Regulation of the Na^+/H^+ Exchanger 1 by BRAF Kinase

by

Aruna Maria Augustine

A thesis submitted in partial fulfillment of the requirements for the degree of

Master of Science

Department of Biochemistry
University of Alberta

Abstract

Mammalian Na+/H+ Exchanger 1 is a ubiquitously expressed membrane protein, which is dedicated to maintaining the acid-base balance in the cell. This balance is brought about by the exchange of one intracellular proton in exchange for extracellular sodium ion. NHE1 is the predominant isoform found in the myocardium and has been implicated in several cardiac diseases including cardiac hypertrophy and ischemic reperfusion induced injury. The NHE1 C-terminal domain is made up of 315 amino acids and is subject to regulation by several protein and protein kinases including the BRAF kinase. In our study we have demonstrated that the BRAF kinase binds to NHE1 C-terminal tail within a region encompassed by amino acids 634 to 710. We also demonstrate that BRAF kinase co-localizes with NHE1 in both AP1 cells as well as HeLa cells, in a serum-dependent manner and the withdrawal of serum results in a loss of co-localization between the two proteins. We further evaluated the role of the threonine 653 amino acid (a target of BRAF kinase phosphorylation) on the NHE1 C-terminal tail with respect to cell proliferation. Mutation of the residue to a non-phosphorylatable amino acid led to a reduction in the rate of cell proliferation.

Additionally, we examined the role of BRAF-NHE1 interaction in melanoma and its effects on various cellular processes. We used specific inhibitors of wild type BRAF (SB590885), mutant BRAF (PLX4720) and NHE1 (EMD87580 and 5-(*N,*N-Hexamethylene) amiloride (HMA)) either alone or in combination to elucidate the role of BRAF-NHE1 interaction in M19, IF6, FM82 and Mel2A human melanoma cell lines. NHE1 did not affect the melanoma cell lines' ability to proliferate. Migration was significantly reduced in the presence of

inhibitors. A combination of BRAF inhibitor and HMA led to a small but significant effect on the rate of migration when compared to NHE1 or BRAF inhibition alone. Invasion was also significantly reduced in the presence of NHE1 or BRAF inhibitors. We also observed varying levels of vimentin among the four cell lines with M19 and Mel2A having high levels of this protein. Mature NHE1 protein was observed only in FM82 and Mel2A but not in M19 or IF6 cell line. These results highlight the importance of NHE1 in the various cellular events associated with tumorigenesis and give a better insight into the underlying mechanism.

We further investigated the role played by stop codon polymorphisms (SCP) in NHE1 localization. We looked at four different SCPs namely, 735STOP, 543STOP, 449STOP and 321STOP. 735STOP localized to the plasma membrane (similar to wild type NHE1) while the other three mutants had cytosolic localization. This study provides us with a better understanding of the vital role played by NHE1 C-terminal tail and how these SCPs can cause deleterious effects within the cell.

Preface

The overlay assay to determine the interaction between BRAF and NHE1 in cardiomyocytes was performed by me and is part of the publication titled "Activation of the Na + /H + exchanger in isolated cardiomyocytes through β-Raf dependent pathways. Role of Thr 653 of the cytosolic tail" *Journal of Molecular and Cellular Cardiology*, *99*, 65–75. The immunofluorescence studies to look at the localization of the various SCPs was also performed by me and is part of the publication titled "Stop Codon Polymorphisms in the Human SLC9A1 Gene Disrupt or Compromise Na+ /H+ Exchanger Function" *PLosOne, 11*(9), 1- 19. I was also involved in the manuscript composition with respect to the data collected and analyzed by me. Dr. Larry Fliegel was responsible for concept formation and manuscript composition.

Dedication

To my beloved grandmother, Aleyamma Kuriakose, who will forever be loved and cherished.

Acknowledgements

I would like to thank my supervisor Dr. Larry Fliegel for this opportunity to work on these projects during my program and for the guidance.

I wish to thank my committee members, Dr. Michael Overduin and Dr. Nicolas Touret for their time and ideas.

I would like to acknowledge the Fliegel lab members, past and present, who have supported me through this journey and have always made the time to help me.

I would like to thank NSERC-CREATE for keeping me afloat for three years and for providing me with the opportunity to travel abroad and attend international conferences.

There are many people in the Department of Biochemistry and Medical Genetics that I would like to acknowledge for their friendship, support and humor during this program.

Table of Contents

List of Tables

List of Figures

List of Abbreviations

Ang II	Angiotensin II
Arg	Arginine
Asn	Asparagine
Asp	Aspartic acid
CAII	Carbonic anhydrase II
CAM	Calmodulin
CaM KII	Calcium-dependent Calmodulin Kinase II
CD	Circular Dichorism
CHO	Chinese hamster ovary
CHP	Caclineurin Homologous Protein
CRD	Cystein rich domain
DMEM	Dulbecco's Modified Eagle's Medium
dNTP	Deoxynucleoside Triphosphate
E.Coli	*Escherchia Coli*
EGF	Epidermal Growth Factor
EL	External Loop
ERK1/2	Extracellular regulated kinase 1/2
ERM	Ezrin-Radixin-Moesin
GDP	Guanosine diphosphate
Glu	Glutamic acid
Gly	Glycine
GST	Glutathione-S-transferase
GTP	Guanosine triphosphate
HA	Haemagglutinin
HEK	Human Embyronic Kidney
HeLa	Henrietta Lacks
His	Histidine
HMA	5-(N,N-Hexamethylene) amiloride
Hsp70	Heat shock protein 70
IGF1R	Insulin like growth factor 1 receptor
Ile	Isoleucine
IPTG	Isopropyl ß-D-thiogalactopyranoside
Leu	Leucine
LPA	Lysophosphatidic acid

Lys	Lysine
MEM	Minimum Essential Media
MMP	Matrix metalloproteinases
MTT	3-(4,5-dimethylthiazol- 2-yl)-2,5-diphenyltetrazolium bromide
NBC	sodium bicarbonate co-transporter
NDCBE	sodium dependent chloride bicarbonate exchanger
NHE	Na+- H+ exchanger
NIK	Nck interacting kinase
NMR	Nuclear Magnetic Resonance
NVRM	Neonatal ventricular rat myocytes
p160ROCK	Rho-associated protein kinase1
p38 MAPK	p38 Mitogen activated protein kinase
p90RSK	p90 ribosomal S6 kinase
PBS	Phosphate Buffered Saline
PCR	Polymerase Chain Reaction
PI3K	Phoshatidylinositol 3 Kinase
PIP2	Phosphatidylionositol 4-5 bisphosphate
PKA	Protein Kinase A
PKC	Protein Kinase C
PKD	Protein Kinase D
PMSF	Phenylmethylsulfonyl Fluoride
PP1	Protein Phosphatase 1
PP2A	Protein Phosphatase 2 A
RAF	Rapidly accelerated fibrosarcoma
RBD	Ras binding domain
RhoA	Ras-homolog A1
RPMI	Roswell Park Memorial Institute Medium
RTK	Receptor tyrosine kinases
SCP	Stop codon polymorphism
SDS-PAGE	Sodium Dodecyl Sulfate-Polyacrylamide Gel Electrphoresis
Ser	Serine
SLC 9A	Solute carrier 9A
SOS	Son of sevenless
TBS	Tris Buffered Saline
Thr	Threonine
TM	Trans-membrane
WT	Wild Type

Chapter 1

Introduction

1.1 Regulation of intracellular pH in mammalian cells

The regulation of cytosolic pH in mammalian cells is a tightly regulated process (1). The acid-base balance is vital for the proper functioning of several key physiological processes in a healthy cell. A subtle shift in the pH dynamics can affect various cellular processes and modulate the activity of several biomolecules, including protein-protein interactions, ligand-receptor interactions, enzyme activity and flux of various ions such as Na^+, Ca^{2+}, K^+ and Cl^- (2, 6).

Several membrane bound transporters are involved in the maintenance of optimal pH (~7.2) and transporters function at a basal level at this pH. The primary acid extruders in the cell include the sodium bicarbonate co-transporter (NBC), sodium dependent chloride bicarbonate exchanger (NDCBE), ATP dependent H^+ pump (H^+- ATPase) and Na^+- H^+ exchanger (NHE). However, the role of each transporter in the maintenance of intracellular pH (pH_i) depends on the cell type (2). Mammalian NHE, particularly NHE isoform 1, is considered to be the predominant exchanger that regulates pH_i especially in the myocardium (3).

1.2. NHE Family of proteins

The transport of sodium ions in exchange for protons across the membrane has been detected in a wide range of organisms, from simple prokaryotes to complex eukaryotes (6). This process is carried out by a family of integral membrane proteins, called the Solute carrier 9A (SLC 9A) family of mammalian NHEs (7). These proteins are classified as secondary active transporters since they do not require the hydrolysis of ATP for the transport of ions. Instead

they rely on the electrochemical gradient that is caused by one of the ions which leads to the counter transport of the corresponding ion (6).

The SLC9A family of NHEs, play a crucial role in maintaining cellular and organellar pH and are involved in a wide array of physiological processes including cell volume regulation, osmolarity regulation as well as salt and water absorption across the epithelia (8-10). Minor fluctuations in the pH_i, associated with NHEs, help modulate cellular proliferation, migration and adhesion (6). The SLC9 gene family is divided into three subgroups, namely, SLC9A1-A9, SLC9B1-B2 (NHA 1-2) and SL9C1 (Sperm-NHE1) (7).

To date, there are ten isoforms (NHE1-10) that have been identified which are encoded by the SLC9A family of proteins. Each isoform differs in terms of cellular localization, tissue specificity, sensitivity to inhibitors, mode of regulation and physiological function (4, 5). NHE isoforms 1-5 are considered as plasma membrane NHEs while isoforms 6-9 are considered as intracellular or organellar NHEs (10). The amino acid identity among the NHE isoforms is highly diverse (20% to 70%) (2). All the NHEs exhibit similar structure in that they have a 12 trans-membrane segment on the N-terminal region which mediates ion transport and C-terminal cytoplasmic tail which play a vital role in posttranslational modification and interaction with other binding partners (7).

1.2.1 SLC9A Family

Pouysségur et al. was the first group to describe a Na^+/H^+ transporter that was not only growth factor activated but also highly sensitive to amiloride. This group further went onto clone the first NHE (NHE1) in 1989 (11). NHE1 is present in almost all mammalian cells and resides on the cell surface. However some studies have shown that NHE1 is absent in α and β-intercalated cells of the kidney as well as the macula densa (12, 13). NHE1 has been shown to accumulate within microdomains of the plasma membrane depending on the cell type and state of the cell (170). In cardiac myocytes NHE1 is concentrated at the intercalated disks and T-tubules. However in polarized cells (epithelial cells), NHE1 is found in the basolateral membrane (10, 14).

NHE2 was first cloned in 1993, by Orlowski et al. and Donowitz et al. (15,16). It is expressed abundantly in the gut and other organs such as heart, skeletal muscle, kidney, brain, uterus, testis, and lung. In epithelial cells, NHE2 has been shown to localize to the apical membrane. A low salt diet resulting in metabolic acidosis causes an increase in NHE2 activity (10,17). However, in both kidney and bowel, absence of NHE2 seems to be compensated by other isoforms such as NHE3 and NHE8 (10).

NHE3 and NHE4 were cloned in 1992 and both are expressed in the gut and kidney. NHE3 is highly resistant to amiloride and its derivatives but NHE4 is only relatively resistant to these compounds (18, 19). Since NHE3 is abundantly expressed in the kidney particularly the apical membrane of the proximal tubule and the ascending thick limb, NHE3 knockout leads to

severe defects in absorption of sodium. NHE5 is highly expressed in the brain and localizes to the plasma membrane and endomembrane. It is also found in skeletal muscle, testis, and spleen. NHE5 demonstrates intermediate sensitivity to amiloride (10, 20).

NHE6 is present in recycling endosomes but also shows a rich plasma membrane distribution in certain cell types. A high expression of NHE6 has been observed in the basolateral membrane of osteoblasts where it aids in removing protons generated as a result of excessive mineralization (21). NHE7 mainly localizes to the trans-Golgi region, however it is also present in brain, skeletal muscles, prostate and pituitary gland. NHE7 is not inhibited by amiloride and its physiological role is not well understood. Some studies show that it may be involved in tumor metastasis (10, 256). NHE8 has been shown to localize to mid and trans-Golgi in HeLa cells and is also present in the apical membrane of kidneys and intestine (22). NHE9 is present in sorting and recycling endosomes, brain and is found in abundance in the plasma membrane of vestibular hair bundles (23). The SLC9C1 encodes for NHE10 expressed in sperm and osteoclasts (30).

Table 1: SLC9A family of Na+/H+ Exchangers (10)

Protein	Expression & Localization	Human Disease
NHE1	Ubiquitous; Plasma membrane	Ischemia Reperfusion induced injury, Cancer, Hypertension
NHE2	Gut, SM, Kd, Ht, Br, Ut, Ts; Plamalemma, apical surface of epithelia	?
NHE3	Gut, Kd, Br; (Apical surface & recycling endosomes)	Congenital Na^+ Diarrhea
NHE4	Stomach, Kd, Br; (Plasma membrane & basolateral membrane of epithelia	?
NHE5	Br (Neurons); Plasmalemma & recycling endosomes	?
NHE6	Ubiquitous; Recycling endosomes	X-linked mental retardation
NHE7	Ubiquitous; Trans-Golgi network & endosomes	Cancer
NHE8	Ubiquitous; Mid to trans-Golgi network, apical plasmamembrane in proximal tubule	?
NHE9	Ubiquitous; Late recycling endosomes	Familial autism; Attention Deficit Hyperactivity Disorder (ADHD)

SM, Skeletal Muscle; KD, Kidney; Ht, Heart; Br, Brain; Ut, Uterus; Ts, Testis.

1.3. NHE1 structural features

Although this exchanger was cloned over 25 years ago, a concrete three-dimensional structure for NHE1 is still lacking due to complications associated with crystallization of membrane proteins. However, experimentally supported models of NHE1 have been proposed. In 2000, Wakabayashi *et al.,* proposed a topology model of NHE1 based on cysteine-scanning mutagenesis and accessibility studies. This model consisted of 12 Trans-membrane (TM) segments with a N-glycosylation site as well as an O-glycosylation site positioned in External Loop 1 (EL1) between TMI and TMII (24). In 2007 Landau *et al.,* used the crystal structure of Na^+- H^+ antiporter from *Escherchia Coli* (EcNhaA) as a template to determine the 3D structure of human NHE1. The Landau model also contains 12 TM segments but differs from the Wakabayashi model in terms of topology and loop extensions. The latter model lacks EL1 and suggests that the first 127 amino acids (spanning TMI and TMII) might be part of a signal peptide that is cleaved in the mature protein and amino acids 315 to 411 form 3 TM segments instead of 1 TM segment (25). However the Wakabayashi model has been supported by other studies, including the Fliegel laboratory. One set of experiments were performed to confirm the presence of the first two TM segments in the whole NHE1 protein. Another series of experiments were conducted to characterize the glycosylation in mature NHE1 protein wherein it was confirmed that asparagine 75 (Asn75) of the first extracellular loop was in fact glycosylated (28).

The human NHE1 protein is made up of 815 amino acids, of which the first 500 amino acids constitute the TM domain that aids in pH sensing and ion translocation across the lipid bilayer. The remainder 315 amino acids form a large cytosolic C-terminal tail that regulates

exchanger activity by binding to other protein partners and is subject to regulation by protein kinase mediated phosphorylation.

1.3.1 N-Terminal Trans-membrane segments

The N-terminal region of NHE1 harbors a short tail consisting of 15 amino acids whose function is still not clear. It extends into the cytosol and is presumed to aid in the anchorage of the first TM segment into the membrane of the cell (29). As mentioned previously, the N-terminal domain of NHE1 consists of 12 TM segments joined by extracellular and intracellular loops. The first two TM segments are joined to each other via an extracellular loop that harbors the two glycosylation sites. The N-glycosylation site aids in targeting the mature protein to the basolateral membrane of polarized epithelial cells (31-33). Interestingly, an inward pointing loop joins TM9 and TM10 (30).

Based on structural modeling studies it appears that TM4 contains residues that line the substrate pore and also determines inhibitor sensitivity (25, 34, 42). NMR studies showed that TM4 did not posses a regular α-helical structure. Rather it had a series of β-turns, an extended structure and a helical region (44,45). Using cysteine scanning mutagenesis and high resolution NMR, Fliegel *et al*., was able to demonstrate that TM6 of NHE1 is a discontinuous helix with amino acids asparagine 227 (Asn227), isoleucine 233 (Ile233), and leucine 243 (Leu243) lining the ion translocation pore (35, 36). Structural studies on the TM7 segment of NHE1 revealed that this segment is predominantly α-helical with an unwound region at residues glycine 261

(Gly261) and glutamic acid 262 (Glu262). TM7 contains several critical residues that not only determine sensitivity to inhibitors but also contribute to protein function (37, 38).

TM9 structure showed that it contained 2 helical regions with an unstructured region in the middle around the functionally important amino acid residue serine 351 (Ser351) and also contains several critical pore-lining residues (41). Functional studies carried out in TM9 demonstrated that this segment is vital for ion translocation as well as drug recognition (42). TM10 was found to be a discontinuous helix with amino acid Leu465 lining the cation pore (46). In addition to these, studies have predicted that the intracellular loops that join TM2-3 and TM10-11, are involved in the allosteric regulation of NHE1 (29, 75, 249).

1.3.2 The C-terminal regulatory domain

The carboxyl terminal region of NHE1 is highly hydrophilic and contains several sites that bind to regulatory proteins and thereby affect exchanger activity. However, very little is known about the structure of the C-terminal tail. The tail is overall intrinsically disordered in several regions. The tail can be divided into two regions, namely, membrane proximal region and membrane distal region (47). Circular Dichorism (CD) studies revealed that this portion of the protein is a mixture of α-helix, β-turn and random coil at 35%, 16% and 49% respectively and this was supported by computer-based prediction, which yielded similar results (46% α-helix, 9% β-sheet and 45% random coil) (48). The studies point to the fact that the membrane proximal region is more compact and structured while the distal portion lacks a well-defined structure. The

unstructured region is thought to aid in phosphorylation and provide flexibility for interaction with other binding partners (48).

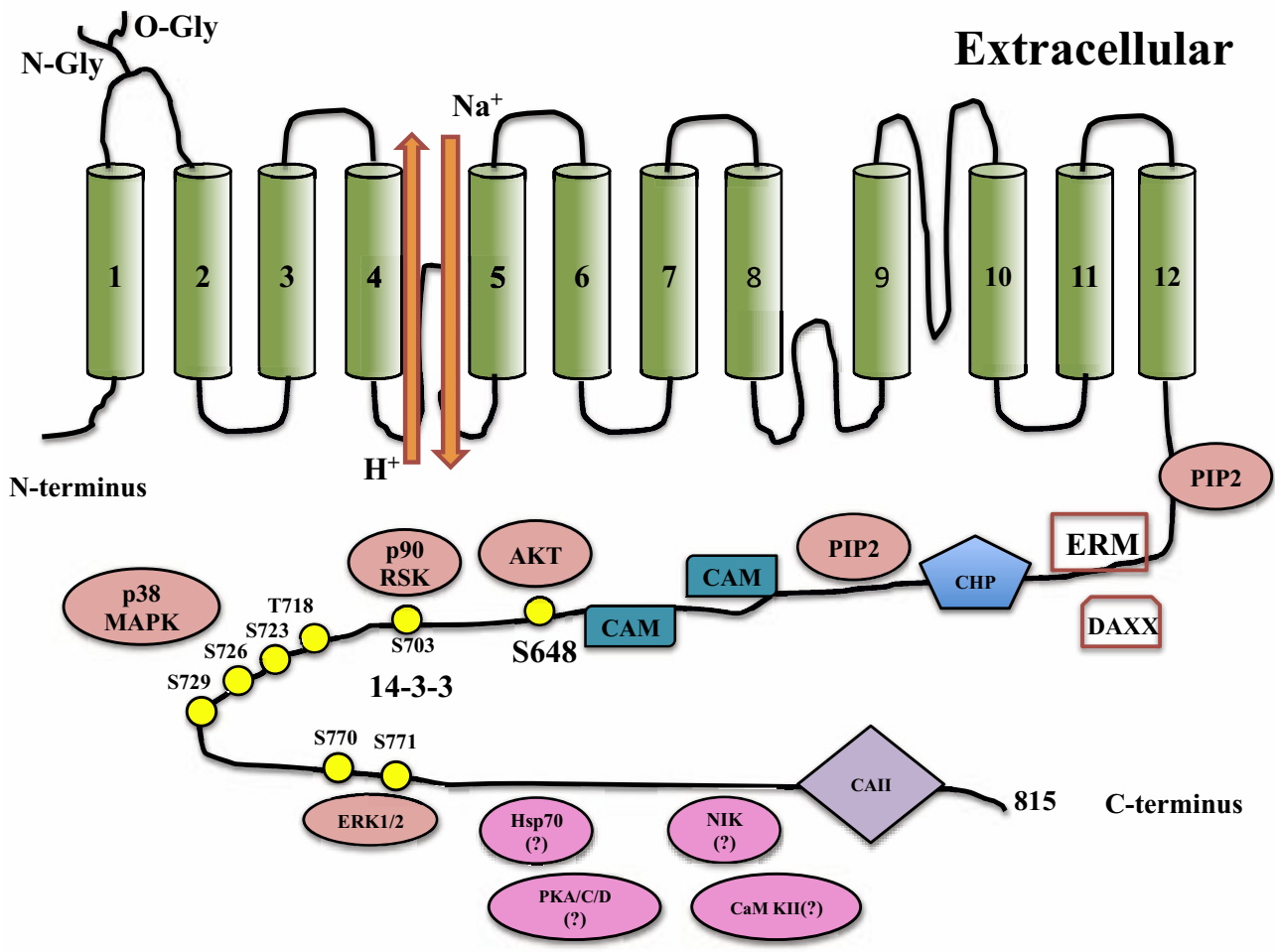

Figure 1: Schematic representation of NHE1 structure (24). NHE1 is made up of 12 Transmembrane segments (labeled 1 to 12) and a large cytoplasmic tail. The C-terminal cytoplasmic tail is bound by and regulated by several proteins and protein kinases. These include PIP2, Phosphatidylionositol 4-5 bisphosphate, ERM, Ezrin-Radixin-Moesin, CHP, Caclineurin Homologous Protein 1 and 2, CAM, Calmodulin, p90RSK, p90 ribosomal S6 kinase, p38 MAPK, p38 Mitogen activated protein kinase, ERK1/2, Extracellular regulated kinase 1/2, Hsp70, Heat shock protein 70, NIK, Nck interacting kinase, PKA/C/D, Protein Kinase A/C/D, CaM KII, Calcium-dependent Calmodulin Kinase II, CAII, Carbonic anhydrase II. Target phosphorylation sites on the C-terminal tail are indicated.

1.4. Regulation of NHE1

The C-terminal tail of NHE1 is vital for the regulation of the NHE1 protein and this process is controlled be several factors such as intracellular acidosis, binding proteins that alter conformation of the tail, protein kinases, post-translational modifications, hormones and growth factors (9).

1.4.1 Cytosolic proton

The intracellular pH affects various cellular processes and therefore is carefully regulated by NHE1. Studies have demonstrated that NHE1 consists of a pH-sensing site, which is different from the H^+ transport site. It was proposed that during sustained intracellular acidosis, the sensor site is bound by H^+ and increases the activity of the exchanger in order to help cells to rapidly recover from the acid load (49). This was demonstrated by experiments conducted in renal brush border membrane vesicles (50). However when the modifier site is not occupied by H^+, NHE1 is not active and thereby protects cells from alkalosis. On the contrary, a very high intracellular acidification abolished Na^+ efflux, which could be due to a competition for the transport site between H^+ ion and Na^+ ion (2).

1.4.2 Regulatory proteins

Studies performed by Wakabayashi *et al.,* with deletion mutations have shown that regulation of NHE1 need not necessarily occur via growth factor induced phosphorylation and rather there might be other regulatory factors that control exchanger activity (51).

Phosphatidylinositol 4,5-bisphosphate (PIP2)

PIP2 is a component of the plasma membrane and functions as a signaling molecule and also regulates the activity of certain ion transporters. Exchangers are thought to bind to PIP2 via motifs that contain cationic and hydrophobic amino acids. The cytosolic domain of NHE1 consists of 2 binding motifs for PIP2, namely, amino acids 513-520 and 556-564 (53). Studies have shown that mutations within these regions caused a significant decrease in the exchanger activity, pointing to the fact that PIP2 interaction is essential to maintain the exchanger's function (53).

Calcineurin homologous protein (CHP) 1 & 2

CHP proteins belong to a family of calcium binding proteins and consist of 3 members, CHP1, CHP2 and CHP3. Studies conducted by Barber *et al.,* demonstrated that CHP1 binds to NHE1 at a specific site within a hydrophobic cluster at amino acids 515-530 and this interaction was vital for growth factor stimulated activation of the exchanger (54-57). Deletion of this specific region led to a loss of growth factor stimulated NHE1 activity (51). Interestingly an

overexpression of CHP1 led to the inhibition of growth factor stimulation of the exchanger (55). One study demonstrated the importance of CHP1 binding to NHE1 to maintain protein stability as well as targeting. Overexpression of CHP1 led to an increase in the levels of NHE1, as well as localization to the plasma membrane (250). NHE1 lacking the CHP1 binding site showed reduced levels of plasma membrane localization, as well as shorter half life when compared to WT NHE1 containing CHP1 binding site (250). The second CHP isoform, CHP2, which has a 60% sequence identity, was shown to interact with NHE1 particularly in malignant cells with a high intracellular pH and promotes transformed cell survival especially during prolonged serum deprivation (58).

Tescalcin

Tescalcin, also known as CHP3, binds to NHE1 at a site different from Calmodulin (CaM) in a calcium dependent manner (59). However this association seems to have an inhibitory effect on the exchanger and the exact binding location is still not known (9).

Ezrin Radixin Moesin (ERM) family of proteins

The ERM family of proteins function as important linkers between NHE1 and the actin cytoskeleton. They are particularly involved in tumor metastasis by regulating actin filament dynamics in conjunction with NHE1 (61). In cardiomyocytes, these proteins have been shown to mediate downstream effects of NHE1 during an acid load via the AKT signaling pathway (62).

The NHE1 C-terminal tail contains 2 binding motifs for ERM proteins located between amino acids 553–564 (60).

Calmodulin

CaM is a 17kDa ubiquitous calcium dependent regulatory factor that binds to NHE1 cytoplasmic tail and activates the protein. CaM binds to two sites on NHE1, a high affinity site located at residues 636–656 constitute and a low affinity site located at residues 657–700 (9, 63). Binding of CaM to the high affinity site aids in the inhibition of the autoinhibitory interaction thereby regulating the exchanger's activity. Deletion and point mutations of positively charged amino acid residues within this region have been shown to reduce the exchanger's activity by 50% in response to growth factor stimuli (63). Interestingly the same group conducted another study and demonstrated that mutations within the CaM high affinity-binding region caused the constitutive activation of NHE1 (251).

Carbonic anhydrase II (CAII)

CAII is a cytoplasmic enzyme that aids in the rapid inter-conversion of carbon dioxide and water to bicarbonate and protons. It binds to NHE1 directly at amino acids 790–802 of the C-terminal tail and enhances the exchanger's activity (67, 68). Since CAII activity produces protons, the interaction between CAII and NHE1 could aid in proton extrusion thereby linking the exchanger to bicarbonate-based pH regulation (68).

Death Domain Associated protein (Daxx)

Daxx protein resides in various locations in the cytoplasm as well as nucleus and has been implicated in ischemic cell death. During ischemic stress, the protein translocates from the nucleus to the cytoplasm where it interacts with NHE1 in competition with Ezrin at the ERM binding motif (70). This results in the inhibition of NHE1 driven downstream activation of the AKT signaling pathway, ultimately resulting in cell death (70).

14-3-3 protein

14-3-3 proteins are a family of highly conserved proteins found in all mammalian cells. These proteins bind to proteins via a specific motif that contains either a phosphorylated serine (Ser) or threonine (Thr) residue. Studies using chinese hamster fibroblast cells demonstrated that 14-3-3 binds to NHE1 at Ser703 residue following its phosphorylation by p90 Ribosomal S6 Kinase (p90 RSK). This interaction offers a protective mechanism wherein, NHE1 de-phosphorylation is prevented and the exchanger is maintained in an active state (71).

Heat Shock Protein 70 (Hsp70)

Hsp70 (also known as DnaK) is a ubiquitously expressed protein and function as chaperones to maintain intracellular protein homeostasis (74). Studies show that the protein binds to the cytoplasmic tail of NHE1 and is thought to aid in protein folding although the specific binding site is still not clear (73). In mouse liver it was demonstrated that Hsp70-NHE1

interaction was required for the involvement of NHE1 in inflammatory response leading to injury (72).

1.4.3 Phosphorylation and Protein Kinases

Phosphorylation of NHE1 C-terminal tail leads to change in the sensitivity of the modifier site to intracellular pH causing an activation of the exchanger (75). It was shown that amino acids 636-815 were vital for growth factor induced *in vivo* phosphorylation of the cytoplasmic tail which accounts for about 50% activation of NHE1 (51, 76).

The NHE1 C-terminal domain is bound and phosphorylated by several kinases. One of the first studies to demonstrate that a kinase directly phosphorylated the C-terminal tail of NHE1 was performed by Fliegel *et al.,* in 1992. *In vitro* assays showed that Ca^{2+}/ calmodulin-dependent protein kinase II (CaM kinase II) directly phosphorylated the distal 178 amino acids of NHE1 (78). However the exact site of phosphorylation is yet to be identified.

Mitogen Activated Protein Kinase (MAPK) and its downstream targets Extracellular-Regulated signal Kinase (ERK 1 and 2) are involved in the phosphorylation of NHE1 in a growth factor dependent manner. Inhibition of this pathway led to ~ 60% reduction in NHE1 stimulation by growth factors in Chinese hamster fibroblast cells (79). Additional studies in rat myocardium highlighted the role of a MAPK downstream effector kinase, p90RSK, in the regulation of NHE1 activity (80). Studies conducted in vascular smooth muscle cells identified Ser703 as a target for p90RSK on NHE1 C-terminal tail and phosphorylation led to an increase in NHE1 activity

ultimately causing ischemic cell death and neuronal cell death (81, 82). Studies preformed in the Fliegel laboratory demonstrated that sustained intracellular acidosis activates NHE1 via an ERK 1/2 dependent mechanism. Specific groups of serine and threonine residues were identified, however Ser770 and Ser771 were shown to be essential in acidosis-mediated activation of the exchanger *in vivo* (83). Further studies in neonatal rat cardiomyocytes demonstrated that phosphorylation of Ser770 and Ser771 contribute to exchanger activation during sustained intracellular acidosis (84).

The p38 MAPK is a group of kinases that is induced by stress stimuli such as cytokines, osmotic shock and heat shock. Studies have shown that p38MAPK modulates NHE1 activity, especially in vascular smooth muscle cells wherein p38MAPK inhibited NHE1 in response to Angiotensin II treatment (86). However in mouse pancreatic β cells, an opposite effect was observed wherein p38 activated NHE1 leading to intracellular alkalinization and subsequent apoptosis perhaps through the phosphorylation of threonine 718 (Thr718), Ser723, Ser726, and Ser729 residues of NHE1 C-terminal tail (89).

The Nck Interacting Kinase (NIK), binds to and regulates NHE1 activity *in vivo*. NIK binds to NHE1 at amino acids 538 to 638, however, the phosphorylation site on NHE1 C-terminal is located more distal to 638 (90). Rho-associated protein kinase1 (p160ROCK) activates NHE1 downstream of Ras-homolog A1 (RhoA) most likely via phosphorylation of the C-terminal tail. The binding motif is considered to lie somewhere between amino acids 635-815 (92).

Although Protein Kinase A and C (PKA, PKC) have been shown to not phosphorylate NHE1 directly, Protein Kinase B (PKB/Akt) has been shown to directly phosphorylate NHE1 at Ser648 (9, 94). Akt is important for growth factor induced cell survival, proliferation and migration and the activation of NHE1 in fibroblasts promotes these processes (94). It should be noted that Akt substrates are often inhibited upon phosphorylation and this was observed in adult rat ventricular myocytes wherein Akt reduced NHE1 activity following intracellular acidosis. This could be possibly due to interference with CaM binding. However, inhibition of Akt led to a reversal of this effect (94, 97).

A study from the Fliegel laboratory published in 2011 demonstrated that a serine/threonine kinase named BRAF bound to NHE1 C-terminal tail both *in vitro* as well as *in vivo* in Henrietta Lacks (HeLa) and Human Embryonic Kidney (HEK) cells. Further studies conducted in human melanoma cell lines demonstrated that the interaction led to an increase in the exchanger's activity in an ERK dependent manner and inhibition of BRAF did not trigger ERK phosphorylation and subsequent activation of NHE1 (3).

Several studies have demonstrated the role of phosphorylation in modulating NHE1 activity, while other studies have highlighted the role of de-phosphorylation in regulating intracellular pH. Protein Phosphatase 1 (PP1) has been shown to directly bind to NHE1 and reduce exchanger activity *in vivo* and inhibition of PP1 led to an increase in proton flux (98). In adult rat ventricular myocytes, Protein Phosphatase 2 A (PP2A) co-localizes with NHE1 and has an inhibitory effect on the exchanger's activity (99).

1.4.4 Growth factor and Hormones

Although phosphorylation plays a vital role in the regulation of NHE1 that is not the only mechanism by which activation occurs. Deletion and point mutation studies in the distal region of NHE1 C-terminal tail (amino acids 636-815) where majority of the phosphorylation sites are located, demonstrated that the exchanger was still able to retain its ability to get activated in the presence of growth factors (51). This supports the idea that there are other factors besides phosphorylation that help modulate ion translocation (113).

The mechanism by which extracellular stimuli regulate the activity of NHE1 is a complex process and not well understood. Growth factors have been shown to phosphorylate serine residues in the C-terminal tail and cause a subsequent increase in the activity of the exchanger (100). Some examples of such growth factors and hormones include, Insulin, Thrombin, Epidermal Growth Factor (EGF), Angiotensin II (Ang II), and Lysophosphatidic acid (LPA) and also serum (9, 102). Thrombin is a serine protease that has been shown to activate the MAPK cascade and subsequent activation of ERK1/2 ultimately leading to the phosphorylation and activation of NHE1 (102). Serum induced phosphorylation occurs via p90RSK which directly targets Ser703 and subsequently leads to 14-3-3 binding and increased NHE1 activity (103). EGF also stimulates NHE1 activity via the MAPK cascade, however in mouse NIH3T3 cells, EGF stimulates NHE1 activity via PKCα (102, 104). In human erythrocytes, insulin activates NHE1 via a Phoshatidylinositol 3 Kinase (PI3K)-PKC pathway (105).

Ang II plays a vital role in protein phosphorylation and ion transport. AngII stimulates NHE1 activity via the AT1 receptor in rat vascular smooth muscle cells (106, 107). In rat hearts it was demonstrated that Endothelin could stimulate NHE1 activity in a PKC dependent manner leading to an increase in intracellular pH and increased sensitivity of cardiac cells to cytoplasmic Calcium (108). AngII can also have a negative effect on NHE1 via the AT2 receptor subtypes (9, 106).

LPA is a phospholipid that functions via G-protein coupled receptors. In fibroblasts, LPA has been shown to stimulate ROCK kinases leading to the phosphorylation of NHE1 at Thr653 residue and subsequent activation of the exchanger. Mutation of this residue to an alanine caused a defect in LPA stimulated activation of the exchanger (112).

Table 2: List of known interacting partners of the NHE1 C-terminal tail (166)

Interacting Partner	Binding Domain/ Phosphorylation site
Phosphatidylionositol 4, 5-bisphosphate	513-520; 556-564
Calcineurin homologous protein	518-537
Ezrin/Radixin/Moesin; Daxx	552-560
Calmodulin	High affinity 636-656; Low affinity 657-700
AKT	Serine 648
p90 ribosomal S6 kinase; 14-3-3	Serine 703
p38 Mitogen activated protein kinase	Threonine 718; Serine 723, 726 and 729
Extracellular regulated signal kinases 1/2	Serine 770 and 771
Carbonic Anyhdrase II	790-802
Protein Kinase A/C/D	Unknown
Tescalcin	Unknown
Nck interacting kinase	538-638; Phosphorylation site unknown
$Ca^{2+/}$Calmodulin dependent kinase II	Unknown
Heat shock protein 70	Unknown
Rho-associated protein kinase1 (p160ROCK)	Proposed to bind between 635-815

1.5. BRAF Kinase: Structure, Function and Regulation

Protein kinases play a central role in cell biology and as discussed previously they bind to and phosphorylate NHE1 C-terminal tail. In humans, the protein kinase family consists of over 518 genes. This family can be subdivide into serine/threonine kinases (~385), tyrosine kinases (~90), tyrosine-kinase like kinases (~ 43) and a smaller sub group with dual specificity (tyrosine-threonine kinases and serine threonine kinases) (177). The MAPK signaling pathway is one of the most well studied cascades particularly in cancer. The MAPK pathway regulates various cellular processes including cell proliferation, differentiation, survival and apoptosis (178). Although not much is known about the link between MAPK and NHE1 via BRAF, a study from our laboratory demonstrated that BRAF binds to NHE1 C-terminal tail and also regulate its activity in various cell lines (3). This study paved the way to explore this link further.

1.5.1 Overview of the MAPK pathway

Under normal physiological conditions, growth factors and mitogens depend on the MAPK cascade to transmit signals from the plasma membrane to the nucleus in order to evade apoptosis and promote cell survival (179, 180). In mammalian cells, the MAPK pathway contains 3 key protein kinases that help relay the information across the cell. These include the MAPKKK which function upstream, intermediate MAPKK and finally the effector MAPK (181). This process is controlled by a ligand dependent activation of receptor tyrosine kinases (RTK), which include insulin like growth factor 1 receptor (IGF1R) and epidermal growth factor receptor (EGFR) (179).

Activation of the RTK by ligand, signals the recruitment of an adaptor protein, growth factor receptor bound protein 2 (Grb2), which subsequently binds and activates son of sevenless (SOS), a Ras guanine exchange factor. Once SOS is activated it catalyzes the exchange of guanosine diphosphate (GDP) for guanosine triphosphate (GTP) thereby converting inactive RasGDP to active RasGTP (179). The active Ras triggers a series of downstream phosphorylation events. First active Ras interacts with MAPKKKs, rapidly accelerated fibrosarcoma proteins (RAF), cause membrane recruitment and subsequent homo or hetero-dimerization and activation (182). Activated RAF kinases then act on MAPKKs (MEK1 and MEK2), which then trigger the activation of downstream MAPKs (ERK1 and ERK2), which target several nuclear and cytoplasmic proteins and activate them via phosphorylation and thereby promote cell proliferation and survival (179).

1.5.2 Structure of BRAF protein-serine/threonine kinases

RAF was first identified in 1983 as part of a retroviral oncogenes (v-Raf) with serine/threonine kinase activity (184). Later the corresponding RAF genes were identified in humans and they consist of 3 members, A-RAF, B-RAF and C-RAF (177). The family of RAF proteins can either form homo-dimers or heterodimers. However the focus of this thesis will be on BRAF kinase.

Each RAF protein shares three conserved regions, CR1, CR2, and CR3. The CR1 region consists of the Ras-Binding domain (RBD) and a cysteine rich domain (CRD) (184). It should be

noted that the CRD can bind two zinc ions. CR2 is a serine/threonine rich domain whose role is less defined (184). Studies have shown that CR2 harbors a site (phosphorylated serine) that can bind 14-3-3 regulatory protein but this binding seems to have an inhibitory effect (177). CR3 is the protein kinase domain located on the C-terminal end of the protein and is regulated by phosphorylation (184).

The BRAF kinase domain has a small N-terminal lobe, which consists of β-sheets and helps anchor ATP. It also consists what is called the P-loop, which has a glycine rich ATP-phosphate binding region (177). The large C-terminal lobe is mostly α-helical and binds several protein substrates including its downstream targets, MEK1/2. The catalytic site lies between these two lobes. The two lobes move in response to signals to form an open or closed state (177, 184). The large lobe contains an activation segment that has a DFG motif (Aspartic acid/Phenylalanine/Glycine). In an inactive state the phenylalanine residue occupies the ATP-binding pocket thereby disrupting it and the aspartic acid residue faces away from the binding pocket and therefore is referred to as the DFG-Asp out conformation. In the active state the aspartic acid side chain faces the ATP-binding pocket to help coordinate Magnesium ions and is called the DFG-Asp in conformation (177).

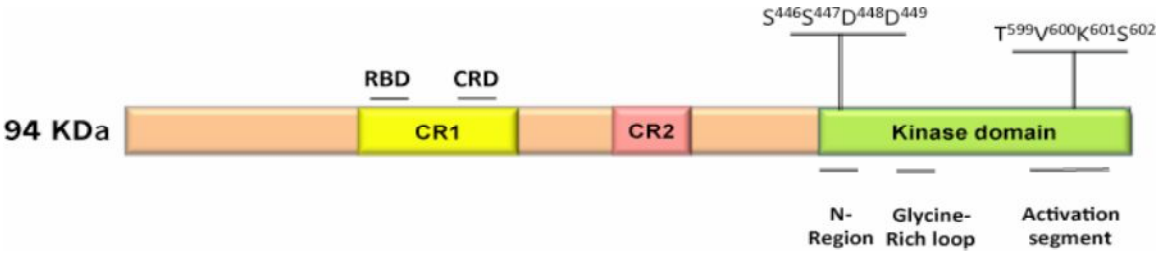

Figure 2: Schematic representation of BRAF containing 3 conserved regions (CR1, CR2 and CR3). CR1 harbors a Ras binding domain (RBD) and Cysteine Rich Domain (CRD). CR3 (activation segment) contains the activation loop, which is essential for its kinase activity (177).

Table 3: Important amino acid residues in human BRAF Kinase (177)

Segment/Domain	Residues
RBD	155-227
CRD	234-280
CR1	150-290
CR2	360-375
CR3	451-717
Glycine rich loop	463-471
14-3-3 binding site	S365, S729
DFG	578
Activation segment (Phosphorylation)	T599, S602
Total number of amino acids	766
Molecular weight (kDa)	94

1.5.3 Regulation of BRAF kinase

Regulation of the RAF kinases is a complex process and involves three key mechanisms, 1. Phosphorylation, 2. Regulation by small GTPases and 3. Scaffolding proteins.

Phosphorylation This mechanism is important for the regulation of a wide variety of cellular proteins and in the case of BRAF it seems to be a conserved mechanism involving both phosphorylation as well as de-phosphorylation (183). Ras binding to BRAF induces phosphorylation at a few key residues and fully induces the protein. However, it should be noted that certain amino acid residues on Raf proteins in general are constitutively phosphorylated. In the case of BRAF Ser445 is constitutively phosphorylated which may explain why this protein's basal activity is at a higher level in cells compared to ARAF and CRAF (177, 183). BRAF activation is dependent on the phosphorylation of Thr599 and Ser602, which lie within the activation segment (177). The kinase activity of the protein relies on the phosphorylation of Ser579 within the activation loop and is thought to be vital to bind downstream substrates (MEK1/2) (177, 183). It is interesting to note that serine residues 151 and 750 and threonine residues 401 and 753 are speculated to be phosphorylation targets of ERK and result in feedback inhibition of the kinase (177).

Small GTPases BRAF activation by Ras is accomplished by binding of the effector domain on Ras to both the RBD as well as CRD on BRAF kinase. This not only allows activation but also aids in the recruitment of BRAF to the membrane. Likewise, Ras related-protein (Rap) GTPases, which are very similar to Ras GTPases, bind BRAF in a similar manner to activate the kinase

(183). Interestingly Rap GTPases binding to CRAF causes inhibition of kinase rather than activation (183).

Scaffolding proteins Using elegant genetic screens in *Drosophila* and *Caenorhabditis elegans* scientists were able to identify a few scaffolding proteins that were important in the activation of RAF kinases and enhancement of MAPK signaling (183). Kinase suppressor of Ras (KSR) is a positive modulator of the MAPK pathway and is proposed to function downstream of Ras. It is a scaffolding protein that can interact with RAF, MEK, ERK and heat shock proteins. KSR contains a C-terminal kinase domain that can directly phosphorylate RAF and activate it. However the exact residue at which phosphorylation occurs remains unclear (183). Sur8/SHOC2 are leucine rich proteins that can form a ternary complex with Ras and RAF and can aid in the activation of BRAF perhaps by bringing the two proteins together (186). Connector enhancer of KSR (CNK), is thought to act downstream of Ras but upstream of RAF and not only activates BRAF but also aids in the recruitment of BRAF to the membrane (187).

As mentioned previously, so far only one study from the Fliegel laboratory has investigated the role of BRAF-NHE1 interaction in cells (3). Recently another study from our group further investigated the role of this BRAF-NHE1 interaction in cardiomyocytes (193). The MAPK cascade and its components, particularly BRAF, play a central role in cellular function and its deregulation is frequently observed in cancer. Given the importance of NHE1 in maintaining pH homeostasis, and its link to this cascade, it is important to explore this pathway in greater depth especially in tumorigenesis.

1.6 NHE1: Physiological functions and pathological role

Although the primary role of NHE1 is to regulate the acid-base balance in the cell, it is involved in a plethora of other cellular functions such as cell volume regulation, cellular proliferation, differentiation, migration and evasion of apoptosis (119). NHE1 has been shown to modulate the expression of several genes of the cell cycle by regulating the intracellular pH. It aids in the G2/M transition to S phase in the cell cycle via a transient intracellular alkalinization. However in NHE1-deficient cells this process is stalled (81).

Studies conducted in P19 embryonal carcinoma cells highlighted the role of NHE1 in cell growth and differentiation. NHE1 deficient P19 cells were defective in growth and also lacked the ability to differentiate into neuronal like cells but the reintroduction of the exchanger reversed this effect (120). NHE1 knock out (KO) mice demonstrated reduced survival and severe growth defects including neurodegeneration and ataxia (121, 122).

Interaction of NHE1 with ERM proteins is required for the maintenance of the cytoskeleton structure and help direct cell migration. NHE1 deficient cells show defects in adhesion properties and a lack of interaction with ERM leads to a loss of cell shape and defective migration (60).

The role of NHE1 in apoptosis depends on the cell type in question. In certain cell types such as breast cancer cells and leukaemic cells, NHE1 aids in the evasion of apoptosis probably through the activation of Akt in response to apoptotic stress (123, 124). However in mouse β-

cells, NHE is activated in response to apoptotic stimuli and leads intracellular alkalinization and progression of apoptosis (89).

1.6.1 Ischemia and Reperfusion

NHE1 is the predominant isoform present in the heart and contributes to proper cardiac function by maintaining intracellular pH homeostasis. However, NHE1 is also involved in injury as a result of ischemia and reperfusion (125). The role of NHE1 in ischemia is relative to the role and activity of two other exchangers, Na^+/K^+ pump and the Na^+/Ca^{2+} exchanger. Under normal physiological conditions, NHE1 remains inactive and the Na^+/K^+ pump functions to extrude sodium from cardiac cells while the Na^+/Ca^{2+} exchanger serves to extrude calcium (126). Myocardial ischemia occurs when the blood flow to the heart is restricted and there is a shortage of oxygen. This condition leads to an inhibition of the Na^+/K^+ pump and causes a rapid accumulation of protons thereby leading to a drop in intracellular pH (126, 127). In addition to this there is a rapid accumulation of metabolites and oxidative stress. The combined effect leads to activation of NHE1 and a subsequent reversal of the Na^+/Ca^{2+} exchanger leading to a large increase in calcium influx. This calcium overload has adverse effects on the myocardium including contractile dysfunction, ventricular arrhythmias and cell death (125, 126).

Since NHE1 plays such a crucial role in Ischemia related injury, there has been a lot of interest in inhibiting this exchanger in order to protect the myocardium, including genetic ablation as well as pharmacological inhibition of NHE1 (128, 129). Initial studies used amiloride to inhibit NHE1 and although there was recovery of myocardial function following ischemic

injury, there were some speculations regarding drug efficacy and toxicity (128, 130, 131). Later studies focused on using a more potent and specific inhibitor of NHE1, cariporide (HOE692). The protective effects conferred by cariporide were far superior compared to others such as Class I Antiarrhythmic agent, Beta-blockers and Angiotensin Converting Enzyme (ACE) inhibitor.

The inhibition of NHE1 with cariporide supports the role of NHE1 in the myocardium and helps reduce the damage that occurs as a result of imbalance in the sodium, protons and calcium levels in the cell. Inhibition confers a protective effect and may help reduce other defects such as ischemia-related arrhythmias and contractile dysfunction (125, 126, 133). However it should be noted that NHE1 inhibition using cariporide is most effective during early ischemic injury (132, 133).

1.6.2 Cardiac Hypertrophy

Cardiac hypertrophy is an enlargement of the heart muscle and this condition is found to accompany other diseases such as heart failure, hypertension and ischemic disease (134). Myocardial G-Protein Coupled Receptors (GPCR) including, AngII, Endothelin-1 (ET1) and adrenergic receptors play a vital role in hypertrophy (135, 136). Mechanical stress in neonatal as well as adult cardiomyocytes can activate a wide array of hypertrophic signaling cascades. Several protein kinases are activated as downstream targets of this external stimulus and these include, MAPK, ERK, p90RSK and PKC (137).

Aside from the proteins listed above, cardiac NHE1 also plays a pivotal role in hypertrophy wherein there is increased expression and activity of the exchanger (125, 139). The increased activity subsequently influences influx of calcium, which triggers several downstream signaling cascades. Inhibition of NHE1 in animal models prevented hypertrophy in animal models (138). The exact mechanism by which NHE1 influences hypertrophy is still not clear, but it should be noted that GPCRs such as AngII, ET-1 and α-Adrenergic receptors are known stimulators of NHE1 (136).

In neonatal ventricular rat myocytes, inhibiting the aldosterone receptor resulted in a protective effect, by preventing aldosterone induced NHE1 expression and subsequent hypertrophy mediated by NHE1 (140). In adult mouse cardiomyocytes, inhibition of CAII prevented hypertrophy since, as mentioned previously, CAII binds to and activates NHE1 activity (67, 68, 141). NHE1 inhibition by amiloride resulted in a reduction of myocardial fiber size and the inhibition of NHE1 with HOE694 suppressed intracellular alkalinization and prevented mechanical stress induced hypertrophy in neonatal cardiac myocytes (137, 142). Recent studies have demonstrated that inhibition of mitochondrial NHE1 abolished increased expression of the exchanger protein and also prevented its effects on Mitochondrial Fission/Fusion (MFF) proteins whose expression is usually affected during *in vitro* cardiomyocyte hypertrophy (143, 144).

1.6.3 Hypertension

Spontaneously hypertensive rats (SHR) serve as an ideal model to study human primary hypertension. Studies from these animal models demonstrated that there is increased activity of NHE1, NHE3 as well as the Na^+-K^+-$2Cl^-$ Co-transporter and a similar defect is observed in patients with hypertension (145). The SHR showed elevated exchanger activity in various cell types such as cultured vascular smooth muscle cells (VSMC), striated muscle cells, platelets, lymphocytes, neutrophils, erythrocytes, mesangial cells and kidney epithelial cells while in patients with hypertension exchanger activity was elevated in erythrocytes, platelets, lymphocytes, and immortalized lymphoblasts (145). In another study, NHE1 activity was increased in about 50% of the hypertensive patients when compared to their normotensive counterparts (148, 149).

Although there are a few theoretical links between NHE1 and hypertension, the exact molecular mechanism underlying this mechanism remains poorly understood. Genetic linkage analysis revealed that NHE1 locus does not play a role in hypertension suggesting that it might be more of a regulatory mechanism that contributes to this pathophysiological effect (150). Another study conducted in cultured vascular and striated muscle cells from SHR revealed that the increased transport activity is not due to increased protein expression, rather it was due to the increased turnover number of the protein (146). An interesting study conducted in SHR vascular smooth muscle cells discovered that p90RSK showed about 1.8-fold increase in its activity in cells stimulated by AngII compared to cells from normal rats. This increase in activity was Calcium dependent (151). Since p90RSK is one of the kinases that regulated transport activity of

NHE1 this could be a possible mechanism by which NHE1 contributes to the pathology of hypertension.

One other potential mechanism linking NHE1 and hypertension is the involvement of Na^+/Ca^{2+} exchanger. NHE1 over activation in vascular smooth muscle cells leads to an overload of intracellular Na^+. This leads to a reversal in the Na^+/Ca^{2+} exchanger and Ca^{2+} accumulation. In chronic conditions this may contribute to abnormal growth of the vascular smooth muscle cells and are susceptible to high-salt-induced hypertension (147, 152). However, it should be noted that strong evidence for this hypothesis is still lacking.

1.6.4 Diabetes

Diabetes Mellitus is a metabolic disease, which is accompanied by improper metabolism of carbohydrates and elevated glucose levels in the blood and urine. The hyperglycemic effect is caused either due to inadequate insulin production or excessive glucagon secretion or insulin resistance (153). Diabetes Mellitus is categorized as Type 1 Diabetes and Type 2 Diabetes. Type 1 Diabetes is an autoimmune disorder wherein the pancreatic beta-cells responsible for producing insulin are destroyed while Type 2 diabetes is a metabolic disorder wherein there is a combination of insulin resistance as well as dysfunctional pancreatic beta-cells (153).

Since elevated NHE1 has been reported to contribute to the pathogenesis of diabetes, the effect of high extracellular glucose was tested in rat vascular smooth muscle cells (154). It was observed that high glucose medium caused a significant increase in the transport activity in a

PKC dependent manner. In addition to this it was observed that high glucose caused a 3-fold increase in NHE1 mRNA levels when compared to control cells (154). In order to demonstrate that NHE1 activity is increased in proximal tubule luminal membrane in conjunction with renal hypertrophy, streptozotocin-induced diabetic rats were used (155). The levels of NHE1 were increased in diabetic condition, however when these animals were treated with insulin the effect was lost (155). Another study conducted in diabetic male-Sprague–Dawley rats demonstrated that NHE1 mRNA levels increased after 6 and 12 weeks of diabetes onset and cariporide treatment along with glucose control was able to attenuate the hyperglycemic effect seen in these rats (156). Taken together these studies highlight the importance/role of NHE1 in diabetes.

1.6.5 Cancer

Cancer is a multistep process that involves the orchestration of several key characteristics that were elegantly described by Hanahan and Weinberg. The six hallmarks include: sustained cellular proliferation, evasion of growth suppressors, invasion and metastasis, replicative immortality, angiogenesis and evasion of cell death (161). However, proton dynamics is considered as an emerging hallmark of cancer, since cancer cells and tissues, irrespective of their genetics, origin or pathology, exhibit a reversal in the pH gradient (162). The reversal leads to an increase in intracellular pH and a decrease within the extracellular milieu, which has been detected during the early stages of tumorigenesis (162). Cytoplasmic pH and ion translocation play an important role in a wide variety of cellular functions such as regulation of mitochondrial activity, enzyme activity, DNA synthesis, growth factor activity and differentiation (158). The imbalance in proton dynamics contributes to neoplastic progression wherein the intracellular

alkalinization promotes cell survival through evasion of apoptosis, proliferation and directed cell migration (159, 160).

Early studies conducted in 1989, aimed to investigate the role of NHE1 in tumor growth in human bladder carcinoma cell line MGH-U1 that were NHE1 deficient (163). These cells either lacked the ability to form tumors or showed severe defects in tumor growth when injected into immunosuppressed mice. Additionally these cells were unable to form spheroids in culture (163). This study shed light into the role of NHE1 in the formation and progression of tumors.

Another study conducted by Reshkin *et al.,* in 2000, investigated the role of aberrant pH in malignant transformation (164). The E7 oncogene from Human Papilloma Virus Type 16 (HPV16) was used to infect NIH3T3 cells, which is a mouse fibroblast cell line. As controls, NIH3T3 cells were infected with an E7 mutant that was defective in inducing transformation. Intracellular alkalinization was high in transformed cells while in controls this was not the case. Inhibition of NHE1 using 5-(N,N-dimethyl) amiloride (DMA) abolished E7 induced cytoplasmic alkalinization. Additionally these cells did not exhibit transformed phenotypes such as higher rates of proliferation, glycolytic metabolism, anchorage and serum-independent growth. In parallel, experiments were conducted in human keratinocytes (HPKIA) to verify the results obtained in NIH3T3 cells. Nude mice were injected with keratinocytes that were infected with HPV16 and then treated with DMA, which delayed development of tumors in these animals. Taken together these results clearly indicate that the first step in oncogene driven transformation is the increase in activation of NHE1 by increasing the affinity of the proton regulatory site and subsequent increase in the exchanger's sensitivity to intracellular protons (158, 164). This

process is not only essential for oncogenic transformation, but is also required for maintenance of the cancerous phenotype (164).

There has been a lot of interest in investigating the role of NHE1 in breast cancer cells. Although NHE1 does contribute to breast cancer metastasis, the exact mechanism by which this occurs remains elusive. In 2003, Reshkin *et al*., investigated the signaling mechanism involved in paclitaxel-dependent apoptosis in breast cancer cells (MDA-MB-435). It was observed that paclitaxel inhibited NHE1 activity in a dose dependent manner and induced apoptosis but did not alter expression levels of NHE1. Additionally, paclitaxel treatment stimulated two kinases, PKA and p38. These two kinases act upstream of NHE1 in the paclitaxel driven apoptotic pathway and interestingly they contribute to an increase in the inhibition of NHE1 by paclitaxel. Inhibition of NHE1 by DMA along with incubation with paclitaxel showed a drastic increase in apoptosis (165). This study was one of the first to demonstrate that NHE1 played a vital role in paclitaxel-induced apoptosis in human breast cancer cells.

A few other studies in breast cancer epithelial cells demonstrated that serum withdrawal stimulates NHE1 activity. This was a result of an increase in the proton affinity by a PI3-Kinase dependent mechanism but is not necessarily accompanied by the direct phosphorylation of the exchanger (158, 166). However two independent reports contradicted this theory and proposed that the increase in NHE1 activity is due to the increased dimerization of the protein rather than contribution from the proton affinity site of NHE1 monomer (167, 168). Fairly recent studies have demonstrated the existence of a signal module consisting of RhoA, ROCK and p38 that contribute to NHE1 activation in serum deprived breast cancer cells (169). Other studies have

demonstrated that CD44, which serves as a receptor for hyaluronic acid, localizes to specific micro-compartments of breast cancer cells and acidifies the extracellular milieu via the activation of NHE1 (170). In MDA-MB-231 cells, an invasive breast cancer cell line, the level of phosphorylated ERK1/2 and p38MAPK was higher than their non-invasive counterparts (MCF-7 cells) and subsequent treatment of the invasive cells with a NHE1 inhibitor, cariporide, affected invasion in these cells (171). All these studies put together provide ample support in terms of the role played by aberrant NHE1 function in breast cancer metastasis.

1.6.6 Genetic disease

Although NHE1 has been implicated in cardiac diseases, hypertension and cancer, previous studies conducted in animal disease show that NHE1 plays a crucial role in certain genetic defects. In order to investigate the role of NHE1 in embryogenesis, gene targeting was used to disrupt the murine exchanger at the 6^{th} and 7^{th} TM domains (172). It was observed that genetic ablation did not cause embryonic lethality, which is likely due to embryogenesis relying on other NHEs or ion transporters. However, homozygous mutants displayed ataxia as well as convulsive seizures just at week 2. An increased level of mortality was observed in the mutant animals before weaning. Histological analysis of these animals revealed abnormalities in the interstitial spaces of glandular gastric mucosa (172).

In parallel there was another study published by Cox *et al.,* where they described a spontaneous mouse mutant that was linked to a null allele of NHE1 (173). The Slow Wave Epilepsy (swe) mice demonstrated defects associated with the central nervous system such as

locomotor ataxia and seizures that were similar to human epilepsies. This was accompanied by severe neurodegeneration in the cerebrum. Only half of the homozygous swe animals survive to weaning but ultimately these animals die by day 40 (173). The phenotypes described above are due to a point mutation in NHE1, which was identified using single nucleotide confirmation polymorphism mapping. An A to T mutation was observed at nucleotide 1639 which converts lysine 442 (Lys442) to a stop codon (AAG-TAG) and therefore the protein is truncated immediately after the 11^{th} TM domain (173). This was the first study to report an inherited NHE1 mutation in murine model.

A study that was published in 2014 by Wessels *et al.,* demonstrated that deletion of huntingtin gene (associated with Huntington's disease) in *Dictyostelium* amoebae resulted in defective chemotaxis in response to extracellular calcium and potassium (29, 185). The huntingtin-knock out cells had defective NHE1 trafficking, in that they were not present at the leading edge of the migrating cell and actin filaments were not well formed. Given the role of NHE1 in cell migration and the observation in this report, there is a possibility that NHE1 might be linked to the huntingtin gene (185). However to date there are no known NHE1 mutations that have been reported in patients with Huntington's disease.

Although there are a few reports based on animal models, not much is known about mutation of human NHE1 and its associated phenotypes. Recently a report used exome sequencing to identify a novel missense mutation in NHE1 among members of a consanguineous family with Lichtenstein-Knorr syndrome (174). Lichtenstein-Knorr syndrome is a progressive autosomal recessive disorder that is linked to ataxia and sensorineural hearing loss syndrome.

The causative mutation occurs on glycine 305 (Gly305), located on the 8th TM domain of NHE1, is converted to an arginine residue (Arg). The Fliegel laboratory in collaboration with Guissart *et al.,* investigated various aspects of this mutant including protein expression, localization/targeting and activity. Gly305Arg showed reduced expression compared to wild type (WT) NHE1 with only 2% of the WT activity. In addition to this, the mutant protein did not show a plasma membrane distribution, rather it showed a cytoplasmic distribution implying that the protein was mis-targeted (174). Taken together this study highlights the role of defective NHE1 in this rare genetic disorder.

Another novel mutation found in NHE1 is N266H wherein an asparagine residue is mutated to a histidine (His) residue. This was discovered through exome sequencing in a group of 119 individuals who had a variety of undiagnosed genetic disorders (176). The patient with this mutation displayed impaired movement and intellectual disability (175). Asn266 maps to TM7 of NHE1 N-terminal domain. The mutation had little to no effect on the expression levels and targeting of the protein. However activity was completely lost when compared to wild type NHE1 (175). Early studies on the structure of NHE1 have indicated that Asn266 lies along the ion transport pore and along with Asp267 is essential for cation binding (25). Therefore the presence of histidine with a large side chain in the place of asparagine at amino acid 266 might disrupt ion translocation pore and this ultimately leads to a loss in exchanger activity. However it is still unclear if this mutation is linked to Lichtenstein-Knorr syndrome or any other genetic disorders but further investigation into the role of such mutants in NHE1 is warranted.

1.7 Thesis Objectives

Our laboratory published a very important finding that BRAF kinase interacts with NHE1 and regulates the exchanger's activity in certain cell types (3). Being the first of its kind, very little is known about the underlying mechanism. The hypothesis of this study was that BRAF kinase binds to and phosphorylates a specific residue/residues on the C-terminal tail of NHE1 and thereby regulates the exchanger's activity.

Therefore the objectives of this thesis are to:

1. Identify the minimal BRAF binding portion on NHE-1 C-terminus *in vitro.*
2. To evaluate the role of NHE-1 BRAF interaction in cell effector functions such as proliferation, migration and invasion.

In addition, a few studies have highlighted the potential role of NHE1 in genetic disorders. However very little is known about the role of stop codon polymorphisms in NHE1 and its functional implications. The final objective of this thesis is

3. To examine the role of stop codon polymorphisms in NHE1 function.

Chapter 2

Materials & Methods

1.1 Protein Expression and Purification (His-tagged constructs)

The Gateway cloning and expression vectors (pDONR201 and pDest14) were purchased from Gibco RBL (**Figures 3A and 3B)**. Restriction enzymes were obtained from New England Biolabs. Oligonucleotides were from by Integrated DNA Technologies. PWO polymerase was purchased from Roche. All other PCR reagents including buffer and dNTPs were purchased from Gibco BRL. Bio-Rad DC Protein Assay Kit was used for protein quantification. The QiaQuick PCR purification kit was used for PCR product purification.

The constructs His155, His117 and His77 **(Figure 3C)** were cloned into a destination vector pDest14 with a C-terminal 6X His tag using the Gateway cloning system. His155 was expressed in *Escherchia Coli (E. Coli)* BL21SI which was induced using 300 mM NaCl, while His117 and His77 constructs were expressed in *E. Coli* Rosetta DE3 which was induced with 1 mM Isopropylthio-D-Galactoside for 6 hours at 37°C. All proteins were purified at 4°C using a column packed with Nickel-NTA which specifically binds His-tagged proteins. The column was washed several times using wash buffer to remove weakly bound proteins and other contaminants. The proteins of interest were then eluted using elution buffer containing 250 mM Imidazole.

1.1.1 Generation of PCR products for cloning

*att*B- PCR products of His117 and His77 were amplified using the Polymerase Chain Reaction (PCR) to enable them to be transferred to the entry vector (pDONR201) and subsequently into the destination vector (pDest14). Specific forward and reverse primers were used to produce His117 and His77. The forward primers were designed to harbor the Shine-Dalgarno (SD) sequence and a kozak consensus sequence for optimal translation of the gene of interest. The reverse primers were designed to contain a 6X His tag to enable protein purification.

The template DNA containing the full length human NHE1 sequence with a triple Haemagglutinin tag (HA-tag) on the C-terminal end (pYN4+ plasmid) was initially denatured at 94°C for 3 minutes (252). The PCR reaction was set up for a final volume of 50 uL containing 200 µM deoxynucleoside triphosphates (dNTPs), 5 µL each of forward and reverse primers, 2.5 µL of pYN4+ plasmid (1 ng final DNA concentration), 2 mM $MgSO_4$, 5 µL of 10X H1F1 buffer, 25.5 µL of sterile double distilled water and 0.5 µL of Taq Polymerase. The PCR cycle was set up using the step down protocol (for 30 cycles) as follows:

Initial denaturation	94°C for 3 minutes
Denaturation	94°C for 1 minute
Annealing	69°C for 1 minute
Extension	72°C for 1 minute
Final extension	72°C for 7 minutes

5 µL of the PCR product was mixed with 6X DNA loading buffer and analyzed on a 1% agarose gel. The specific PCR product was visualized using ultraviolet light for the expected size of the product (487 bp for His117 and 358 bp for His77).

1.1.2 Entry and Expression clones

The Gateway Cloning Kit was used to generate the constructs for protein expression in *E. Coli.* First, an entry clone using pDONR201 was created using the BP reaction components, which included 1X Tris EDTA buffer (pH 8.0), BP reaction buffer, pDONR201 plasmid (15 ng final concentration), PCR product and 2 µL of the BP clonase enzyme. The reaction was set up on ice and then incubated at 25°C for 1.5 hours. 1 µL of Proteinase K (a serine protease) was added to the reaction mix and incubated at 37°C for 10 minutes to terminate the reaction. 1 µL of BP reaction was transformed into competent DH5α cells by electroporation. Cells were grown in LB media for 1 hour and then plated on LB plates containing 50 µg/mL Kanamycin was used to select the clones that have the PCR product (Gene of interest) successfully inserted into the pDONR201 vector backbone. To further confirm the insertion, the pDONR201His117 or pDONR201His77 was digested using BspE1 and PvuII restriction endonucleases. The reaction was set up as follows (final volume of 20 µL): 0.5 µl of RNase (final concentration 0.25 mg), 1µL of each restriction enzyme, 5 µL of DNA, 1.5 µL of 10X NEB buffer 3 and 11 µl of sterile double distilled water. The reaction mixture was incubated at 37°C for 1.5 hours and analyzed on 1% Agarose gel under ultraviolet light. Once the correct entry clones were confirmed the gene of interest was moved to the Destination vector (pDest14) using LR reaction.

The LR reaction was set up on ice for a final volume of 10 µL and contained the following: 2 µL of LR reaction buffer, 4 µL of 1XTE buffer (pH 8.0), 1 µL of entry clone (100-300 ng/20 µL), 300 ng/20 µL of pDest14 vector, 0.5 µL of Topoisomerase I and 2 µL of LR clonase enzyme mix. The reaction mix was thoroughly mixed and incubated for 1 hour at 25°C. 1 µL of Proteinase K was added to the reaction mix and incubated for 10 minutes at 37°C to terminate the reaction. To confirm the insertion of the gene of interest into the destination vector, 1 µL of LR reaction was transformed into competent DH5α cells by electroporation. The cells were grown in LB media for 1 hour and then spread onto LB plates containing 100 µg/mL ampicillin to specifically select the positive clones. The pDest14His117 or pDest14His77 was digested using BspE1 and PvuII restriction endonucleases as described previously.

1.1.3 Expression and Purification of Proteins

The constructs (pDest14His117 and pDest14His77) were transformed into RosettaDE3 *E.Coli* strain by electroporation. The cells were grown in LB media for about 1 hour and plated onto LB-Amp plates and incubated at 37°C overnight. An individual colony was chosen to inoculate 1L of LB Amp media the following day and the culture was grown at 37°C for 2.5 hours with agitation at 250 rpm until the optical density of the culture reaches 0.5 at 600 nm. The cells were induced with 0.5 mM Isopropyl ß-D-thiogalactopyranoside (IPTG) and allowed to grow for 6 hours at 37°C. The cultures were pelleted at 6000 rpm for 15 minutes at 4°C and the pellet was washed with wash buffer once. The pellet was thoroughly resuspended in 30 mLs of resuspension buffer containing Protease Inhibitors ((0.1 mM phenylmethylsulfonyl fluoride (PMSF) and 0.1% (v/v) protease inhibitor cocktail). The cells were lysed using a sonicator four

times at 70% amplitude on ice (each cycle was set for 45 seconds with a 0.5 second on and off pulse). The cell suspension was centrifuged at 12,000 rpm for 15 minutes at 4°C. The cleared cell lysate was applied to a column containing 2 mL of Ni-NTA beads that were previous equilibrated with loading buffer. The column was thoroughly washed using wash buffer and the bound His-tagged proteins were eluted using Elution buffer. The eluted proteins were concentrated using appropriate Amicon protein filters. The concentrated solutions were stored in 50 µL aliquots in -80°C freezer until further use.

1.1.4 Cell Culture, Transfection and Cell Lysis

HeLa Cells were cultured and maintained in Dulbecco's Modified Eagle's Medium supplemented with 10% Bovine Growth Serum and 1% penicillin streptomycin. HeLa cells were plated on 10 cm dishes and allowed to grow until they reach about 85% confluency. Once the cells reached the required confluency they were transfected with pEBGGST-BRAF plasmid using Lipofectamine 2000 reagent (Invitrogen) according to manufacturer's protocol. The media was changed the following day to allow the cells to recover. For each 10 cm dish, 21 µg of DNA was added to 500 µL of Opti-MEMI reduced serum medium (Invitrogen) and 38 µL of Lipofectamine 2000 reagent was added to 500 µL in Opti-MEMI medium. The solutions were incubated separately at room temperature for 5 minutes and then combined and further incubated for 20 minutes at room temperature to aid in the formation of DNA-Lipofectamine complexes. The entire 1 mL of the mixture was added dropwise to each plate containing serum free growth media and allowed to incubate at 37ºC for about 4 to 6 hours. 10% serum was added and cells were incubated at 37°C in 5% CO2 for 24 hours.

On the second day post-transfection cells were carefully scraped off with a sterile cell scraper with 10 mL lysis buffer (1X Tris Buffered Saline (TBS) with 1% Triton X-100 containing protease inhibitors (0.1 mM phenylmethylsulfonyl fluoride (PMSF) and 0.1% (v/v) protease inhibitor cocktail) per dish. The cell suspension was immediately frozen at -80°C. Cells were lysed by slowly thawing cells on ice and centrifuged at 14000 rpm at 4°C for 15 minutes to remove any cell debris.

1.1.5 HeLa Cell Overlay assay

50 µg each of His tagged proteins (His182, His155, His117, His77 and HisCHP) were loaded onto a 13% Sodium Dodecyl Sulfate-Polyacrylamide Gel Electrphoresis (SDS-PAGE) gel and resolved at 120 V. The proteins were transferred onto a nitrocellulose membrane at 300 mA for 1 hour at room temperature. The Nitrocellulose blot was first stained with ponceau S stain to visualize the loaded proteins. The blot was then thoroughly washed with double distilled water and then blocked with 10% (w/v) skimmed milk in 1X TBS for 5 hours at room temperature. 10 mL of fresh transfected HeLa cell lysate was added to the blot and incubated overnight at 4°C. The primary antibody was made up in 1% (w/v) skimmed milk in 1X TBS and was added (mouse monoclonal Anti-BRAF Antibody from Santa Cruz 1:4000) and incubated for about 16 hours at 4°C. The blot was thoroughly washed and incubated with secondary antibody made up in 1% (w/v) skimmed milk in 1X TBS (peroxidase conjugated goat anti-mouse antibody 1:3000) for 2 hours at room temperature. Protein bands were visualized using the Amersham Enhanced Chemiluminescence system.

Table 4: Primers used for Gateway cloning experiment

Primer Name	Primer Sequence
NHE 5'Gate634 (Forward)	5'GGGGACAAGTTTGTACAAAAAAGCAGGCTTAGAAGGAGATAGAACCATGatcctgaggaacaacttgcagaagac 3'
Gat750Hisstp (Reverse)	5'GGGGACCACTTTGTACAAGAAAGCTGGGTCCTATTAGTGATGGTGATGGTGATGctttgcaggatcccggctcaaccctaa 3'
Gat710Hisstp (Reverse)	5'GGGGACCACTTTGTACAAGAAAGCTGGGTCCTATTAGTGATGGTGATGGTGATGcggctcataggccagtgggtctgagcc 3'
NOTE:	NHE 5'Gate 634 was used as forward primer for the two constructs. Lower case: Fragment of human NHE1 C-terminal Upper case: attB1 (underlined) sequence, SD and kozak consensus sequence.

Figure 3A:

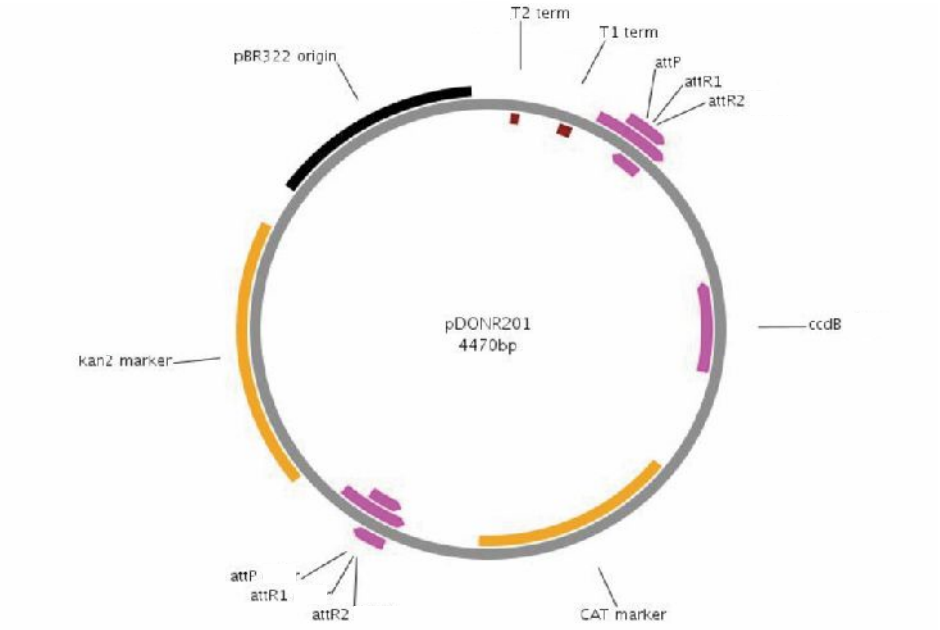

Figure 3A: Map of pDONR201 entry clone vector (PlasMapper).

pDONR201 was used to clone genes encoding His117 and His77. The vector contains two *att*P sites that aids in recombination (BP reaction) between the PCR product containing two *att*B sites. The vector also contains a Kanamycin resistance gene (Kan2 marker), Chloramphenicol Acetyltransferase gene (CAT marker), Transcription termination sequences (T1 and T2 Term) as well as ccdB gene present in the pDONR201 vector backbone that is lethal to most *E.Coli* strains. Once the PCR product is inserted into this specific region the ccdB gene is disrupted.

Figure 3B:

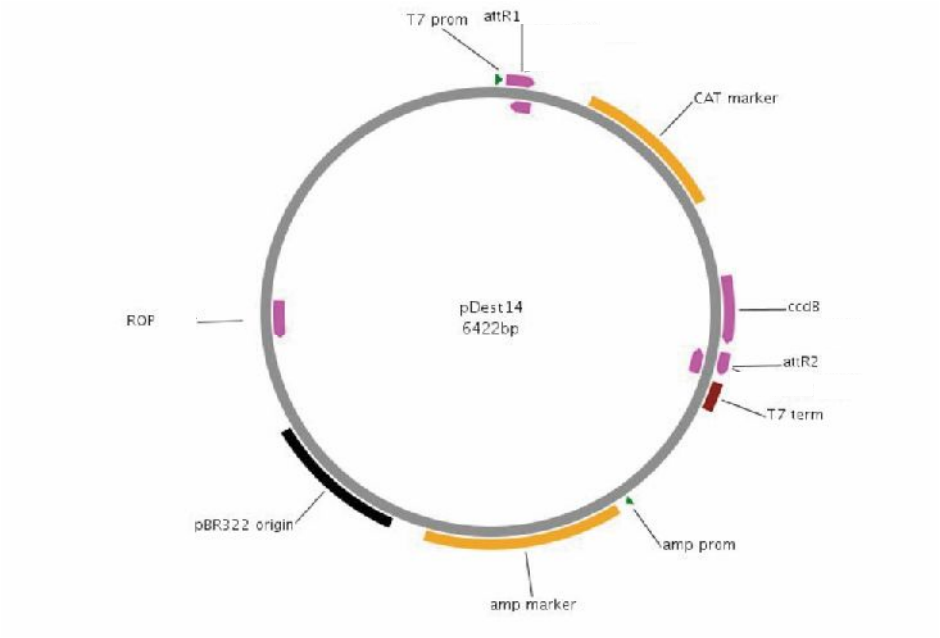

Figure 3B: Map of pDest14 vector (PlasMapper).

The pDest14 vector was used for subcloning cDNA that encodes for His117 and His77 proteins. The vector contains *att*R1 and R2 sites within which the cDNA of interest is inserted. The vector also contains T7 promoter (T7 Prom), Ampicillin resistance gene (Amp marker), Chloramphenicol Acetyltransferase gene (CAT marker) as well as a ccdB gene. The ccdB gene in its native form is lethal to most *E. Coli* but is disrupted upon insertion of cDNA of interest.

Figure 3C:

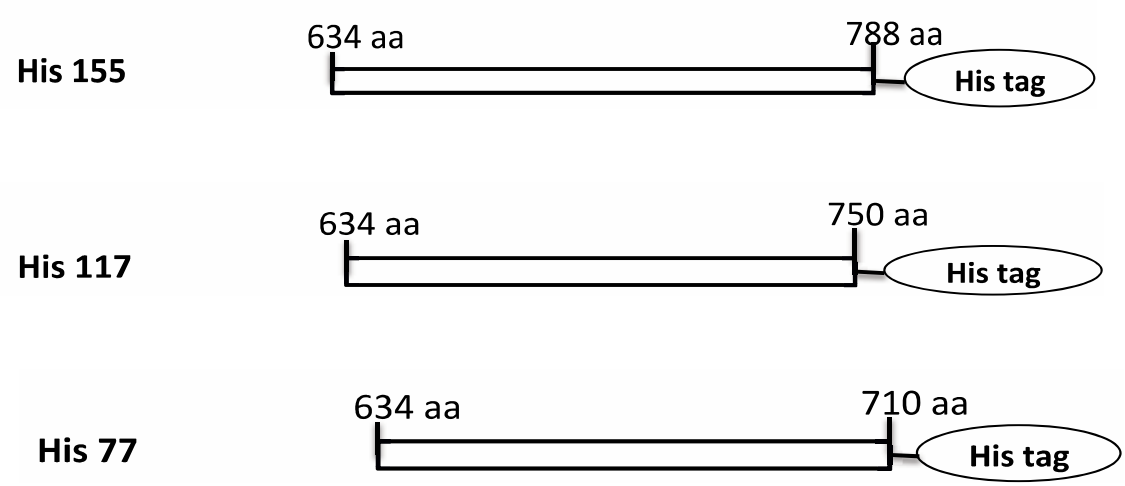

Figure 3C: Schematic representation of NHE1 C-terminal constructs.

The constructs were designed to express a portion of the NHE1 cytosolic domain with a 6X Histidine tag on the C-terminal end to aid in protein purification. His155 contains amino acids 634 to 788; His177 contains amino acids 634 to 750; His77 contains amino acids 634 to 710.

Table 5: Buffers used in His-tagged protein purification

Buffer Name	Composition	
Wash Buffer	Tris HCl pH 7.4	20 mM
Resuspension Buffer	Tris HCL Triton X-100 NaCl EDTA pH 7.4	20 mM 1% 200 mM 0.75 mM
Loading Buffer	NaCl Tris-HCl Imidazole Glycerol pH 8.0	300 mM 10 mM 20 mM 3%
Elution Buffer	NaCl Tris-HCl Imidazole Glycerol pH 8.0	300 mM 10 mM 250 mM 3%

1.2 Immunofluorescence study

1.2.1 Cell Culture:

HeLa Cells were cultured and maintained in Dulbecco's Modified Eagle's Medium supplemented with 10% Bovine Growth Serum and 1% penicillin streptomycin. AP1 cells stably expressing CFP-tagged NHE1 were cultured in α-Minimal Essential Medium (MEM) supplemented with 10% BGS, 1% penicillin streptomycin and 400 μg/mL of Geneticin (G418). Cells were maintained at 37°C with 5% CO_2. The cells were then plated onto coverslips and allowed to grow up to 60% confluency and one set of coverslips were cultured in the presence of media containing 10% serum while the other set was cultured in media containing 0.5% serum for 16 hours and processed as described below.

1.2.2 Immunofluorescence:

HeLa cells and AP1 cells were grown on coverslips were fixed with 4% paraformaldehyde for 15 minutes at room temperature and washed briefly with 1X Phosphate buffered saline (PBS). Cells were then permeabilized with 0.2% Triton X-100 for 10 minutes and then blocked with 5% goat serum (blocking buffer) for 1 hour and then incubated with the primary antibody in the same blocking buffer for a maximum of 2 hours at room temperature. Secondary antibody in blocking buffer was then added for 1.5 hours in the dark and excess antibody solution was removed by rinsing in 1X PBS thrice. The cells were stained with DAPI (300 nM) for 15 minutes in the dark. Cells were mounted on a slide with mounting media.

HeLa cells were stained with primary antibodies that included, mouse monoclonal anti-NHE1 antibody (BD Biosciences) and goat anti-mouse antibody conjugated to Alexa fluor 488 (Jackson Immunoresearch Labs). The two antibodies were used at a 1:200 dilution NHE1. Primary rabbit anti BRAF antibody (Abcam) and secondary goat anti-rabbit antibody conjugated to Alexa 594 (Jackson Immunoresearch Labs) were both used at a 1:200 dilution to detect BRAF. AP1 cells were stained with mouse monoclonal anti-BRAF antibody (Santa Cruz) and secondary donkey anti-mouse antibody conjugated to Cy3 (Jackson Immunoresearch Labs) to detect BRAF. The CFP-tag on the NHE1 stably expressed in AP1 cells aided in the visualization of NHE1.Images were obtained with a Leica SP5 confocal laser-scanning microscope with a 63X objective. Lasers and laser intensity were 405 Diode for DAPI, 10% detection at 435– 465 nm. Argon for Alexa 488 and CFP 20% at 510– 560 nM. HeNe for Alexa 594 and Cy3 30% at 580–680 nm. Images were obtained using Leica Application suite-AF software (Leica Microsystems).

1.3 Neonatal Rat Ventricular Cardiomyocyte Experiment

1.3.1 Isolation and Culturing of Neonatal Rat Ventricular Cardiomyocytes:

5 to 6 day old rats were decapitated and the heart was carefully removed and placed in 10 mL of Solution I. A small volume of Solution I was added to a petri dish and hearts were placed and cut within the dish. A scalpel was used to remove atria and leave behind the ventricles. The ventricles were then transferred to a fresh volume of Solution I and cut into very small pieces. The contents were carefully transferred to a jacketed Erlenmeyer flask with a stir bar. Once the pieces settled the supernatant was carefully removed without disturbing the ventricular pieces. 20

mL of Solution II was added to the Erlenmeyer flask which was stirred at a low speed for 20 minutes at 37°C. The supernatant was carefully transferred to a 50 mL A Corning tube containing 20 mL of Solution III was placed on ice. These steps were repeated three times and each time Solution II and Solution III was added at a volume of 15 mL, 8 mL and 7 mL (each) respectively. The myocyte solution was filtered using a cell strainer and combined and divided into two tubes of 40 mL solution each. The cardiomyocyte solution was centrifuged at 2000 rpm for 8 minutes. After carefully aspirating the supernatant, the pellet was resuspended in 16 mL of Solution IV in each tube. The solution was plated on 10 cm Primaria™ (Falcon) culture dishes for 30 minutes. The dish was removed and carefully washed with the existing solution. The following day the old media was carefully aspirated and 10 mL of fresh media was added.

On Day 3, cells were washed using warm PBS ABC thrice and 10 mL of Solution V was added. The media was changed everyday. By Day 5, a monolayer of spontaneously beating cells was obtained.

1.3.2 Cardiomyocyte Cell lysis

The cardiomyocyte monolayer was gently rinsed with ice-cold Phosphate Buffered Saline (PBS), and placed on ice. Proteins were extracted from cells using 10 mL of overlay lysis buffer (1X PBS containing 1% Triton X-100 and protease inhibitors (0.1 mM phenylmethylsulfonyl fluoride (PMSF) and 0.1% (v/v) protease inhibitor cocktail) per 10 cm dish. Cells were scraped on ice with disposable scraper and the cell suspension was transferred to 50 mL corning tube and immediately frozen at -80°C. The cell suspension was thawed slowly on ice and centrifuged at

14000 rpm at 4°C for 15 minutes to remove cell debris. The supernatant was used for subsequent experiments.

1.3.3 Cardiomyocyte overlay assay

50 ug of proteins (His tagged C-terminal construct 182 and His tagged Calcineurin Homologous protein) were separated on 13 % SDS-PAGE and transferred to nitrocellulose. 4X SDS PAGE loading dye (30% glycerol, 3% 2-mercaptoethanol, 6% SDS, 0.13 M Tris at pH 6.8, and 0.133 mg/mL bromophenol blue) was mixed with protein in a 1:5 ratio. The sample was then loaded on 13% SDS-PAGE gel, which ran for approximately 1.5 hours at 80 V until the dye front reached the end of the gel. Proteins on the SDS-PAGE gel were transferred to a nitrocellulose membrane using a current for 1 hour at 350 mA at room temperature. The nitrocellulose membrane was stained with 1X ponceau S stain to visualize equal loading of proteins. The blots were thoroughly washed to remove residual ponceau stain. The nitrocellulose membrane was blocked for 5 hours at room temperature with 10% (w/v) skimmed milk in 1X Tris Buffered Saline (TBS). The blots were then incubated with 10 mL of cardiomyocyte lysate in overlay lysis buffer overnight. The following day the blots were thoroughly washed in 1XTBS and incubated with antibody to specifically detect BRAF. Primary antibody dilutions were made in 1% (w/v) skimmed milk in 1X TBS and blots were incubated at 4°C overnight. Dilutions were as follows: mouse monoclonal anti-BRAF antibody (1:3000) and secondary antibody were peroxidase conjugated goat anti-mouse used at a dilution of 1:4000. Protein bands were visualized using the Amersham Enhanced Chemiluminescence system.

1.3.4 Proliferation assay for threonine 653 mutants

AP1 cells stably expressing either WT NHE1 or mutant NHE1 (T653A, T653D) were seeded in a 6-well dish at 10,000 cells/well and allowed to attach overnight. Cells were harvested at 0 hour, 24 hours and 48 hours using trypsin and the reaction was stopped with 1mL complete Alpha-MEM media. The cell suspension was pelleted at 3000 rpm for 5 minutes and the pellet was resuspended in 0.5 mL of media. 10 μL of trypan blue was added to an equal volume of cell suspension and the cells were counted manually using a hemocytometer with 10 μL of the suspension loaded. The proliferation data was normalized to the 0 hour time point of the cells expressing WT NHE1.

Table 6: Neonatal Rat Ventricular Myocyte Culture Solutions

SOLUTION	COMPOSITION
Solution I	1X HBSS (Hank's Buffered Salt Solution); 20 mM HEPES; 1% Penicillin/Streptomycin
Solution II	0.1% Collagenase; 1X HBSS; 20 mM HEPES; 1% Penicillin/Streptomycin
Solution III	20% Fetal Bovine Serum; 1X HBSS; 1% Penicillin/Streptomycin
Solution IV	DMEM F12 (Gibco) media $NaHCO_3$ 2.438 g/L BSA 10 g/L Fetuin (Sigma F-2379) 0.25 g/L Penicillin Streptomycin 1% Insulin 0.005 g/L Transferrin 0.005 g/L Selenium 10 ng/mL $CaCl_2$ 80 µg/L L-Ascorbic acid 20 µg/L MEM-Nonessential amino acids (Sigma A-4403) 1X Vitamin 100X (Gibco) 1X BSA-Palmitate 2 mL/L pH 7.3
BSA-Palmitate	BSA 1.2 g per 20 mL of water (in the dialysis bag) Dialyze Solution: 20 mL EDTA (0.5 M); 100 mL PBSA; 870 mL water; 10mL Palmitate (1.4 g in 10 mL of 95% Ethanol) Dialyzed overnight at 4°C.
Solution V	DMEM F12 (Gibco) media $NaHCO_3$ 2.438 g/L Fetal Bovine Serum 10% HEPES 30 mM Penicillin Streptomycin 1% Insulin 10 µg/mL Transferrin 10 µg/mL Linoleic acid 5 µg/mL BSA 2 mg/mL MEM-Nonessential amino acids (Sigma A-4403) 1X Vitamin 100X (Gibco) 1X Selenium 10 ng/mL Pyruvic acid 3 mM pH 7.3
PBS A PBS B PBS C	NaCl 10 g/L KCl 0.25 g/L NA2HPO.7H2O 2.71 g/L KH2PO4 0.25 g/L CaCL2.2H2O 1.32 g/L MgCl2.6H2O 2.13 g/L PBS ABC= 400 mL of PBS A+ 50 mL PBS B+ 50 mL PBS C

2.NHE1 regulation in Melanoma

2.1 Cell Culture:

Human melanoma cell lines, M19, IF6, FM82 and Mel2A were a generous gift from Dr. David Schrama (Dept. of Dermatology, Wuerzburg, Germany) and were cultured in Roswell Park Memorial Institute Medium (RPMI) 1640 medium with 10% fetal bovine serum and 1% penicillin streptomycin. All cells were maintained at 37°C with 5% CO2.

2.2 Cytotoxicity Assay:

Melanoma cells were cultured in a 96-well plate overnight at specific densities (M19 at 20,000 cells/well and IF6, FM82 and Mel2A at 12,000 cells/well). Cell cytotoxicity to increasing concentrations of various inhibitors or combination of inhibitors was assessed by spectrophotometric analysis of MTT ((3-(4,5-dimethylthiazol- 2-yl)-2,5-diphenyltetrazolium bromide) at 570 nm and background subtraction at 630 nm using the BioTek Synergy MX microplate reader (BioTek Instruments Inc.). Inhibitors or a combination of inhibitors was added to specific wells and incubated for 32 hours before assessing cytotoxicity. The cytotoxicity data was represented as % cell viability and was normalized to untreated controls. For cell viability assays, drug concentrations used were SB590885, 5 μM; PLX4720, 10 μM; HMA, 50 nM; EMD87580, 10 μM.

2.3 Cell Proliferation Assay:

Melanoma cells were seeded in a 6-well dish at 20,000 cells/well and allowed to attach overnight. Cells were either left untreated (controls) or treated with specific inhibitors. Cells were harvested at 0 hour, 24 hours and 48 hours using trypsin and the reaction was stopped with 1 mL complete RPMI 1640 media. The cell suspension was pelleted at 3000rpm for 5 minutes and the pellet was resuspended in 0.5 mL of media. 10 μL of trypan blue was added to an equal volume of cell suspension and the cells were counted manually using a hemocytometer with 10 μL of the suspension loaded. The proliferation data was normalized to the 0 hour time point for each condition. The concentration of drugs used were HMA, 50 nM; EMD87580, 10 μM.

2.4 Migration Assay

Melanoma cells were seeded in a 12 well dish in complete RPMI 1640 media and allowed to attach overnight. A scratch was made using a sterile 200 μL pipette tip and the wells were either left untreated (control) or treated with Mitomycin-C at 1 μg/mL only or in combination with various inhibitors. The rate of migration (percentage gap closure) was monitored over a period of 24 hours and 32 hours using Image Pro Plus software. The final concentrations of drugs used were SB590885, 5 μM; PLX4720, 10 μM; HMA, 50 nM; EMD87580, 10 μM.

The % Gap Closure was calculated using the following formula:

% Gap Closure = ((distance of gap at T 0 hour - distance of gap at T 24 hours or T 32 hours)/distance of gap at T 0 hour))* 100.

2.5 Invasion Assay:

Transwell inserts (8 μm pore size) were coated with Matrigel made at a 1:10 dilution with RPMI 1640 media containing 0.5% serum. Melanoma cells were seeded onto the coated inserts at 100,000 cells/insert in media containing 0.5% serum either in the absence of inhibitors (control) or presence of inhibitors. The lower chamber was supplemented with media contained 10% serum with or without inhibitors. The cells were allowed to invade over a period of 24 hours and the coated inserts were thoroughly cleaned and stained with Giemsa. Quantification of invasion was by manual measurement of numbers of cells traversing the membrane, and was imaged at 10X magnification with Image Pro Plus software using a Leica DM IRB microscope. A total of 5 fields per insert were used for quantification. The final concentrations of drugs used were SB590885, 5 μM; PLX4720, 10 μM; HMA, 50 nM; EMD87580, 10 μM.

2.6 Cell Lysis and Western Blot Analysis of proteins:

Melanoma cells were grown to confluency in 10 mm dishes, gently rinsed with ice-cold phosphate buffered saline (PBS), and placed on ice. Proteins were extracted from cells using 100 uL radioimmunoprecipitation assay (RIPA) lysis buffer containing 50 mM Tris, pH 7.4, 150 mM NaCl, 1% (v/v) Nonidet P-40, 0.25% (w/v) sodium deoxycholate, 0.1% (v/v) Triton X-100, 1 mM EGTA, protease inhibitors (0.1 mM phenylmethylsulfonyl fluoride (PMSF) and 0.1% (v/v) protease inhibitor cocktail) and incubated on ice for 2 minutes. Cells were scraped on ice with a disposable scraper and the cell suspension was transferred to eppendorf tube and centrifuged at

14000 rpm at 4°C for 5 minutes. The supernatant was removed and tested for protein expression using SDS-PAGE.

Proteins (50 – 100 μg) were separated on 10 % SDS-PAGE and transferred to nitrocellulose. 4X SDS PAGE loading dye (30% glycerol, 3% 2-mercaptoethanol, 6% SDS, 0.13 M Tris at pH 6.8, and 0.133 mg/mL bromophenol blue) was mixed with lysate in a 1:5 ratio. The sample was then loaded on 10% acrylamide SDS-PAGE gel, which ran for about 1 hour at 80 V and then at 130V until the dye front reached the end of the gel. Proteins on the SDS-PAGE gel were transferred to a nitrocellulose membrane for 1.5 hours at 350 mA at room temperature. Nitrocellulose membrane was blocked for an hour at room temperature with 10% (w/v) skimmed milk in 1X Tris Buffered Saline (TBS). Primary antibody dilutions were made in 1% (w/v) skimmed milk in 1X TBS and blots were incubated at 4C overnight. Dilutions were as follows: mouse monoclonal anti-BRAF antibody (1:3000); 1:1000 mouse monoclonal anti-vimentin antibody; 1:2000 mouse monoclonal anti-NHE1 antibody; 1:1000 rabbit anti-GAPDH antibody. Secondary antibodies were peroxidase conjugated goat anti-mouse or goat anti-rabbit used at a dilution of 1:4000. Protein bands were visualized using the Amersham Enhanced Chemiluminescence system. Quantification was done using Image J 1.48 software (National Institutes of Health, Bethesda, MD, USA).

2.7 Statistics:

All data are expressed as means ± SE and plotted with KaleidaGraph 4.1 (Synergy Software, US). Results for proliferation and migration assay are from four independent

experiments while results for invasion are from three independent experiments. Results for western blot analysis is from four independent experiments. Results for the proliferation of AP1 cells expressing WT NHE1 or mutant NHE1 (Thr653A or Thr653D) are from four independent experiments. Statistics was calculated using Wilcoxon Mann-Whitney rank sum test and a p-value less than 0.05 was considered to be statistically significant.

3. Stop Codon mutations in NHE1

3.1 Cell Culture

AP1 stable cell lines (Wild type, 735, 543, 449 and 321) were cultured in Alpha-MEM media supplemented with 10% Bovine Growth Serum, 1% penicillin streptomycin and G418 while the chinese hamster ovarian cells (CHO) were cultured in the absence of G418. All cells were maintained at 37°C with 5% CO_2.

3.2 Immunofluorescence

Cells were grown as described above on coverslips and fixed with 4% paraformaldehyde in PBS for 15 minutes at room temperature and washed twice with PBS for 10 minutes. Cells were permeabilized for 10 minutes with 0.2% Triton X-100 and then blocked with 5% goat serum (blocking buffer) for 45 minutes and then incubated with the primary antibody in the same blocking buffer for a maximum of 1 hour at room temperature. Secondary antibody in blocking buffer was added for 1 hour in the dark and this was removed by washing three times. The cells

were stained with DAPI (300 nM) for 10 minutes in the dark. Cells were mounted on a slide with appropriate mounting media. Primary antibodies that were used includes, monoclonal anti-HA antibody used at 1:200 dilution; mouse monoclonal anti-NHE1 antibody (BD Biosciences) at 1:200 dilution; rabbit polyclonal anti HA antibody (Santa Cruz) at a dilution of 1:200. Secondary antibodies included goat anti-mouse antibody conjugated to Alexa fluor 488 (Jackson Immunoresearch Labs) was used at 1:200; goat anti-rabbit antibody conjugated to Alexa 647-Atto 647 (from Rockland Inc.) was used at a 1:200 dilution. Images were obtained with a Leica SP5 confocal laser-scanning microscope with a 63X objective. Lasers and laser intensity were 405 Diode for DAPI, 10% detection at 435– 465 nm. Argon for Alexa 488, 20% at 510– 560 nM. HeNe for Alexa 647, 33% at 640– 700 nm. Images were obtained using Leica Application suite-AF software (Leica Microsystems) and processed identically.

Chapter 3

Results

1. NHE1-BRAF binding studies

1.1 Introduction

A novel study from the Fliegel laboratory demonstrated that several kinases and proteins from lysate obtained from rat heart extract was able to bind to the C-terminal tail of rabbit NHE1 (3). This study, for the first time, demonstrated that BRAF kinase could bind to the cytoplasmic domain of NHE1. In addition this study also demonstrated that BRAF kinase regulates NHE1 activity in certain cell types such as HeLa cells and melanoma cells (3).

BRAF is member of the Ras-RAF-MEK-ERK signal cascade and helps transduce mitogenic signals from the plasma membrane to the nucleus. This results in the activation of a repertoire of biological processes that promote cell proliferation and survival (179, 180). Studies have shown that the MAPK cascade plays a vital role in orchestrating various events in mammalian cardiogenesis (192). However whether this signaling cascade plays a direct or indirect role in cardiac morphogenesis remains unclear (192).

The role of NHE1 in the heart has been well studied. It is vital for contractile function and its role in pathology of various cardiac diseases including cardiac hypertrophy, ischemia reperfusion induced injury, arrhythmias and cell death are well documented (125, 126). Although previous studies have demonstrated the role of MAPK cascade in cardiac NHE1 regulation via ERK1/2, the interaction between BRAF kinase and NHE1 particularly in the heart is yet to be

explored (79-82). Neurohumoral factors have been shown to trigger cardiac hypertrophy via the signaling components of the MAPK cascade, especially RAF and ERK1/2 (253). Given that NHE1 regulation relies heavily on either phosphorylation by protein kinases and/or interactions with various protein partners, it is imperative to investigate the downstream signaling mechanism involving NHE1 and BRAF kinase particularly in the myocardium (166). In this report we investigate the interaction between NHE1 and BRAF and evaluate the role played by the target phosphorylation site located on NHE1 in cellular proliferation.

1.2 Results

1.2.1 Analysis of in-vitro association of BRAF and NHE1

In order to investigate the minimal BRAF binding portion located on the NHE1 C-terminal domain, His-tagged constructs of varying lengths of NHE1 C-terminus were cloned, expressed and purified as described in the methods section. First HeLa cells were transiently transfected to overexpress Glutathione-S-transferase (GST)-tagged BRAF. Lysates from HeLa cells were run on a gel and transferred to a blot to check for expression of GST-tagged BRAF. Results are presented in Figure 1.2.1A. In parallel, 50 μg His tagged proteins were resolved on a SDS PAGE gel, transferred to a blot and stained with ponceau S to detect the proteins. His182 was used as the positive control and HisCHP was used as the negative control based on previous results obtained in the Fliegel laboratory (3). An overlay assay was conducted with the HeLa cell lysate and the resulting blots were visualized for binding of BRAF to NHE1 C-terminal domain. Results are presented in Figure 1.2.1 B. The BRAF protein bound strongly to the positive control

(His182) while it did not bind to the negative control (HisCHP). BRAF did bind effectively to all three truncated NHE1 C-terminal proteins, His155, His117 and His77.

1.2.2 Analysis of in-vitro association of NHE1 with cardiomyocyte BRAF

Previous experiments from the Fliegel laboratory have demonstrated that BRAF from rat heart extracts strongly binds to an affinity column that consisted of NHE1 C-terminal tail (3). We wanted to investigate if this binding could occur using the overlay assay with a portion of NHE1 C-terminal tail (His182). Cardiomyocytes from Neonatal ventricular rat myocytes (NVRM) were isolated and cultured as described in the methods section. Lysates were prepared from the cardiomyocytes and used for the overlay experiment. His-tagged proteins, His182 and HisCHP were used as positive and negative controls respectively. The resulting blot was visualized for association between BRAF obtained from cardiomyocyte cells and NHE1 C-terminal domain. Results are presented in Figure 1.2.2. Endogenous BRAF from NVRM lysates strongly associated with His182 but did not bind to HisCHP.

1.2.3 Analysis of Co-localization between NHE1 and BRAF

Since the previous experiments demonstrated that BRAF binds to NHE1 C-terminal tail *in vitro* we wanted to investigate if BRAF co-localizes with NHE1 in intact cells. It is well known that BRAF is translocated from the cytoplasm to the membrane upon Ras activation in order to facilitate the well-orchestrated downstream events in the MAPK cascade (182). To examine the co-localization we used AP1 cells that stably expressed CFP tagged NHE1. BRAF

was visualized using an antibody specific for the BRAF protein. This experiment was conducted in cells supplemented with 10% serum or in serum-deprived conditions wherein the cells were supplemented with only 0.5% serum. Since AP1 cells are chinese hamster ovarian cell lines, we used HeLa cells to investigate the co-localization between the two proteins in human cells. The experiment was conducted in serum supplemented or serum deprived conditions as mentioned previously. Results are presented in Figure 1.2.3 A. In the presence of serum, BRAF co-localizes with NHE1 in both AP1 cells as well as HeLa cells as indicated by the yellow hue in the merge column. However, the withdrawal of serum resulted in a loss of this association.

Additional controls were tested to ensure that the signals bleed through between the CFP and Cy3 collection window. Results are presented in Figure 1.2.3 B &C. The CFP channel does not bleed into the Cy3 channel and likewise the Cy3 channel does not bleed into the CFP channel.

In addition to this, a time course experiment was conducted. HeLa cells were cultured in serum deprived conditions for 16 hours and then 10% serum was added to these cells at time 0 hour and the co-localization of the protein was monitored by immunofluorescence over a period of 2, 12 and 24 hours. Results are presented in Figure 1.2.3 D. It was observed that during the time course the co-localization pattern was reestablished in the previously serum starved cells.

1.2.4 Effect of mutating BRAF target phosphorylation site on cell proliferation

Experiments conducted in the Fliegel laboratory, using *in vivo* phosphorylation and mass spectrometry analysis, revealed that amino acid threonine 653 located on the NHE1 C-terminal tail, is the target for phosphorylation by BRAF kinase (193). In order to investigate the effect of this phosphorylation site in cell proliferation we conducted experiments in which the threonine residue was mutated to either a non-phosphorylatable amino acid (alanine) or a phosphomimetic (aspartic acid). AP1 cells were used for this experiment that stably expressed the native or mutated protein. Cells were cultured as described in methods and a cell count was done to evaluate cell proliferation at 0, 24 and 48 hours. Results are represented in Figure 1.2.4. AP1 cells stably expressing Wild Type (WT) protein or T653D mutant had similar proliferation rates while the cells expressing the T653A mutant showed a significant reduction in the rate of cell proliferation.

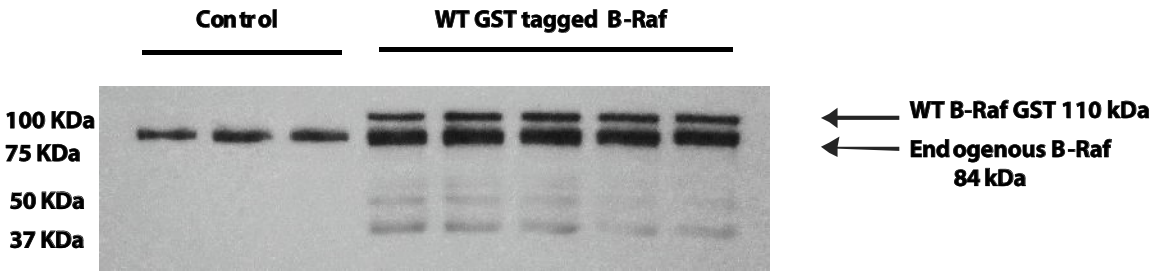

Figure 1.2.1 A: Overexpression of BRAF in HeLa Cells.

HeLa cells were transiently transfected with the plasmid pEBG BRAF-GST using lipofectamine. Cells were harvested 48 hours post-transfection and cell lysates were analyzed for GST-tagged BRAF expression using Anti-BRAF antibody. The first three lanes were lysates obtained from untransfected HeLa cells containing only endogenous BRAF protein. Lysates in lanes 4 to 8 express GST-tagged BRAF as well as endogenous BRAF.

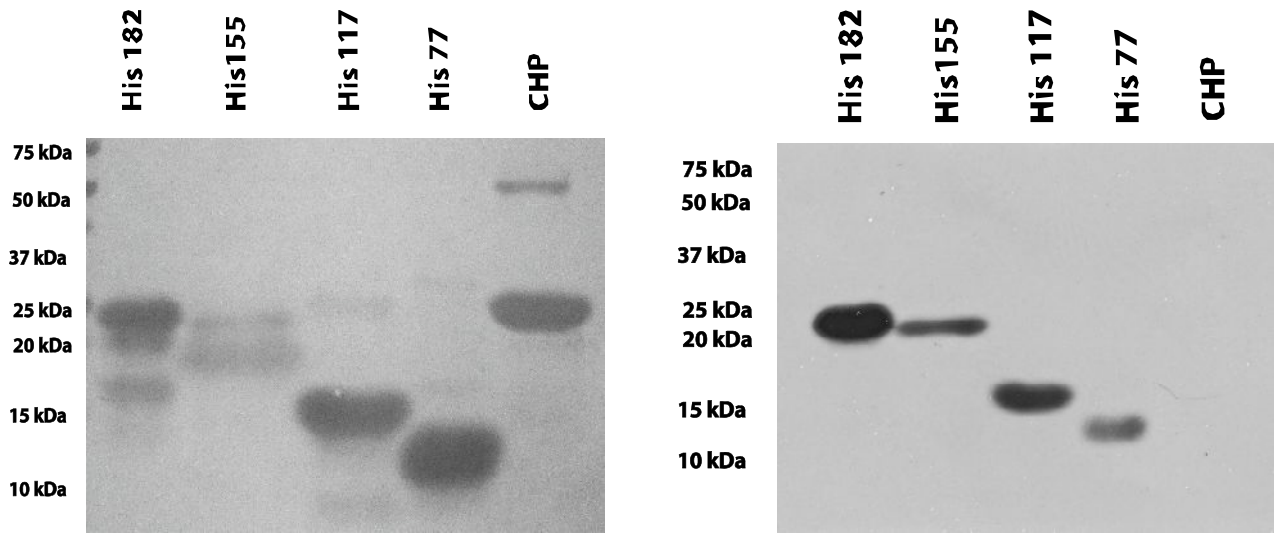

Figure 1.2.1 B: Overlay assay to analyze NHE1-BRAF interaction.

The panel on the left hand side is a ponceau S stain of the nitrocellulose blots containing the His-tagged proteins prior to overlay assay. The panel on the right is nitrocellulose membrane blotted for BRAF protein using Anti-BRAF antibody after incubating the blot with HeLa whole cell lysate containing enriched BRAF protein. This experiment was conducted 4 times to confirm results.

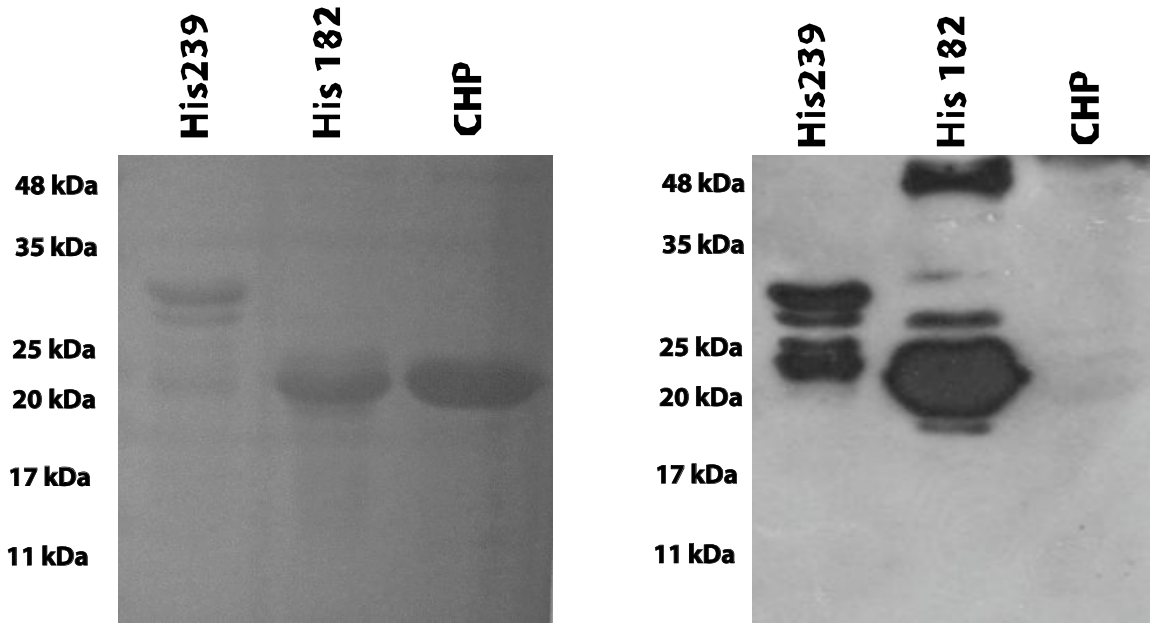

Figure 1.2.2: Overlay assay to analyze NHE1-BRAF interaction in cardiomyocyte cell lysate.

The panel on the left hand side is a ponceau S stain of the nitrocellulose membrane containing the His-tagged proteins prior to overlay assay. The panel on the right is the nitrocellulose membrane blotted for BRAF protein using anti-BRAF antibody. This membrane was visualized after incubating it with cell lysate obtained from cardiomyocytes expressing endogenous BRAF protein. n =4.

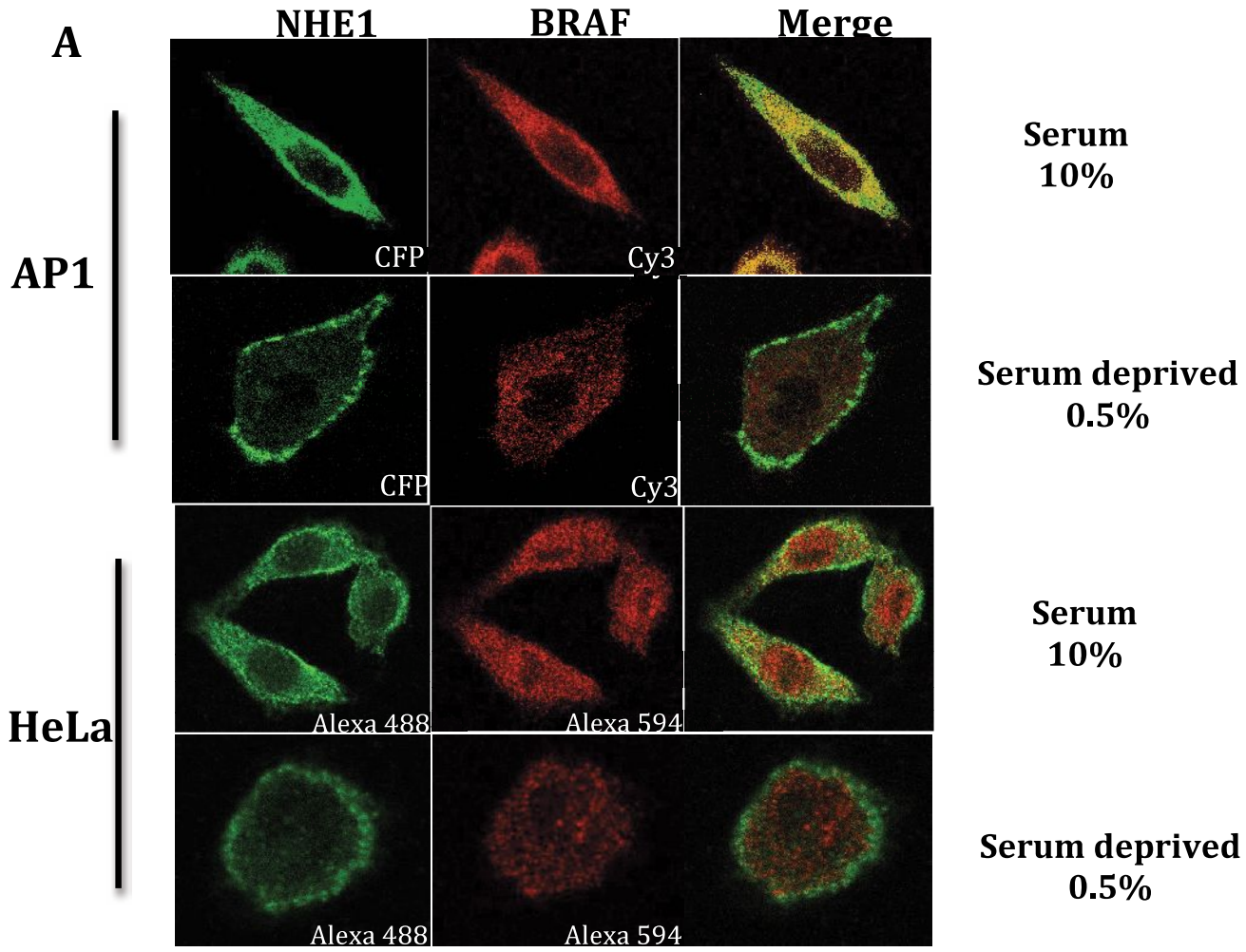

Figure 1.2.3 A: Co-localization of BRAF and NHE1 in AP1 cells and HeLa cells.

Upper panel: AP1 cells stably expressing CFP-tagged NHE1 were used in the presence or absence of serum. Cell imaging was performed as described previously.

Lower panel: HeLa cells were used in the presence or absence of serum. Specific antibodies against NHE1 and BRAF were used to look at co-localization between the two proteins. Cells were serum starved for 16 hours.

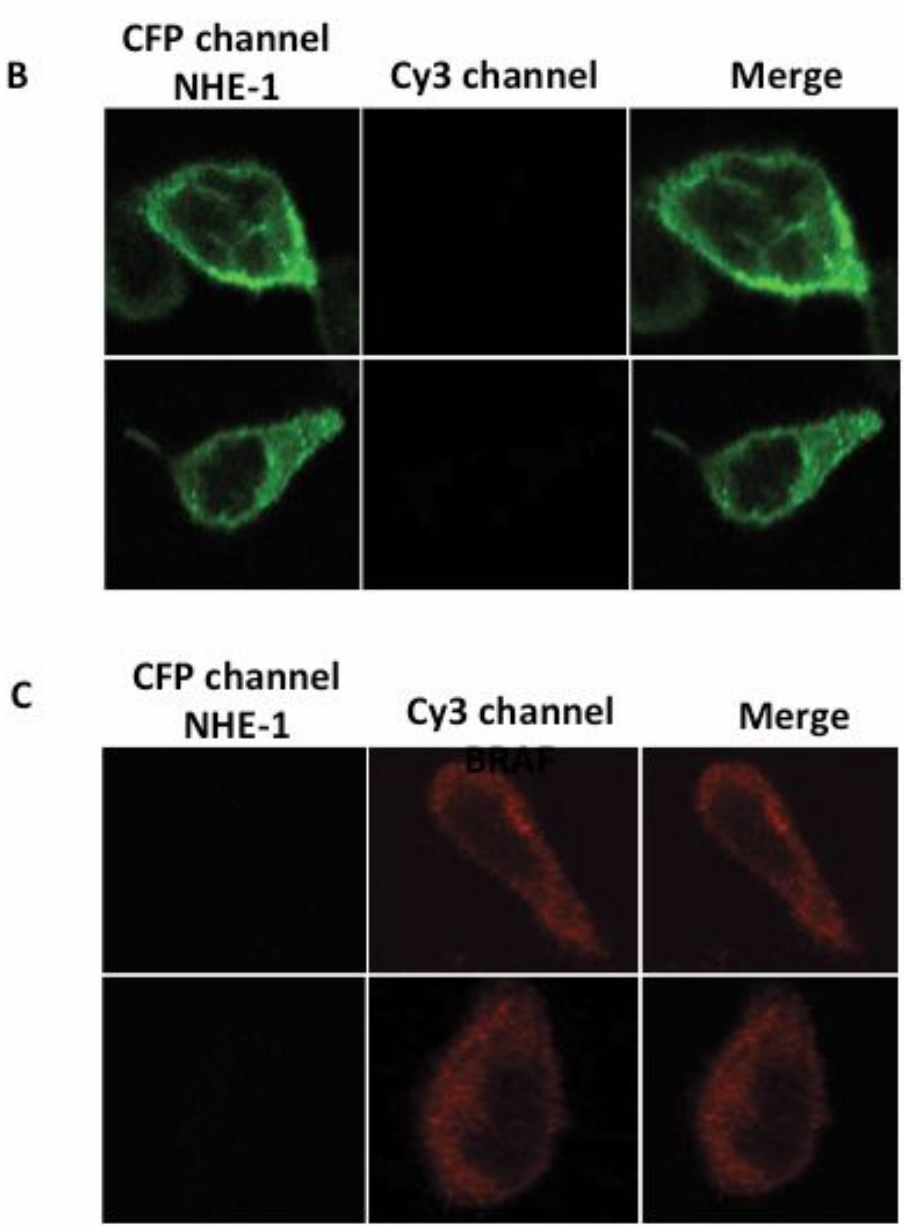

Figure 1.2.3 B&C: Controls for Co-Localization experiment.

Figure A CFP bleed through in Cy3 channel; AP1 cells stably expressing CFP tagged NHE1 were visualized in the Cy3 channel. Figure B AP1 cells stably expressing WTNHE1 were incubated with antibody specific for BRAF (red) and visualized in the CFP channel.

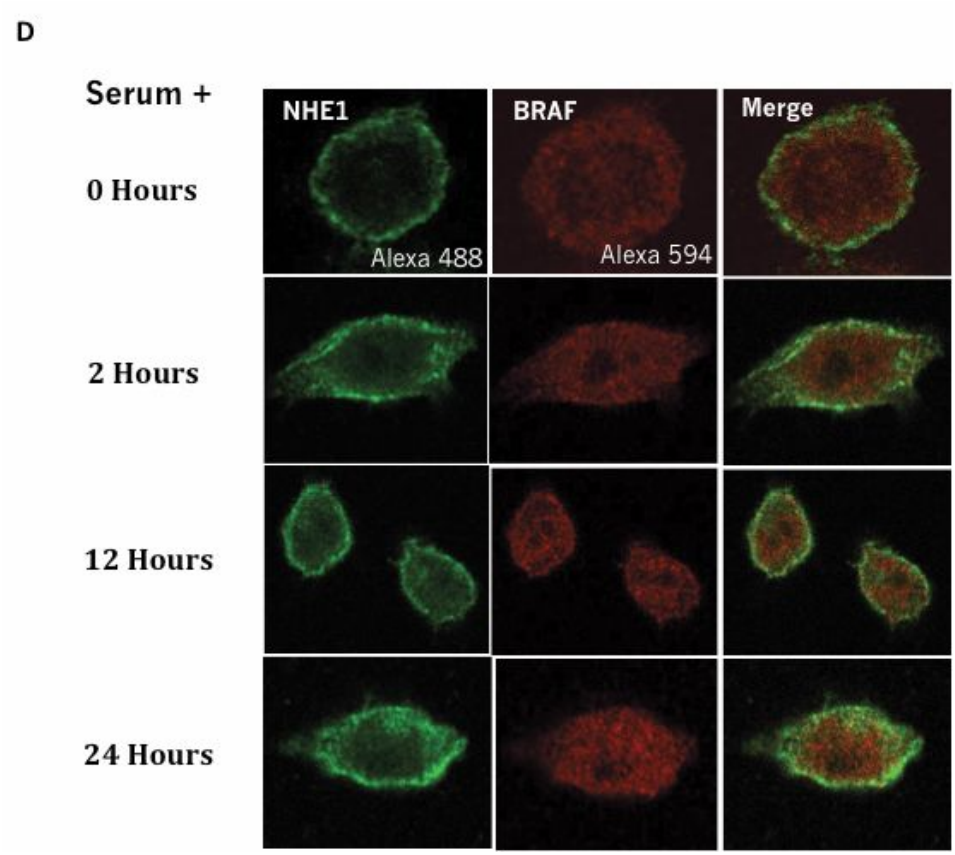

Figure 1.2.3 D: Time-course experiment for BRAF-NHE1 Co-localization.

Serum starvation experiments were performed in HeLa cells. Cells were supplemented with 0.5% serum (starvation) for 16 hours. Co-localization between NHE1 and BRAF was observed by adding back serum to the starved cells at various time points of 2, 12 and 24 hours respectively.

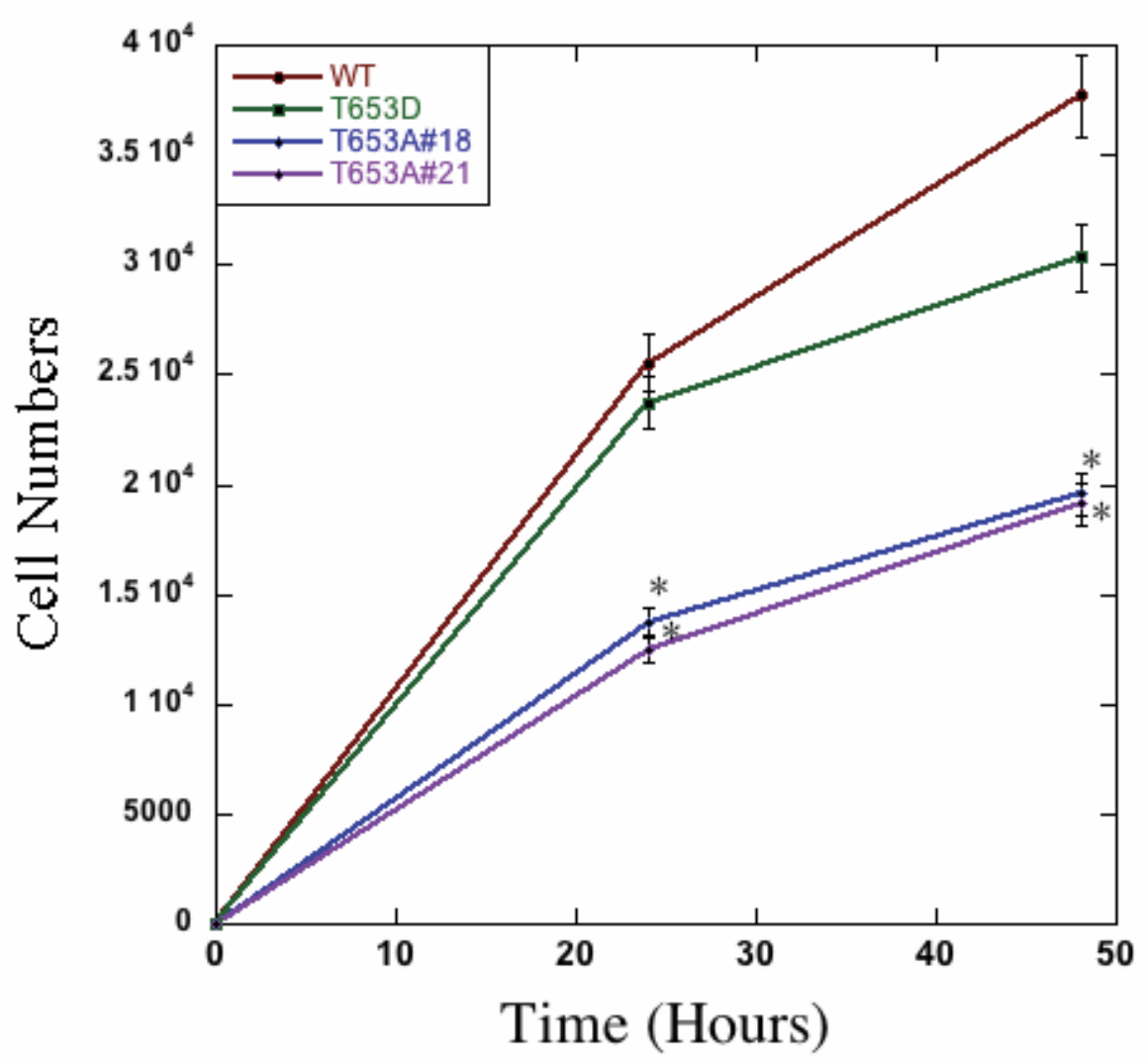

Figure 1.2.4: Cell proliferation of Threonine 653 mutants

Cell proliferation was assessed in AP1 cells stably expressing WTNHE1/ T653D/ T653A. Data was collected at 24 hours and 48 hours respectively. Results are the mean of ± SE of 4 experiments. * p Value <0.0001

2. NHE1 regulation in Melanoma

2.1 Introduction

Aberrant MAPK signaling is a classic feature of melanoma development and progression, which mostly includes activating mutations in BRAF (199). Genotype studies conducted on melanoma samples have revealed that 40-50% of melanomas contain BRAF mutations and 70-90% of these mutations are caused by a missense mutation that changes a valine amino acid to a glutamic acid amino acid at position 600 (V600E). This mutation destabilizes the auto-inhibitory interaction between the glycine rich loop and activation segment and causes the kinase to be constitutively activated. Mutant BRAF then binds to its downstream signaling target, MEK and thereby trigger aberrant or increased MAPK activity (179). A smaller subset of melanomas harbor NRAS mutations that are present in about 15 - 20% of the cases, which causes RAS to be in a GTP-bound active state (179,198).

These malignant melanoma cells rely on glycolytic metabolism even under aerobic conditions, which results in a rapid accumulation of protons within the intracellular environment. In turn the cells secrete the intracellular protons causing a reversal of the pH gradient wherein there is an acidification of the extracellular environment (194). This ability seems to be directly linked to tumor aggressiveness (158). This reversed pH gradient lays the foundation for a complex multistep metastatic cascade, which involves increased cell proliferation, loss of cell-cell contacts, increased cell motility, migration, invasion and evasion of apoptosis (195, 196). Although several mechanisms contribute to development and progression of carcinogenesis,

activated NHE1 plays a central role in the development and maintenance of the reversed pH gradient (158).

As described previously, the Fliegel laboratory has demonstrated that melanoma cells with BRAF V600E mutation had a higher resting intracellular pH, which was directly correlated to increased NHE1 activity when compared to cells with WT BRAF (3). In addition to this it was observed that BRAF inhibition with either chemical inhibitors or Si-RNA knockdown led to a decrease in NHE1 activity (3). Given that BRAF not only interacts with NHE1 but also somehow modulates the exchanger's activity we wanted to investigate the effects of BRAF inhibition and NHE1 inhibition in various metastatic processes in melanoma cells which include proliferation, migration and invasion. We used 4 different melanoma cell lines for this purpose as illustrated in Figure 2.1. M19 cells endogenously express WTBRAF while IF6, FM82 and Mel2A express mutant BRAF (V600E).

2.2 Results

2.2.1 Effect of inhibitors on melanoma cell toxicity and viability

To investigate the role of NHE1 and BRAF in melanoma cell effector functions, inhibitors of NHE1 or BRAF were used in these experiments. We initially determined the optimal concentration of the inhibitors, either alone or in combination, to evaluate the role of the exchanger and the kinase in the melanoma cells. We investigated the cytotoxic effect of HMA (NHE1 inhibitor) at varying concentrations of 1 nM to 10 μM on M19 cells as well as the effect

of 1 μM, 5 μM and 10 μM SB590885 (WT BRAF inhibitor). Cytotoxicity was evaluated after 24 hours post treatment and cell viability was evaluated 32 hours post treatment. There was no change in cell viability up to 1 μM of HMA and SB590885 up to 10 μM as observed in Figure 2.2.1 A & B. Cell viability was assessed with a combination of the two drugs (HMA: 50 nM and SB590885 5 μM) against untreated controls. M19 cells demonstrated about 80% cell viability (Figure 2.2.1 C).

Similar experiments were conducted on the remaining melanoma cells lines (IF6, FM82 and Mel2A) as described previously. However for cell toxicity only the NHE1 inhibitor was tested for these cell lines and not mutant BRAF inhibitor (PLX4720) since previous experiments conducted in the Fliegel laboratory demonstrated that these cell lines did not exhibit toxicity in the presence of 10 μM PLX4720 (3). Results are presented in Figures 2.2.1 D to I. Both IF6 and FM82 did not show a change in cell viability up to 1 μM of HMA while Mel2A cell line did not survive at this concentration. When the cell lines were exposed to a combination of HMA and PLX4720 at 50 nM and 10 μM respectively, IF6 and FM82 demonstrated ~80% cell viability while Mel2A demonstrated ~75% cell viability.

2.2.2 Effect of inhibitors on melanoma cell proliferation

First we wanted to investigate if the cells that harbor mutant BRAF (IF6, FM82 and Mel2A) proliferate faster than cells that harbor WT BRAF (M19). Cells were cultured as described earlier and the rate of cell proliferation was analyzed at 0, 24 and 48 hours respectively for all the four cell lines. Results are presented in Figure 2.2.2 A. It was observed that cell lines

carrying mutant BRAF did indeed proliferate faster than the cell lines that did not, with Mel2A showing the highest rate of cell proliferation followed by FM82 cells, which was followed by IF6 cells. M19 cells showed the slowest rate of proliferation.

Next we wanted to investigate the effect of NHE1 inhibition on the 4 cell lines. The cells were treated either with 10 μM EMD87580 or 50 nM HMA and the rate of cell proliferation was assessed after 24 hours and 48 hours. Results are presented in Figures 2.2.2 B to E. Interestingly, NHE1 inhibition did not have an effect on the rate of cell proliferation in any of the four cell lines irrespective of the presence or absence of mutant BRAF.

2.2.3 Effect of inhibitors on melanoma cell migration

Migration is a fundamental process that drives various cellular processes during development, wound healing and metastasis. Increased NHE1 activity has been shown to contribute to increased cell proliferation in cancer cells (194, 200-202). In order to investigate the role of NHE1 and BRAF interaction in the migration of melanoma cells, we performed a scratch assay. The cells were treated either with NHE1 inhibitor or BRAF inhibitor or a combination of both. In addition to this, since these cells showed different rates of cell proliferation, they were treated with Mitomycin C (1 μg/mL). Mitomycin C is an antitumor antibiotic, which prevents cell division (254). This drug was used to ensure that the migration rates among the melanoma cell lines was not influenced by differences in the rate of cell proliferation. The images were obtained over a period of 24 hours and 32 hours. M19 cells were treated with SB590885, which specifically inhibits WT BRAF while the other three cell lines

were treated with PLX4720 since it targets mutant BRAF (V600E). Results are presented in Figures 2.2.3 A-D.

M19 cells showed only ~55% gap closure at 32 hours. Addition of Mitomycin C caused a small but significant effect on the cell's ability to migrate when compared to untreated controls. Cells treated with either the NHE1 inhibitor or WT BRAF inhibitor showed a small but significant effect on the migration of M19. Although EMD87580 + SB590885 treatment did not cause a change in the migration when compared to SB590885 only treated cells, HMA+SB590885 caused a significant reduction in migration rates (Figure 2.2.3 A).

FM82 and IF6 showed ~90 to 95% gap closure at 32 hours. Addition of Mitomycin C did not cause a significant effect in the cells' ability to migrate when compared to untreated controls. However addition of NHE1 inhibitors (EMD87580/HMA) or mutant BRAF inhibitor (PLX4720) caused a significant reduction in migration rates. FM82 displayed about 25-30% migration in the presence of inhibitors (Figure 2.2.3 B). IF6 displayed about 50% migration when compared to untreated controls (Figure 2.2.3 C). Treatment with a combination of HMA+PLX4720 led to a small but significant reduction in migration rates when compared to PLX4720 only treated cells in both FM82 as well as IF6 (Figures 2.2.3 B & C respectively).

Migration rates of untreated Mel2A cells were the highest when compared to other cell lines with complete gap closure at 32 hours. Addition of Mitomycin C did not cause a significant effect in the cell's ability to migrate. However, addition of either NHE1 inhibitor or mutant BRAF inhibitor caused a significant reduction in the cell's ability to migrate (~50% with NHE1

inhibition and ~40% with mutant BRAF inhibition). As observed with FM82 and IF6 cell lines, Mel2A also displayed a small but significant reduction in the migration rate when treated with a combination of HMA+PLX4720 (Figure 2.2.3 D).

2.2.4 Effect of inhibitors on melanoma cell invasion

Another key feature of actively metastasizing cells is their ability to form invadopodial structures. These are specialized membrane protrusions that are vital for the cancerous cells to target secondary sites (203-205). Since there is growing evidence that NHE1 is important in the formation of invadopodial structures, we wanted to investigate the role of the NHE1 protein and BRAF kinase in this process (158). We conducted an elegant method to look at the invasive potential of the melanoma cell lines using Boyden chamber inserts as described in methods. Cells were harvested and plated in the inserts that were coated with matrigel. Invasion was monitored for each cell line in the presence or absence of specific inhibitors after 24 hours. Results are presented in Figures 2.2.4 A-C.

FM82 cell lines showed the highest invasive potential with almost 350 cells invading per field (Figure 2.2.4 B) followed by Mel2A cells that showed about 250 cells invading per field in untreated controls (Figure 2.2.4 C). NHE1 inhibition or BRAF inhibition caused a significant reduction in the invasive potential of both these melanoma cell lines. It appears that the invasive potential of these cell lines is almost lost in the presence of inhibitors. Untreated M19 cells were barely invasive with only about 50 cells invading per field and the addition of NHE1 or BRAF

inhibitors did not affect the invasive potential of this cell line (Figure 2.2.4 A). Interestingly the IF6 cell lines (untreated control cells) did not invade the matrigel layer (data not shown).

2.2.5 NHE1, BRAF and Vimentin expression in Melanoma cell lines

Next we wanted to determine if the expression levels of various proteins differed among the cell line that expressed WT BRAF versus those cell lines that expressed mutant BRAF. A simple western blot was carried out to evaluate the expression of NHE1 protein, BRAF kinase and vimentin protein across the 4 cell lines. Results are presented in Figures 2.2.5 A & B.

FM82 cells and Mel2A cells expressed mature NHE1 protein while the glycosylated form is absent in both M19 and IF6 cells. BRAF expression remains fairly unchanged across all the four cell lines (Figure 2.2.5 A). However, the relative expression of vimentin varies across the 4 cell lines. Mel2A shows the highest levels of the protein followed by M19 cell lines. IF6 and FM82 have very low levels of vimentin (Figure 2.2.5 B).

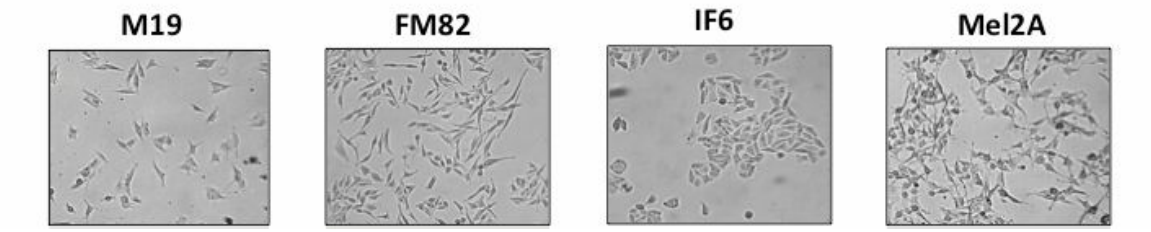

Figure 2.1: **Microscopic images of human melanoma cell lines**.

M19, FM82, IF6 and Mel2A cells were cultured in RPMI 1640 medium supplemented with 10% FBS and 1% penicillin streptomycin. Images were taken using a 10X objective in a bright field setting.

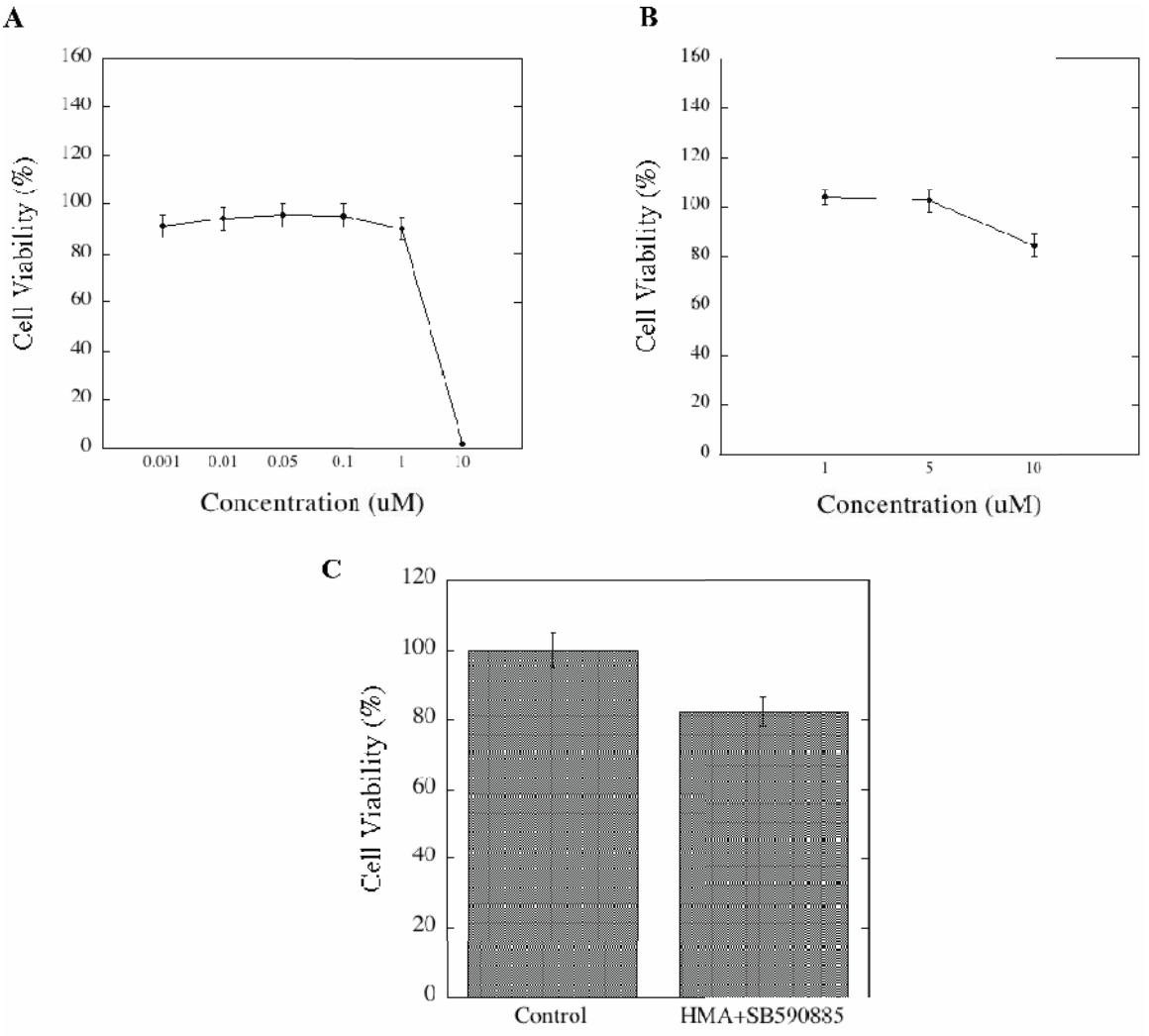

Figure 2.2.1 A, B &C: **Cytotoxicity and Cell Viability in M19 Melanoma Cells.**

A&B: Varying concentrations of NHE1 inhibitor (n=3) and BRAF inhibitor (n=5) were tested using the MTT assay as described in methods. Results are the mean of ± SE of 3 and 5 experiments respectively. HMA, 0.001 to 10 μM; SB590885, 1, 5 and 10 μM.

C: Cell viability was assessed in the presence of a combination of NHE1 and BRAF inhibitor as indicated. HMA, 50 nM: PLX4720, 10 μM. Results are the mean of ± SE of 4 experiments.

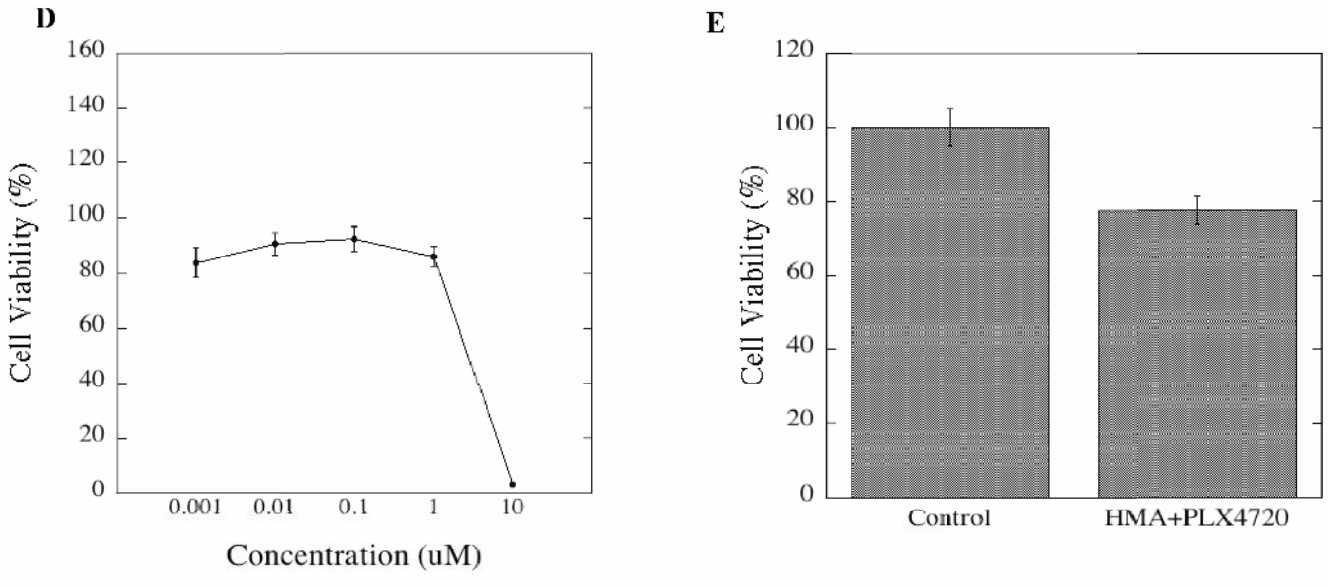

Figure 2.2.1 D&E: **Cytotoxicity and Cell Viability in IF6 Melanoma Cells.**

D: Varying concentrations of NHE1 inhibitor on cell viability was examined using MTT as described in methods. E: Cell viability was assessed in the presence of a combination of NHE1 and BRAF inhibitor as indicated. HMA, 50 nM; PLX4720, 10 μM. Results are the mean of ± SE of 4 experiments.

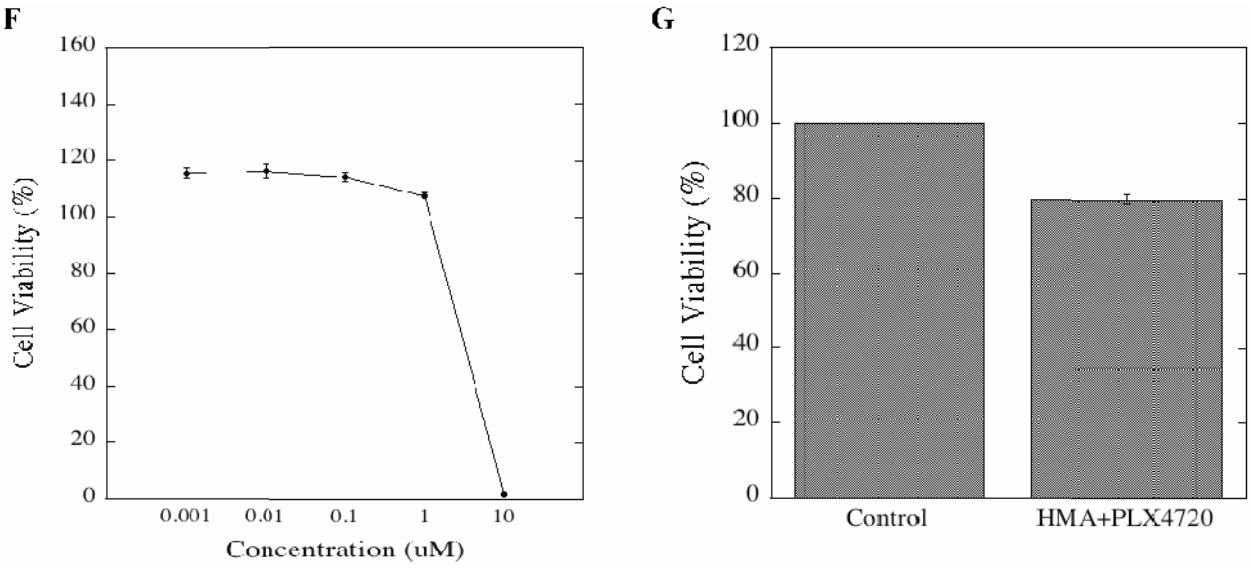

Figure 2.2.1 F&G: **Cytotoxicity and Cell Viability in FM82 Melanoma Cells.**

F: Varying concentrations of NHE1 inhibitor on cell viability was examined using MTT as described in methods. HMA, 0.001 to 10 μM. G: Cell viability was assessed in the presence of a combination of NHE1 and BRAF inhibitor as indicated. HMA, 50 nM; PLX4720, 10 μM. Results are the mean of ± SE of 4 experiments.

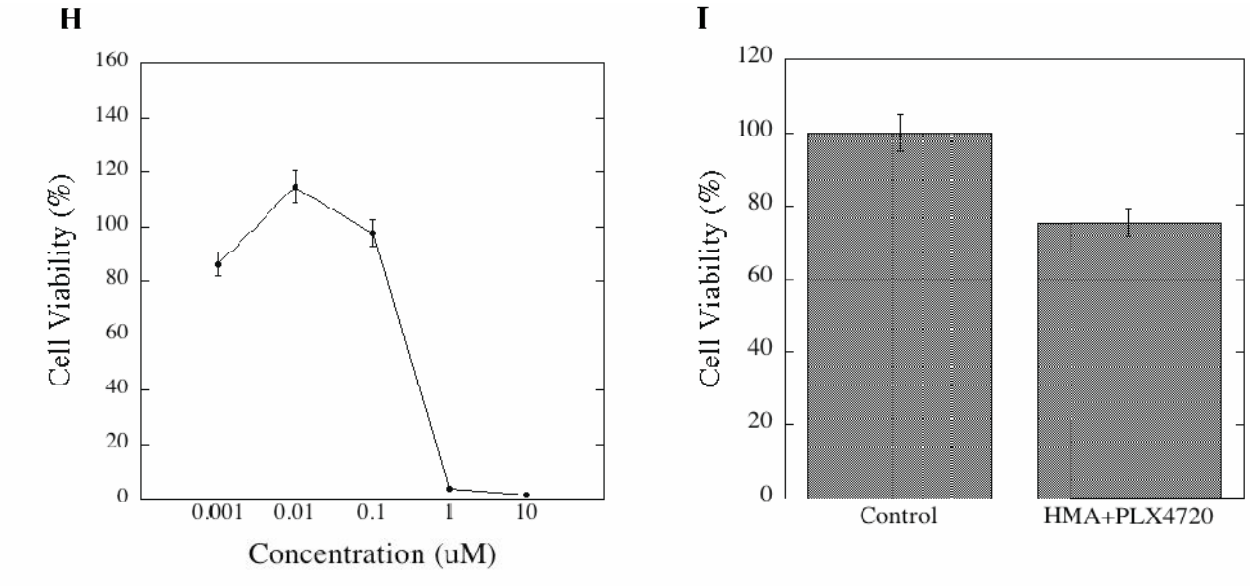

Figure 2.2.1 H&I: **Cytotoxicity and Cell Viability in Mel2A Melanoma Cells.**

H: Varying concentrations of NHE1 inhibitor on cell viability was examined using MTT as described in methods. HMA, 0.001 to 10 μM. I: Cell viability was assessed in the presence of a combination of NHE1 and BRAF inhibitor as indicated. HMA, 50 nM; PLX4720, 10 μM. Results are the mean of ± SE of 4 experiments.

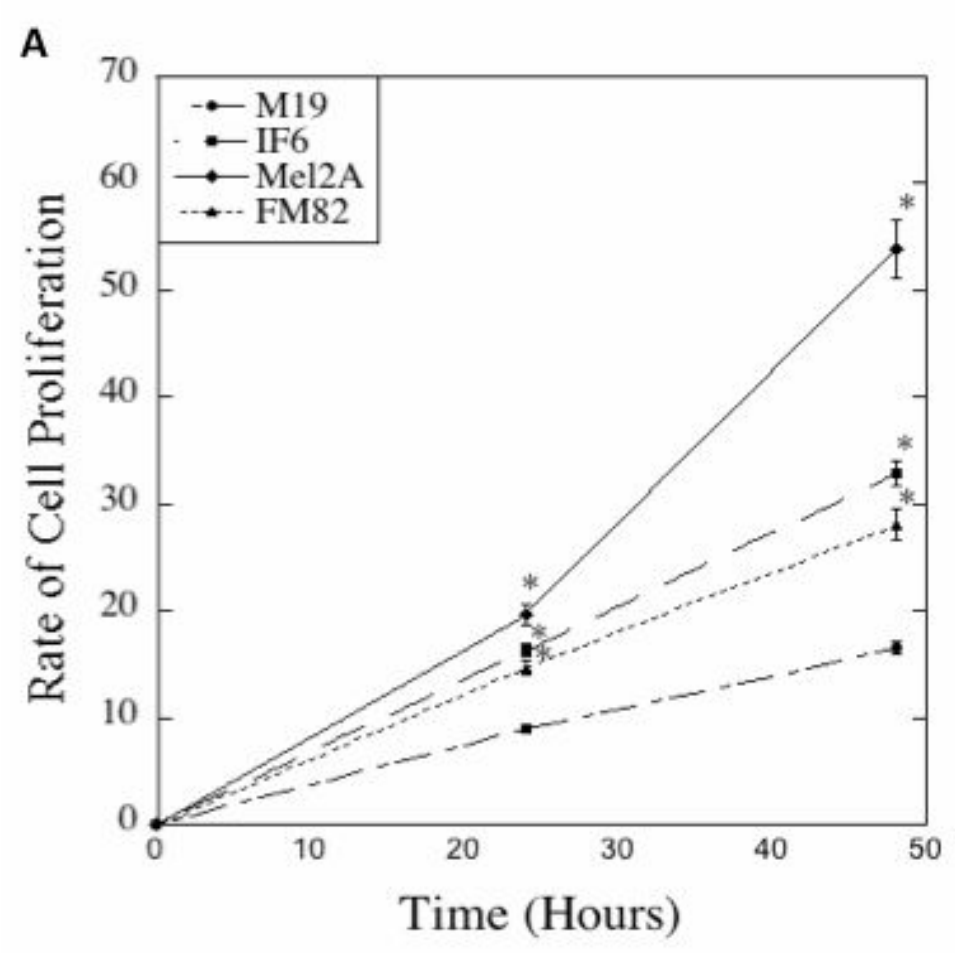

Figure 2.2.2 A: Rate of cell proliferation in Melanoma Cells.

M19, IF6, FM82 and Mel2A were cultured as described in methods and the cell proliferation was assessed at 24 hours and 48 hours. Mel2A, IF6 and FM82 showed a significant increase in proliferation compared to M19 cells. Results are the mean of ± SE of 4 experiments;

* p value <0.0001.

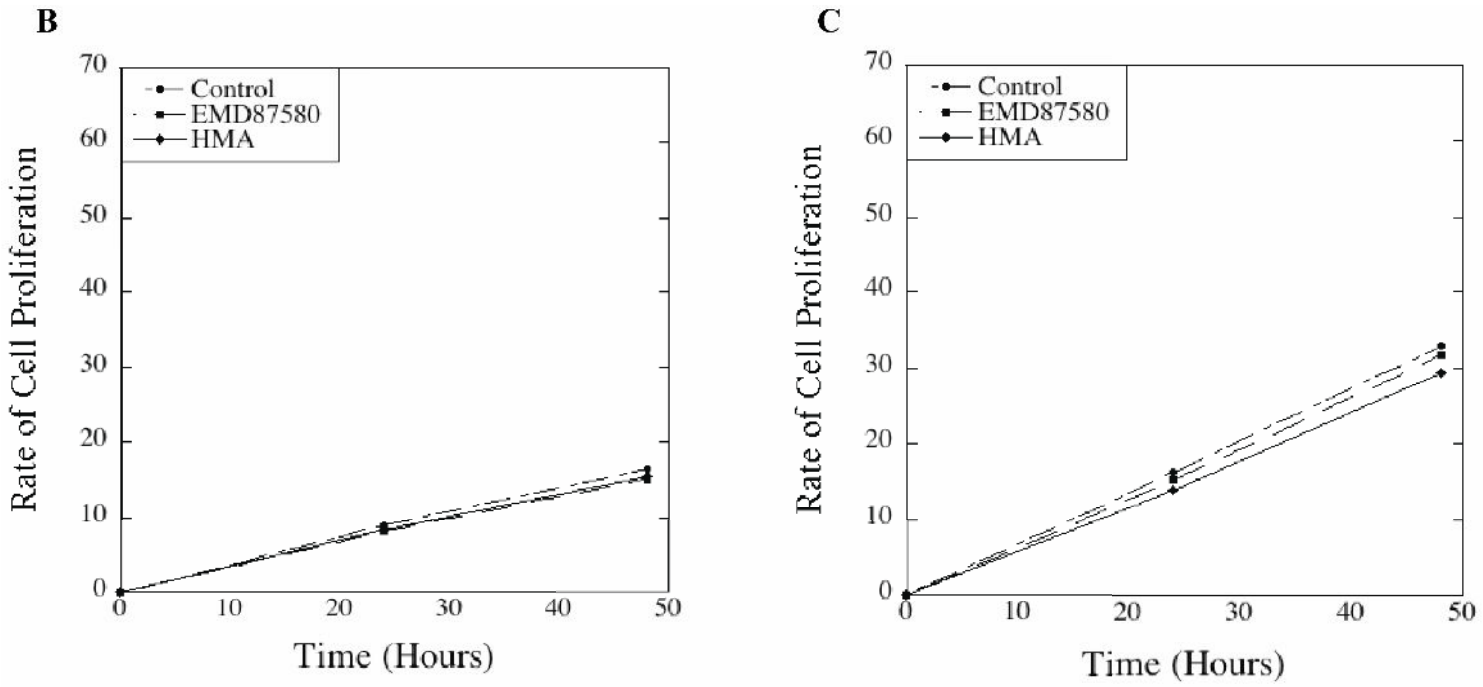

Figure 2.2.2 B & C: Rate of cell proliferation in Melanoma Cells.

M19 and IF6 were cultured as described in methods and the cell proliferation was assessed at 24 hours and 48 hours in the presence of two NHE1 inhibitors, EMD87580 and HMA at 10 μM and 50 nM respectively. Results are the mean of ± SE of 4 experiments.

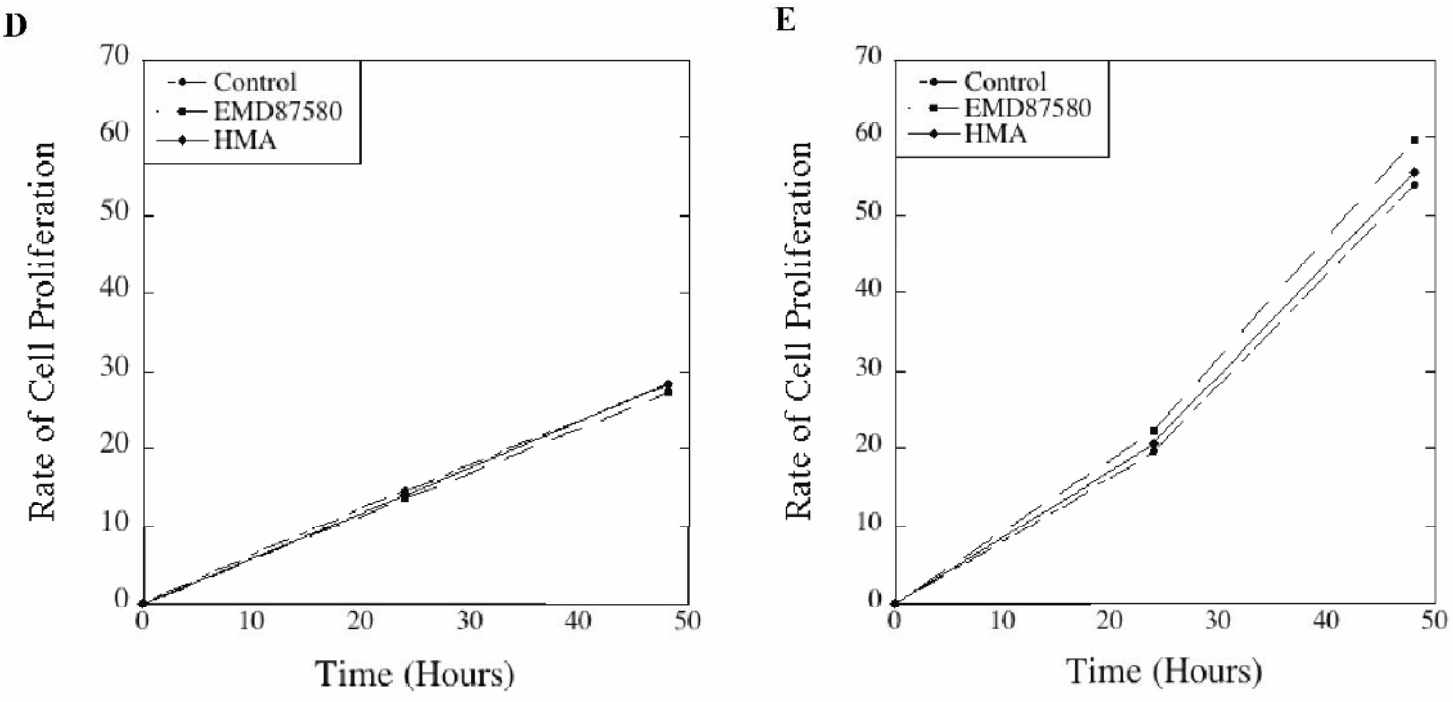

Figure 2.2.2 D & E: Rate of cell proliferation in Melanoma Cells.

FM82 and Mel2A were cultured as described in methods and the cell proliferation was assessed at 24 hours and 48 hours in the presence of two NHE1 inhibitors, EMD87580 and HMA at 10 μM and 50 nM respectively. Results are the mean of ± SE of 4 experiments.

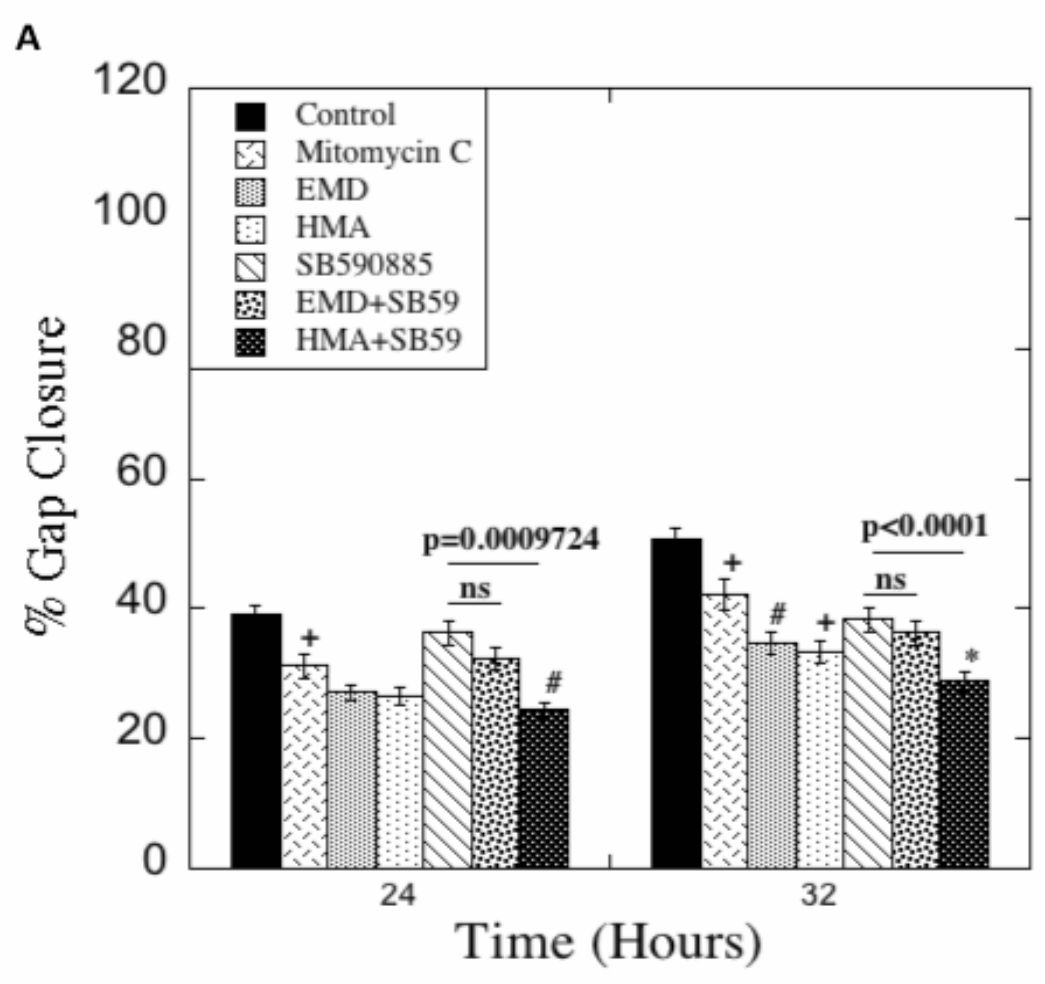

Figure 2.2.3 A: Rate of cell migration in M19 Melanoma Cells.

M19 cells were cultured as described in methods and the cell migration was assessed at 24 hours and 32 hours in the presence of either NHE1 inhibitors or BRAF inhibitors or both. The concentration of compounds used are as follows: Mitomycin C 1 μg/mL, EMD87580 10 μM, HMA 50nM, SB590885 5 μM. Results are the mean of ± SE of 4 experiments. * p Value <0.0001, # p Value <0.001, + p Value <0.05

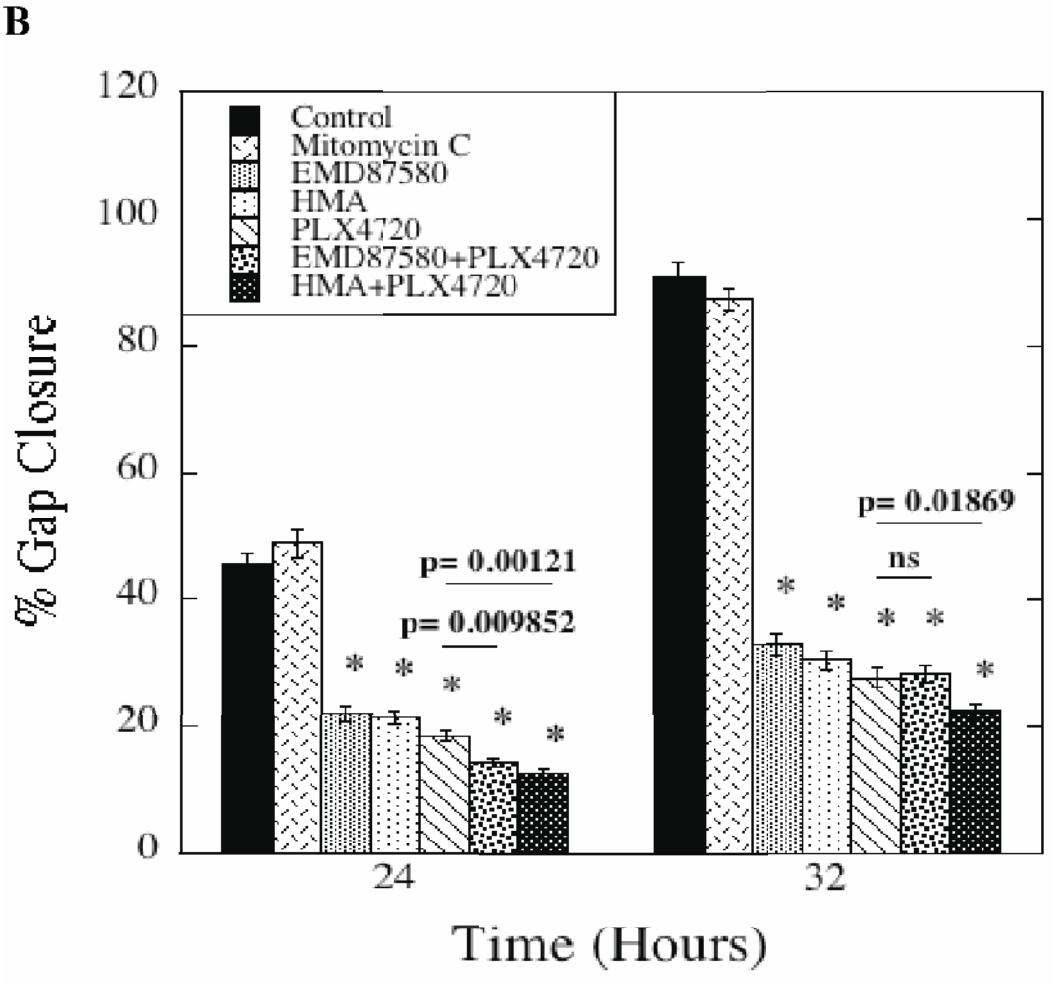

Figure 2.2.3 B: Rate of cell migration in FM82 Melanoma Cells.

FM82 cells were cultured as described in methods and cell migration was assessed at 24 hours and 32 hours in the presence of either NHE1 inhibitors or BRAF inhibitors or both. The concentration of compounds used are as follows: Mitomycin C 1 μg/mL, EMD87580 10 μM, HMA 50 nM, PLX4720 10 μM. Results are the mean of ± SE of 4 experiments.

* p Value <0.0001.

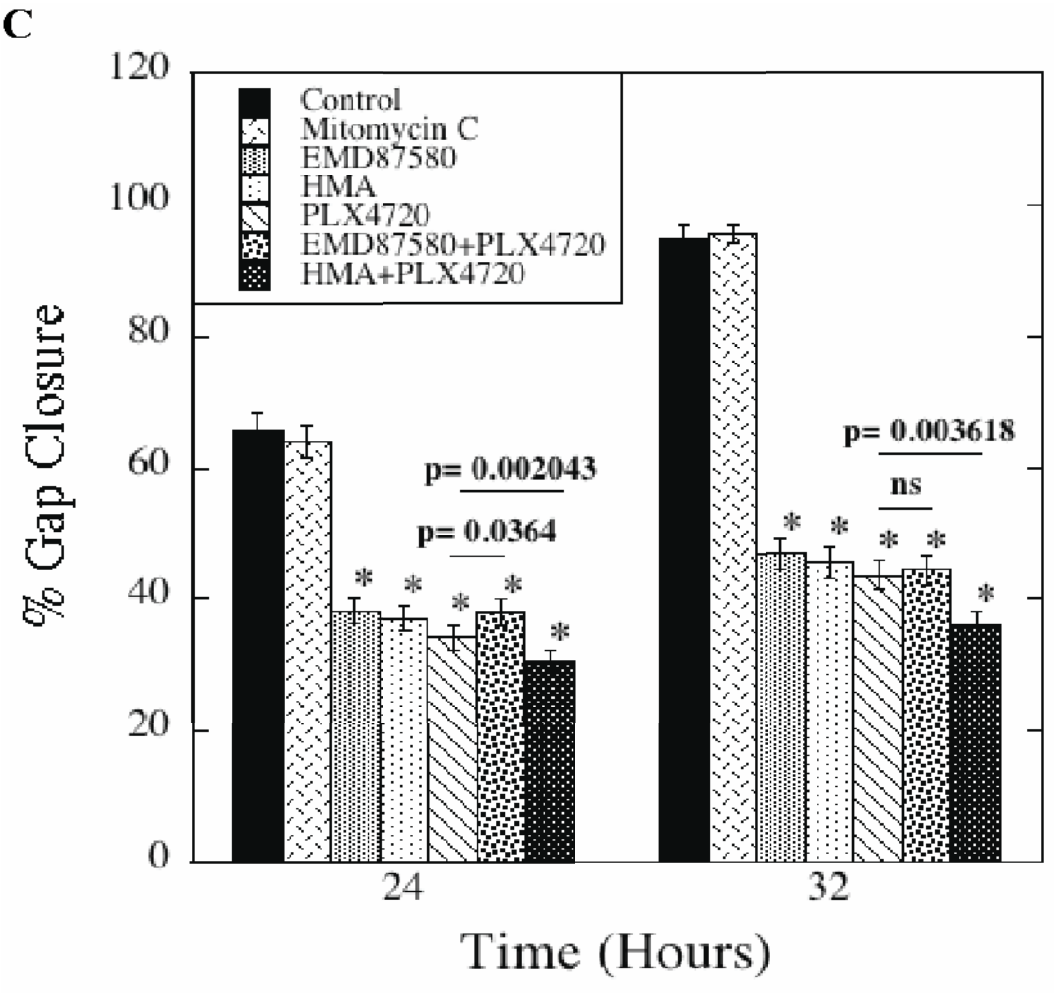

Figure 2.2.3 C: Rate of cell migration in IF6 Melanoma Cells.

IF6 cells were cultured as described in methods and cell migration was assessed at 24 hours and 32 hours in the presence of either NHE1 inhibitors or BRAF inhibitors or both. The concentration of compounds used are as follows: Mitomycin C 1 μg/mL, EMD87580 10 μM, HMA 50 nM, PLX4720 10 μM. Results are the mean of ± SE of 4 experiments.

* p Value <0.0001.

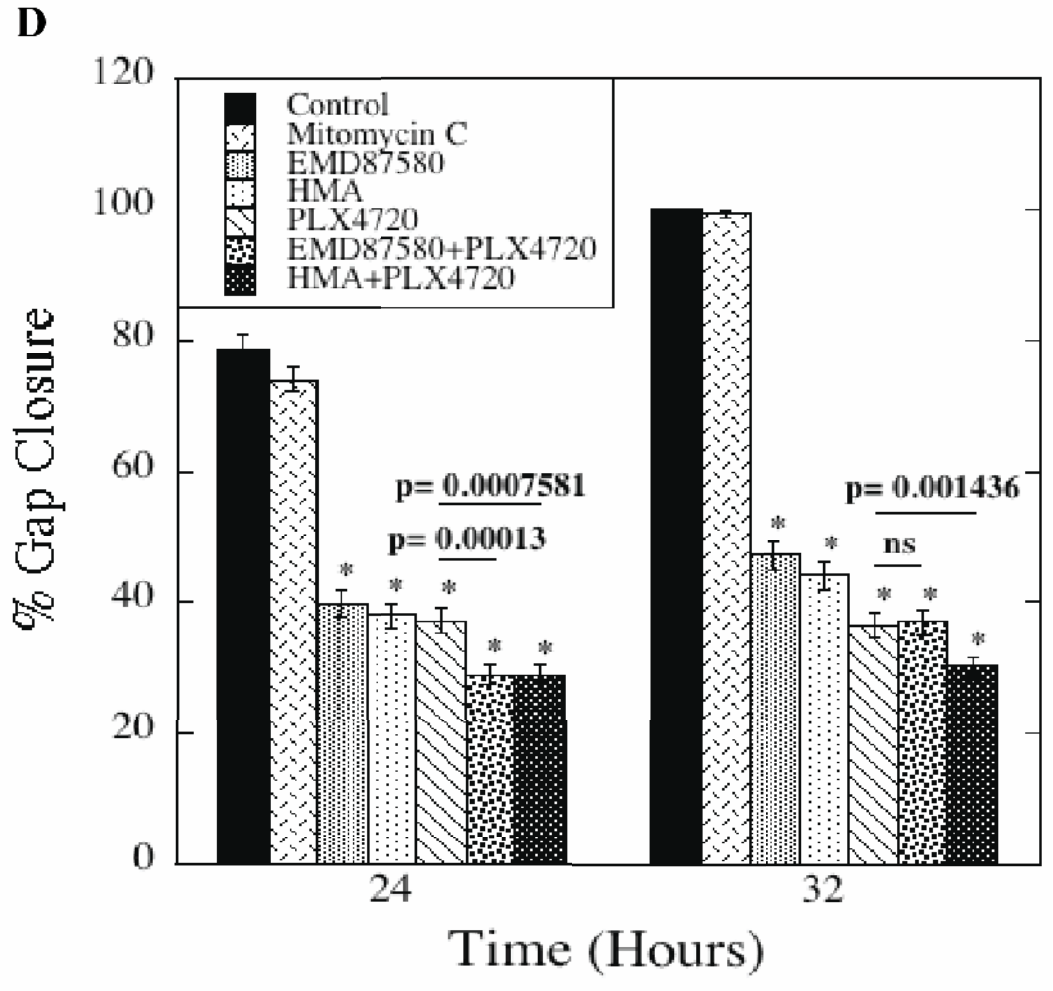

Figure 2.2.3 D: Rate of cell migration in Mel2A Melanoma Cells.

Mel2A cells were cultured as described in methods and cell migration was assessed at 24 hours and 32 hours in the presence of either NHE1 inhibitors or BRAF inhibitors or both. The concentration of compounds used are as follows: Mitomycin C 1 µg/mL, EMD87580 10 µM, HMA 50 nM, PLX4720 10 µM. Results are the mean of ± SE of 4 experiments.

* p Value <0.0001.

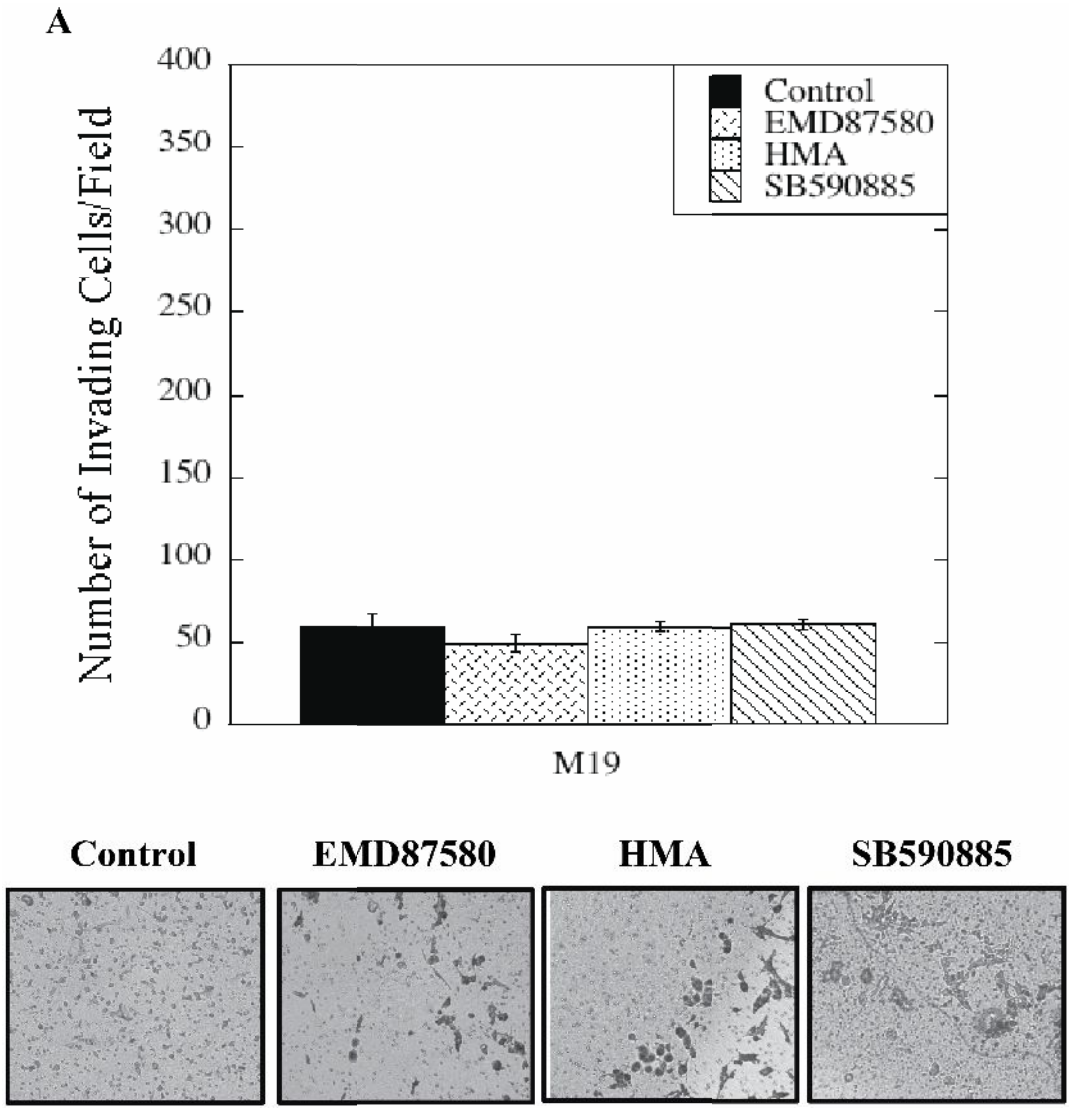

Figure 2.2.4 A: Cell invasion in M19 Melanoma Cells.

M19 cells were cultured as described in methods and invasion was assessed at 24 hours in the presence of either NHE1 inhibitors or BRAF inhibitor. The concentration of drugs/inhibitors used are as follows: EMD87580 10 μM, HMA 50 nM, SB590885 5 μM. Results are the mean of ± SE of 3 experiments.

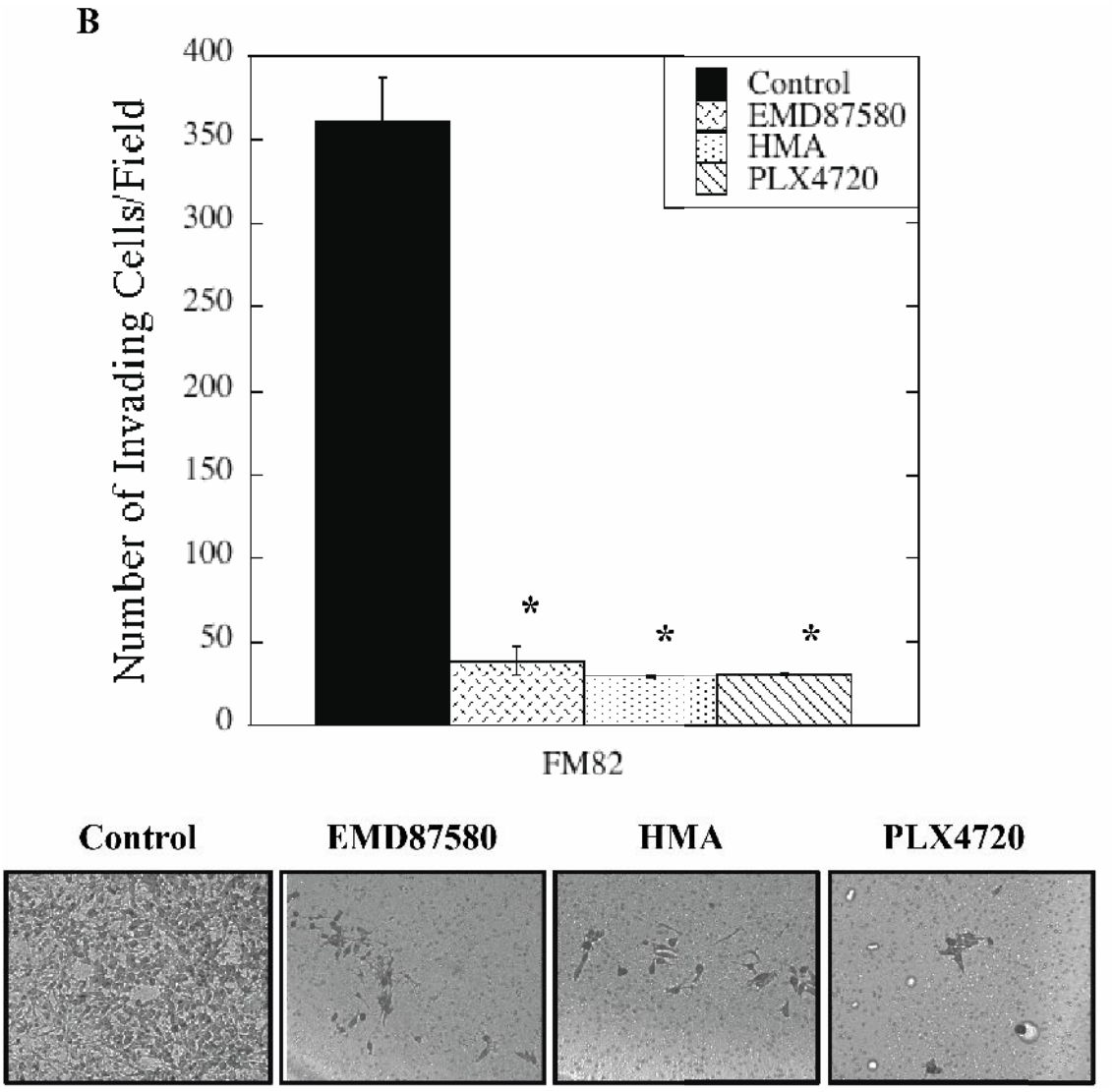

Figure 2.2.4 B: Cell invasion in FM82 Melanoma Cells.

FM82 cells were cultured as described in methods and invasion was assessed at 24 hours in the presence of either NHE1 inhibitors or BRAF inhibitor. The concentration of compounds used are as follows: EMD87580 10 μM, HMA 50 nM, PLX4720 10 μM. Results are the mean of ± SE of 3 experiments. * p Value < 0.0001.

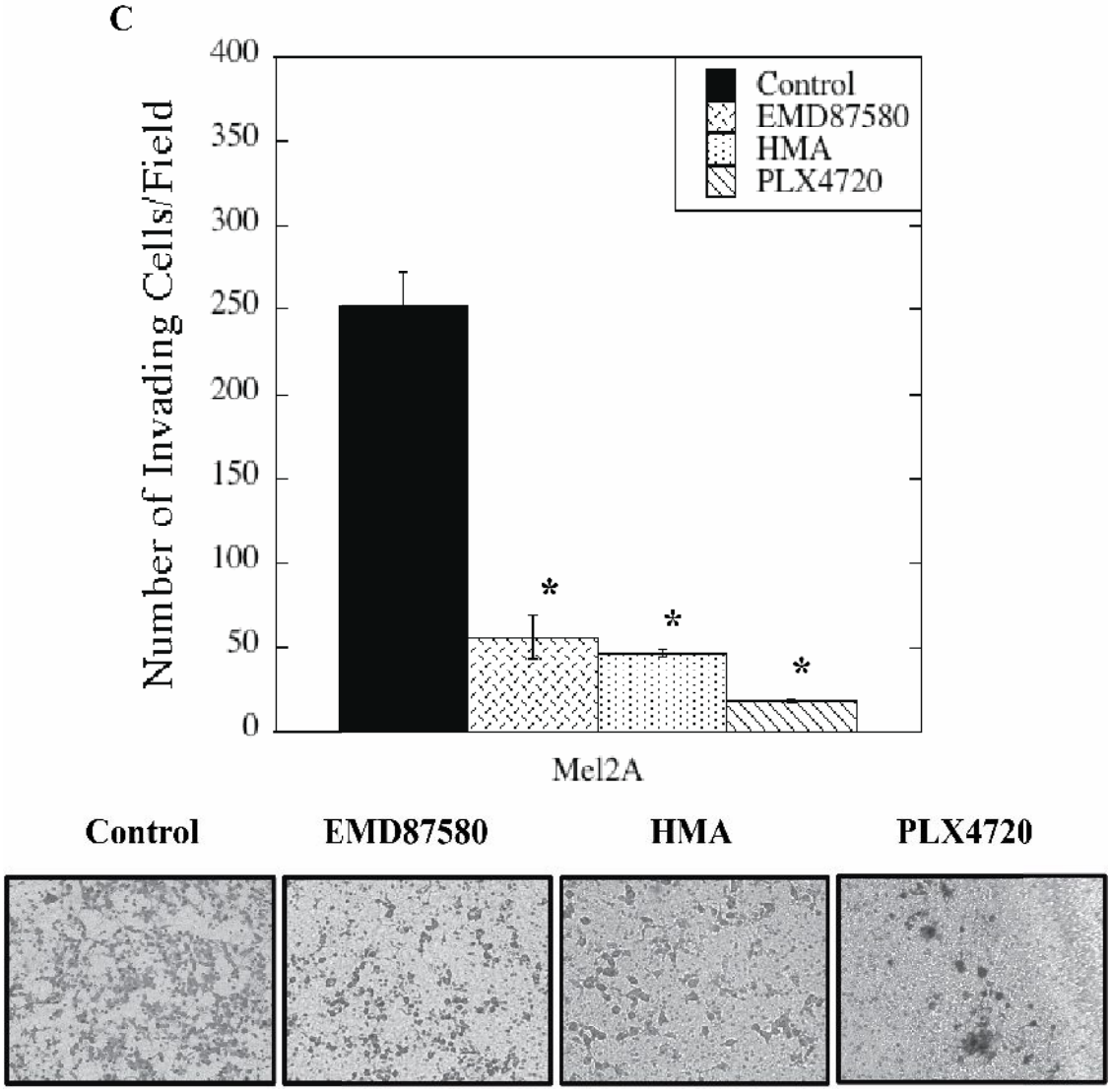

Figure 2.2.4 C: Cell invasion in Mel2A Melanoma Cells.

Mel2A cells were cultured as described in methods and invasion was assessed at 24 hours in the presence of either NHE1 inhibitors or BRAF inhibitor. The concentration of compounds used are as follows: EMD87580 10 μM, HMA 50 nM, PLX4720 10 μM. Results are the mean of ± SE of 3 experiments. * p Value < 0.0001.

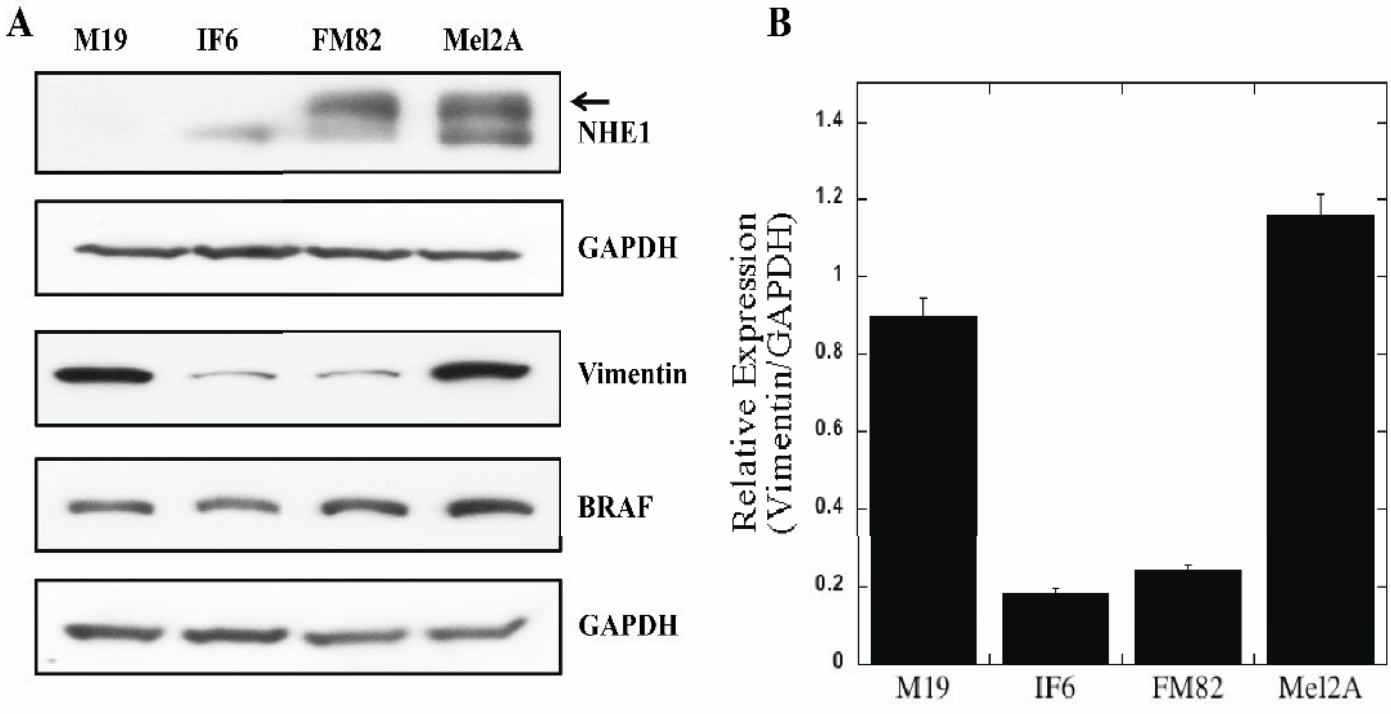

Figure 2.2.5 A&B: Expression blots for proteins in Melanoma cells.

The four human melanoma cell lines (M19, IF6, FM82 and Mel2A) were cultured as described in methods and fresh lysate from each cell line was used for western blotting. 50 µg of total protein was loaded for BRAF and Vimentin blots while 100 µg of total protein was loaded for the NHE1 blot. A: Expression blots showing various proteins obtained from Melanoma cell lysate. B: Relative expression of Vimentin in M19, IF6, FM82 and Mel2A cell lines. GAPDH was used as the loading control. Results are the mean of ± SE of 4 experiments.

3. Stop codon Polymorphisms in NHE1

3.1 Introduction

As mentioned previously, the mammalian NHE1 is involved in several pathological diseases. Although defects in NHE1 have been studied in murine models, there is limited information available on mutations in human NHE1. One study reported a mutation at Gly305 to Arg, which was linked to Lichtenstein-Knorr syndrome and the Fliegel Laboratory further validated this report (174). Another study focused on asparagine 266 to histidine mutation, which led to a loss in the exchanger's activity (175). With the advent of whole genome sequencing, it has been easier to detect mutations across the entire spectrum of the human genome. A study called the 1000 genome project was aimed at understanding the relationship between the genome and phenotype and was effective in detecting over 11 million single nucleotide polymorphisms in multiple human populations (188).

The effect of single nucleotide polymorphisms, especially stop codon polymorphisms (SCP) in the SLC9A1 gene are yet to be investigated in detail. Genes harboring premature termination codons lead to truncation of the translated product and appear to be more deleterious than other polymorphisms (189). In addition, these products may have reduced expression, undergo non-sense mediated mRNA decay and display defects in localization (190).

The 1000 genome project was instrumental in detecting SCP within the SLC9A1 gene at 735, 449 and 321 amino acids. A study conducted in the Fliegel laboratory investigated the

effects of these mutations with respect to expression, activity and targeting (191). In this study we examine the localization of the various SCP (735STOP, 449STOP and 321STOP), which explains why the activity and expression of 2 out of the 3 mutants is drastically affected when compared to WTNHE1. Our report is the first of its kind to investigate the effects of SCP on NHE1 protein function and targeting.

3.2 Results

3.2.1 Localization of SCP proteins

In order to examine the localization of the proteins carrying premature stop codons, AP1 stable cell lines were created including WTNHE1 in the Fliegel laboratory. The cells were subject to immunofluorescence imaging to visualize localization of NHE1 protein. DAPI staining was used to detect healthy cells. Results are presented in Figure 3.2.1. The 735STOP mutant was predominantly localized to the plasma membrane similar to full length NHE1. However, the 449STOP and 321STOP mutants displayed intracellular localization. The 523STOP mutant was used as an additional control and this mutant also displayed cytoplasmic retention.

3.2.2 Effect of Co-expression of SCP proteins and full length NHE1

In the next set of experiments, we wanted to investigate the effect of co-expressing full length NHE1 and truncated NHE1. We transiently expressed 735STOP mutant or 321STOP mutant in CHO cells that possess their own endogenous NHE1. Results are presented in Figure

3.2.2 A. It was observed that 735STOP was able to localize to the plasma membrane but the 321STOP displayed an intracellular localization and the presence of full length NHE1 did not alter its cellular localization. Additional controls (as presented in 3.2.2 B) were included to ensure that the antibody used to detect C-terminal tail of full length endogenous NHE1 in CHO cells did not target 735STOP as it contained majority of the NHE1 C-terminal tail. Results indicated that the NHE1 antibody was highly specific to the distal portion of NHE1 that did not encompass the translated region lying upstream of amino acid 735.

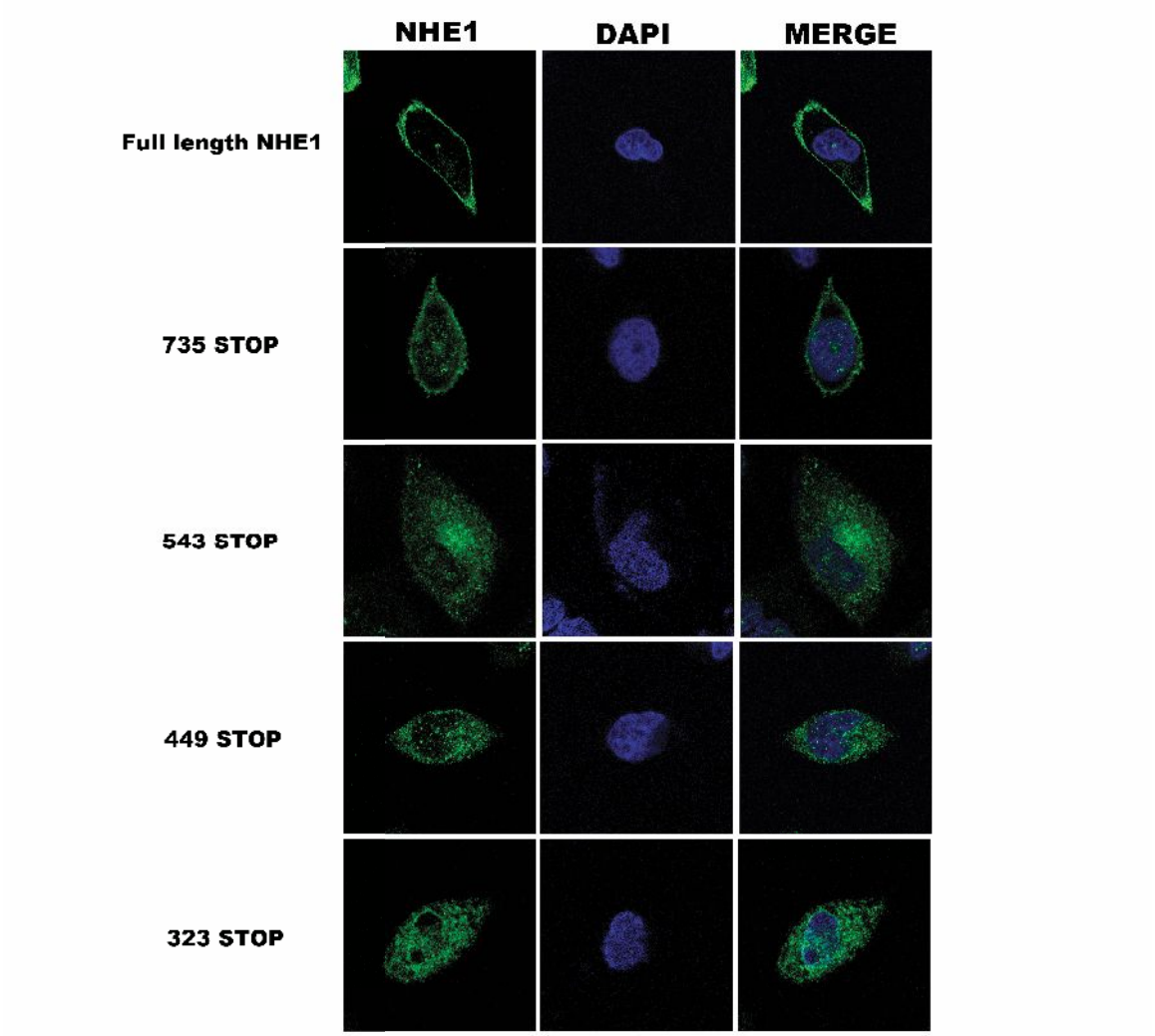

Figure 3.2.1: Localization of full-length and mutant proteins in AP1 stable cell lines.

Full length and mutant NHE1 proteins were stable expressed in AP1 cells and the NHE1 protein was detected using anti-HA antibody (Green). DAPI was used to stain the nucleus. The left panel shows the location of the NHE1 protein (full length/mutant) within the AP1 cell. The panel on the right hand side shows an overlap between DAPI and NHE1. n = 3.

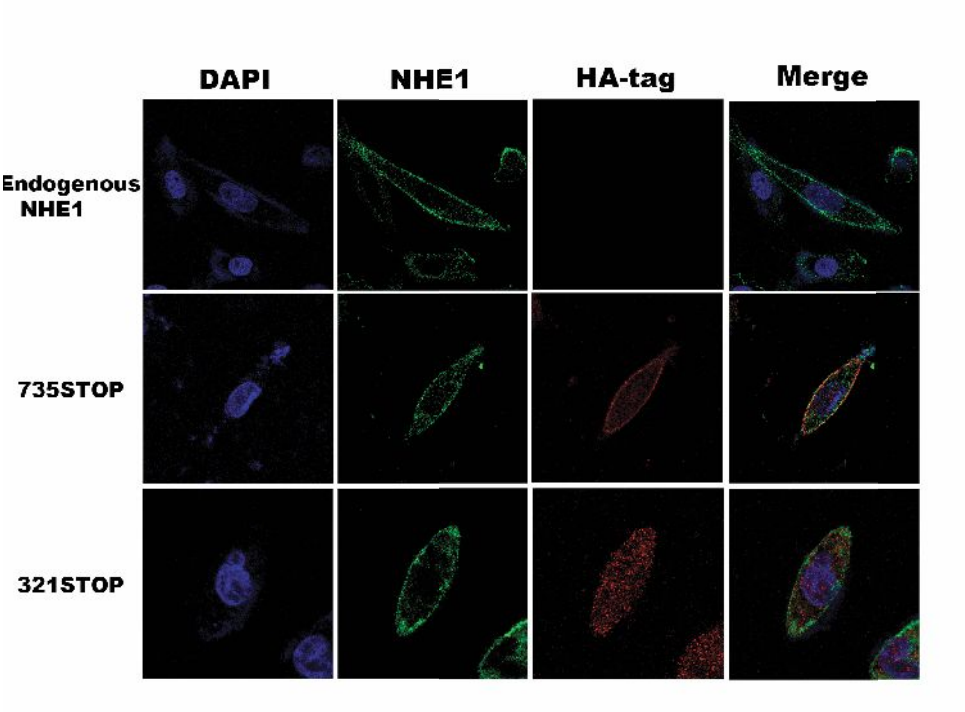

Figure 3.2.2 A: Co-expression of full-length NHE1 and mutant NHE1 in CHO cells.

735STOP and 321STOP mutants were transiently expressed in CHO cells. DAPI was used to detect the nucleus in the left panel, endogenous NHE1 was detected using an anti-NHE1 antibody in the second panel. The mutants were detected using anti-HA antibody since they possess a HA-tag on the C-terminal end. The images were merged to look at the overlay. n =3.

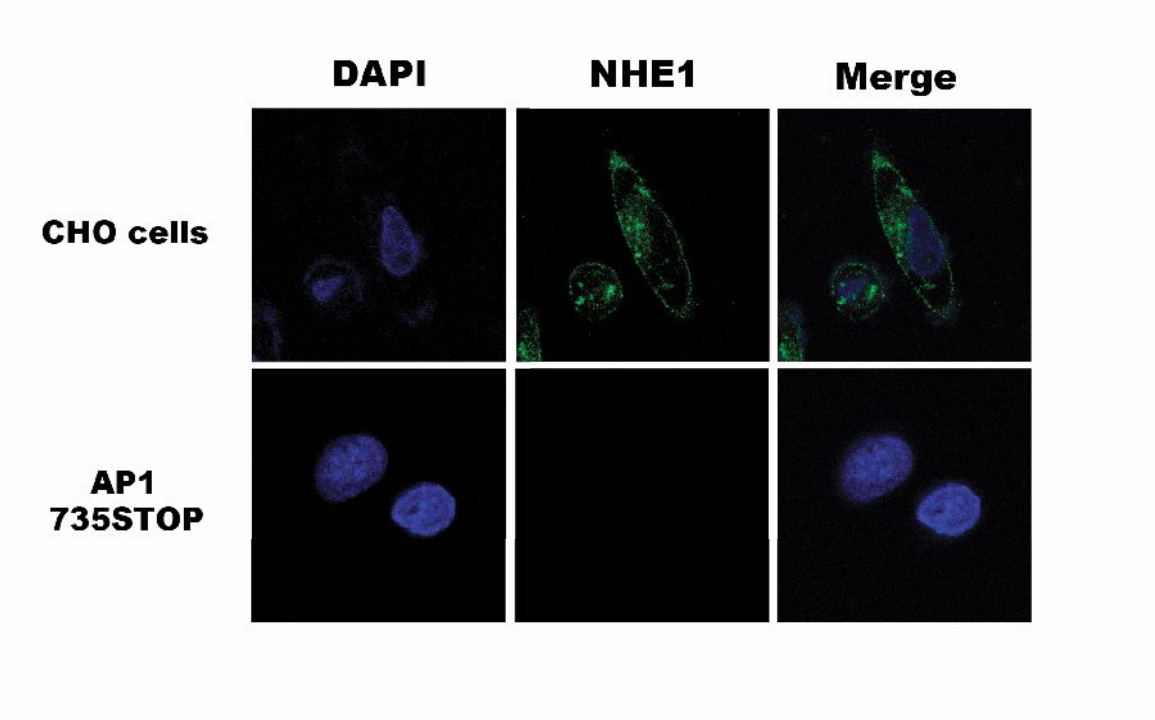

Figure 3.2.2 B: Controls to test Anti-NHE1 Antibody.

CHO cells expressing endogenous NHE1 and AP1 cells stably expressing 735STOP were stained with DAPI on the left. Anti-NHE1 antibody was used to stain both cells in the middle panel. The right panel shows image overlay with only full length NHE1 being detected using the antibody. n =3.

Chapter 4

Discussion

1. NHE1-BRAF binding studies

1.1 Discussion

Cardiovascular disease is one of the leading causes of death around the world and heart failure in particular, is a major cause of mortality (192). The NHE1 protein has been shown to play a pivotal role in the pathology of cardiovascular diseases including cardiac hypertrophy and ischemia reperfusion induced injury. During acute myocardial ischemia, the lack of oxygen catalyzes anaerobic respiration resulting in a rapid accumulation of lactate and protons in the cell (207). This leads to an increase in Na^+ influx via NHE1 and the subsequent inactivation of Na^+-K^+ ATPase during ischemia, exacerbates the Na^+ load triggering a reversal of the Na^+- Ca^{2+} Exchanger. Excessive amounts of Ca^{2+}in the cell leads to injury associated with ischemia. Several studies in animal models have demonstrated a strong correlation between the accumulation of Ca^{2+} following Na^+ influx in ischemic non-reperfused myocardium (208-212). In addition to this, studies have also demonstrated that treatment with NHE1 inhibitors results in reduced cardiac injury and enhanced recovery following ischemia (208).

Tremendous success from animal studies with respect to cardio-protective effects of NHE1 inhibition led to the development of NHE1 inhibitors and subsequent clinical evaluation of these drugs. However NHE1 inhibition failed to demonstrate clinical efficacy and in some cases caused severe side effects resulting in significant increase in cerebrovascular events and increased mortality (208). Although the cardio-protective effects of NHE1 were offset by the

side effects, NHE1 still proves to be a viable target and it is imperative to understand the regulation of NHE1 in cardiac cells.

The Fliegel laboratory discovered that BRAF kinase from rat heart extracts bound to the C-terminal tail of NHE1 in a commercial protein kinase screen, wherein an array of antibodies were used to detect the various protein kinases that bound to the tail (3). Following this discovery, they also demonstrated the interaction of BRAF kinase from enriched HeLa cell lysates with truncated versions of the C-terminal tail (His239 and His182) (3). Since there is no information available on the exact minimal binding portion of BRAF kinase to NHE1 C-terminal tail, the current study was aimed at identifying the target-binding region. Various truncations within amino acids 634 and 815 of the NHE1 C-terminal tail were created to asses the interaction with BRAF kinase. The *in vitro* overlay assay demonstrated that BRAF kinase bound strongly to all three constructs (His155, His117 and His77). This finding indicates that the minimal BRAF binding portion lies somewhere within amino acids 643 and 710 of the NHE1 C-terminal region. This is not surprising since previous studies have indicated that the distal unstructured portion of NHE1 C-terminal tail is a target for several protein kinases (48). Additionally, it should be noted that the amino acid residue (threonine 653) phosphorylated by BRAF kinase is located within this minimal BRAF binding region (193). Interestingly, one report has demonstrated the presence of a proline rich sequence in MEK1. This sequence is essential for BRAF binding and activation of MEK1 in response to growth factor stimulation (257). However the NHE1 C-terminal tail, especially within the region encompassed by amino acids 643 and 710, does not contain a proline rich sequence indicating that this might be highly specific for MEK1 and not for other targets of BRAF.

We further designed and attempted to express smaller constructs encompassing amino acids 634 to 680 of the NHE1 C-terminus (His47). However challenges in cloning and protein expression prevented us from identifying a narrower target-binding site. To determine if BRAF kinase obtained from NVRM bound to NHE1 C-terminal tail we conducted similar experiments wherein His182 was immobilized on membranes. Our results demonstrate that endogenous cardiac BRAF kinase bound to His182 *in vitro* further supporting our idea that the target BRAF binding site is located within the distal portion of the NHE1 C-terminus. Since the MAPK pathway has been implicated in the pathogenesis of cardiac hypertrophy, this result helps gain a better understanding of how the key player of this pathway (BRAF) is involved in the process through NHE1 (253).

After confirming the BRAF-NHE1 interaction *in vitro*, we next examined the localization of these protein partners within intact cells. Since growth factors and hormones including serum have been shown to play a crucial role in NHE1 activation, we examined the effect of serum withdrawal in NHE1-BRAF interaction (9, 102). Our study showed that the two proteins co-localize in the presence of serum while serum withdrawal, resulted in a lack of association between the proteins. This could be due to the fact that serum withdrawal results in the lack of growth factor stimulation of the MAPK cascade. Growth factors are vital for the activation of Ras, which subsequently binds to and recruits its downstream target (BRAF) from the cytoplasm to the plasma membrane wherein it can interact with other proteins such as NHE1. In the absence of growth factors, BRAF remains in the cytoplasm and does not bind to NHE1 as demonstrated in our experiments conducted in AP1 cells as well as HeLa cells.

To further validate the findings, serum starved cells were supplemented with serum over a time course. The results from the current study indicate that co-localization is reestablished between the two proteins which highlights the importance of serum not only in the activation of BRAF but also in its recruitment to the plasma membrane to interact with the membrane protein (NHE1). Interestingly, an earlier study has demonstrated the importance of serum in NHE1 activation via the phosphorylation of NHE1 C-terminal tail at serine 703 residue via p90RSK (80-82, 103). It is proposed that phosphorylation of the NHE1 tail may cause conformational changes within the tail and thereby aid in docking/ interaction of other proteins and kinases on the C-terminal tail. It is possible that serum withdrawal prevents exchanger activation by p90RSK as a result of which, the BRAF binding site remains inaccessible. However, the addition of serum is able to activate NHE1 via p90RSK, induce a conformational change in the C-terminal tail and BRAF is able to gain access to the specific binding site.

Although the minimal BRAF binding region remains elusive, a study conducted in the Fliegel laboratory was instrumental in identifying the BRAF kinase's target amino acid residue (threonine 653) on the NHE1 C-terminal domain (193). Mutation of this residue into a non-phosphorylatable amino acid (alanine) had an interesting effect on cell proliferation. Stable AP1 cells expressing T653A mutant showed a drastic reduction in the rate of cell proliferation in comparison to AP1 cells stably expressing WTNHE1 or T653D mutant. The MAPK cascade is involved in promoting cell division and cell survival (179, 180). Therefore mutating the BRAF phosphorylation site leads to a lack of NHE1 activation via phosphorylation and subsequently affects cell proliferation in these mutants. This is an interesting observation compared to another

group that demonstrated that mutation of T653A leads to an increase in cell proliferation (213). This difference in observation between our study and the study conducted by Wallart *et al.,* can be due to the fact that they used Chinese Hamster Lung Fibroblasts (CCL39) versus our study that used Chinese Hamster Ovarian cell lines (AP1), where the signaling mechanism contributing to cell proliferation may vary. Wallart's study demonstrates that ROCK I and ROCK II phosphorylate T653 on NHE1 C-terminus tail unlike our study where BRAF kinase plays a pivotal role in phosphorylation and regulation.

Additionally, a study conducted by Peter *et al.,* in yeast cells discovered that cytosolic pH regulated Ras/PKA activation and promoted cell growth and proliferation. An increase in intracellular pH led to a decrease in cell growth in those cells (213, 214). Although this study was conducted in yeast cells, there is a possibility that a similar regulatory mechanism occurs in mammalian cells. The current report from the Fliegel Lab indicates that the T653A mutant showed reduced activity when compared to WTNHE1 (193). Therefore another explanation is that in these cells expressing the mutant protein, defective proton extrusion leads to a more acidic intracellular pH, which prevents the activation of Ras/PKA pathway. This in turn prevents the downstream signaling pathway that is involved in promoting cell division and therefore the AP1 T653A cells show reduced cell proliferation compared to WTNHE1.

1.2 Summary & Future Directions

Regulation of intracellular pH is crucial in maintaining normal physiology of cardiac cells. This current study provides a deeper insight into the molecular mechanisms that lie

downstream of BRAF kinase- NHE1 interaction in AP1 cells, HeLa cells as well as NVRM. Our report is the first of its kind to demonstrate the potential BRAF binding site located on the NHE1 C-terminal domain and explore the effects of serum deprivation on NHE1-BRAF co-localization. BRAF not only binds to NHE1 but also regulates the NHE1 activity. The current study further highlights the role of threonine 653 residue with respect to cell proliferation, which might be crucial for cardiac remodeling and maintenance via the MAPK-BRAF-NHE1 cascade.

It is still unclear if BRAF binding to NHE1 promotes the pathophysiology of cardiac diseases (253). Earlier studies have demonstrated that Ras, Raf-1 and MEK1 exist as a complex in the cytoplasm (216). Future experiments can focus on deleting regions within the BRAF binding portion (amino acids 634 to 710) in human NHE1 to help define the specific minimal BRAF binding portion. IP experiments combined with mass spectrometry can be performed with constructs expressing full length NHE1 or partly deleted NHE1. Certain signaling molecules that exist as part of the Ras, Raf and MEK complex may bind only to full length NHE1 but not to the NHE1 with deletions in its C-terminal tail. The results can be compared and used to identify other key players in the BRAF signaling cascade to better understand its role of BRAF-NHE1 interaction in cardiomyoctyes. Additional experiments can be conducted with the T653A mutant since NHE1 is thought to act as a scaffolding protein for other protein complexes. It will be interesting to explore the effect of mutating the BRAF phosphorylation site on the assembly of such kinase complexes.

Since the majority of the experiments in this thesis were conducted in either AP1 cells or HeLa cells, future experiments should be conducted in cultured NVRM to gain a deeper insight

into the role of BRAF in cardiac cells. Co-localization studies can be conducted in cultured cardiomyocytes in the presence or absence of specific BRAF inhibitor (SB590885). Additionally NVRM cells can be designed to express mutant NHE1 (T653A and T653D) using an Adenoviral expression system (255). The co-localization between endogenous BRAF and mutant NHE1 can be examined to evaluate if the presence of the mutation results in a lack of binding of the kinase to the exchanger.

Another interesting area would be to explore the role of BRAF in cardiac cell death. Lovostatin and Doxorubicin have been shown to induce cardiotoxicity and cell death via the activation of apoptotic pathways (217, 218). Cardiomyocytes expressing WTNHE1 and T653A mutant can be treated with such drugs and cell death can be analyzed by immunoblotting for Caspase 3 and Poly ADP Ribose Polymerase cleavage, which are indicators of apoptosis. Additionally, the cells can be assessed for levels of cardiac troponin 1 which is an important biomarker for cardiac injury (219). Studies have shown that ischemic reperfusion induced injury leads to an increase in NHE1 expression and apoptosis. Subsequent inhibition of NHE1 led to a decrease in the levels of apoptosis in isolated rat cardiomyocytes (258, 259). If BRAF kinase plays a crucial role in cell death by binding to and activating NHE1 then the loss of the phosphorylation site would provide a protective effect to these cells and they will be able to evade apoptosis.

To fully understand the effect of BRAF on NHE1 *in vivo* it would be ideal to create transgenic mice that harbor T653A mutation on the NHE1 C-terminal tail. These mice can be subjected to myocardial injury either using invasive or noninvasive techniques to simulate

ischemia reperfusion injury and cardiac hypertrophy in the animals (231,232). Our hypothesis states that NHE1 is phosphorylated by BRAF and that leads to an increase in the NHE1 activity and a mutation at the target site negates this effect. This experiment will help delineate the role of BRAF in an animal model. My hypothesis is that mice expressing WTNHE1 are more susceptible to cardiac injury than mice with the T653A mutation. Since the T653A mutant cannot be phosphorylated by BRAF and *in vitro* experiments have demonstrated that the mutants have lowered NHE1 activity, the presence of this mutation may serve a cardio protective role in these animals unlike WT animals. Taken together these experiments will help define the complex pathophysiological role played by NHE1-BRAF interaction in ischemic reperfusion induced injury as well as in cardiac hypertrophy and perhaps aid in designing combinatorial therapy to effectively treat cardiac diseases.

2. NHE1 regulation in Melanoma

2.1 Discussion

Melanoma is a form of aggressive skin cancer, which arises when melanocytes undergo a process of neoplastic transformation including dysplasia, hyperplasia, invasion and metastasis (221). About 80% of deaths from skin cancer are associated with melanoma and only 14% of the patients demonstrate a 5-year survival rate (222). Several genetic and proteomic studies have demonstrated the molecular mechanism associated with the development and progression of melanoma. However, prognosis and treatment of this disease has been extremely challenging.

BRAF kinase, particularly the BRAF V600E mutant, has been found in a majority of the melanoma cases. The mutant kinase is implicated in various mechanisms involved in the development and progression of the disease including, constitutive activation of the downstream signaling molecules MEK and ERK leading to unchecked replicative potential, increased migration, evasion of apoptosis, invasion and angiogenesis (222). In addition to this, cancerous cells have a perturbed acid-base balance compared to normal cells due to increased NHE1 activity wherein the extracellular pH (pHe) tends to be more acidic and intracellular pH (pHi) tends to be highly alkaline and this promotes tumorigenesis (223). Although the Fliegel laboratory demonstrated that BRAF kinase regulates NHE1 activity in melanoma cells, more information regarding the underlying mechanism is warranted and the current study aims to define the role of this interaction in melanoma.

2.2 Role of NHE1 in melanoma cell proliferation

In order to elucidate the role of NHE1-BRAF interaction in melanoma cells, 4 human melanoma cell lines were chosen, namely, M19, IF6, FM82 and Mel2A. The 4 cell lines demonstrated varying rates of cell proliferation, with cell lines that harbor V600E mutant showing higher rates of cell proliferation compared to M19 that expresses WT BRAF. This difference is due most likely due to constitutive activation of the MAPK signaling pathway, which triggers unchecked cell proliferation. Therefore cells that harbor V600E (Mel2A, FM82 and IF6) showed greater rates of cell proliferation when compared to M19 cells. Previous studies from the Fliegel laboratory have shown that intracellular pH is more alkaline due to the activation of NHE1 in Mel2A, FM82 and IF6 cells and this effect is attenuated in the presence of EMD87580 (3). The same study also demonstrated that using Sorafenib (a multi kinase inhibitor) to inhibit BRAF caused a significant reduction in NHE1 activity in IF6, FM82 and Mel2A cell lines but not in M19 cells clearly indicating that mutant BRAF causes aberrant activation of the exchanger. This result was further supported by Si-RNA knockdown of BRAF in Mel2A cells, which resulted in a significant reduction of NHE1 activity (3). Interestingly, in the present study, NHE1 inhibitors (EMD87580 and HMA) did not show an effect on cell proliferation in the mutant BRAF cell lines. Although some reports in fibroblasts have indicated that NHE1 might play a role in cell proliferation via Akt we were unable to establish a correlation between NHE1 and cell proliferation in the human melanoma cell lines that we tested (94). This could be due to the fact that the cell signaling pathways differ between fibroblasts versus human melanoma cell lines. We hypothesize that cell growth and proliferation in melanoma cells may be under a

different signal regulation. Therefore inhibition of NHE1 does not affect their ability to divide because other signaling pathways compensate for this effect.

2.3 Role of NHE1 in melanoma cell migration

Metastatic behavior has been commonly linked to local fluctuations in cell volume. pH and cell migration are a central component of this process (195). A complex interplay between ion channels, components of the cytoskeleton and signaling pathways is required for this process (195). Our hypothesis was that mutant BRAF would constitutively activate NHE1, which triggers several downstream signaling cascades that promote cell migration. In the current study we examined the role played by NHE1-BRAF interaction in cell migration.

Cell migration was higher in cells expressing mutant BRAF with Mel2A having the highest rate followed by IF6 and FM82 over a period of 32 hours. Treatment of these cells with NHE1 inhibitors (EMD87580 10 μM; HMA 50 nM) or with mutant BRAF inhibitor (PLX4720 10 μM) caused a significant reduction in cell migration rates which highlights the role of NHE1 and BRAF in this metastatic process. However, a combination of NHE1 and BRAF inhibitors only produced significant results when HMA was used versus EMD87580. Before performing migration experiments, we ensured that the effect of combinatorial treatment with inhibitors at the respective concentrations was not a result of cytotoxicity; rather it was a direct effect on cell migration itself. A possible explanation as to why HMA treatment was more effective in curbing cell migration compared to EMD87580 could be due to its efficacy. Early reports have demonstrated that HMA is about 200 to 500 fold more potent when compared to other NHE1

inhibitors, which could explain why a combination of HMA and PLX4720 shows a better effect on melanoma cells that express mutant BRAF (224). However experiments have to be conducted in the melanoma cell lines to determine if the concentration of HMA (50 nM) used inhibits NHE1 more than 10 μM of EMD87580. There is also a possibility of synergistic effect caused when using HMA+PLX4720 versus EMD87580+PLX4720 however that hypothesis remains unclear at this point.

Interestingly we observed a similar effect on M19 cells wherein a combination of HMA and SB590885 caused a significant reduction in cell migration when compared to BRAF inhibition alone with SB590885. It could be possible that in these cell lines the MAPK is more active than in normal melanocytes but not as highly active as in the more aggressive cell lines that harbor mutant BRAF. Therefore using a combination of BRAF and NHE1 inhibitors causes an increased effect on cell migration given how potent HMA is in comparison to EMD87580.

2.4 Role of NHE1 in melanoma cell invasion

Another phenomenon of the metastatic cascade is the ability of cancerous cells to invade, leading to a dissemination of malignant tumors. Invasion involves the formation of cell protrusions containing filamentous actin and other components of the cytoskeleton and this confers the ability of tumor cells to invade distant sites (220, 225). Several studies have suggested that NHE1 plays an important role in invasion (particularly in breast cancer cells) and therefore we wanted to examine its role in human melanoma cells (169-171). We hypothesize that mutant BRAF binds to and activates NHE1 constitutively through phosphorylation and

promotes invasive potential of certain melanoma cell lines. In the present study we attempt to demonstrate the role played by NHE1-BRAF interaction in invasion.

We observed that M19 cells expressing WT BRAF demonstrated basal levels of invasiveness, which is expected because these cell lines do not possess a constitutively active BRAF protein. Therefore the treatment with BRAF or NHE1 inhibitor did not alter their basal invasive potential. However the FM82 and Mel2A cell lines with the BRAF V600E mutation showed a higher invasive potential. Inhibition of NHE1 or BRAF caused a significant reduction in the invasiveness of these cell lines. In FM82 cell lines the invasiveness was lower than the basal levels of M19 cell lines when treated with the inhibitors. Mel2A cells demonstrated similar levels of invasiveness to M19 upon NHE1 inhibition but when treated with a BRAF inhibitor the levels were lower than M19 cells. We did not proceed with a combinatorial treatment since individual treatments affected the cells' invasive potential so much as to cause them to become nearly non-invasive. Therefore we would not have observed much difference in invasiveness in the presence of both BRAF and NHE1 inhibitors.

Interestingly, IF6 cells lines expressing mutant V600E BRAF did not invade at all (data not shown). This was a surprising find since IF6 cells showed higher levels of cellular proliferation and migration when compared to M19 cells. One study conducted experiments in nude mice using a panel of melanoma cell lines of which IF6 was chosen due to its non-metastatic potential (266). This study showed that IF6 cells did not show strong adhesion to Hyaluronic acid (HA) (226). HA is a glycosaminoglycan present in the ECM where it binds to CD44 and activates various signaling pathways, including the activation of matrix

metalloproteinase (MMP), which aids in tumor progression (227). IF6 cells also demonstrated lower levels of CD44 when compared to the metastatic cell lines. Another study conducted in MDA-MB-231 breast cancer cells, demonstrated that binding of HA to CD44 activated NHE1 via Rho kinase and promoted tumor cell invasion by causing an acidic extracellular microenvironment. Inhibition of Rho kinase however caused a reversal of this effect (228). It is possible that in IF6 cells there is a defect in this pathway and that contributes to its inability to invade even in the absence of NHE1 or BRAF inhibitors.

2.5 Protein expression in melanoma cells: NHE1 and Vimentin

Another striking feature of malignant cells is their cellular morphology. Aggressive tumor cells tend to lose their epithelial polarization during a process called epithelial to mesenchymal transition (EMT) (195). The EMT phenomenon requires a cascade of well-coordinated cellular events including NHE1. In turn, the mesenchymal cells are able to disseminate from the primary tumor site and enter the bloodstream to invade distant sites (195). Mel2A cells and FM82 cells have a mesenchymal shape, which is not surprising as they harbor mutant BRAF and are more aggressive. However M19, which expresses WT BRAF, also demonstrated a mesenchymal morphology and IF6 cells that harbors mutant V600E BRAF had a more rounded epithelial like morphology which was unexpected. We next wanted to examine the expression of a cytoskeletal protein that contributes to cell shape and determines cell migration and invasion. For this purpose we chose vimentin protein, which is an intermediate filament protein whose expression has been linked to increased migration and invasiveness of cancerous cells (229).

We tested for basal levels of NHE1, BRAF and vimentin expression in all 4 melanoma cell lines. BRAF levels remained unchanged among the 4 melanoma cell lines. However the levels of NHE1 and vimentin seemed to differ across the 4 cell lines. FM82 and Mel2A showed high levels of mature NHE1. IF6 only had the immature protein whereas the mature band was not seen. M19 showed a complete lack of NHE1 protein. It is possible that the levels of NHE1 are very low in IF6 and M19. In the current study 100 ug of total protein was loaded per lane which may not be enough to visualize the protein because the previous study from the Fliegel Laboratory demonstrated that the afore mentioned cell lines exhibit NHE1 activity (3). Therefore it is not possible that M19 and IF6 completely lack endogenous NHE1. However it is interesting to note that the mature, active form of NHE1 is missing in M19 cells, which might explain their slow migration rates as well as basal levels of invasion. In the case of IF6, the lack of mature NHE1 protein might be one of the contributing factors to its inability to invade.

On the other hand the relative expression of vimentin was highest in Mel2A cells, which is not surprising since these are highly invasive cell lines with strong mesechymal morphology. A recent large-scale proteomics study with melanoma cell lines included patient samples with varying levels of aggressiveness and examined important biomarkers up regulated in aggressive tumors (240). Out of the 300 proteins that were analyzed, the study revealed that vimentin levels were higher among melanoma samples especially when they are adjacent to the blood vessels, which is an indication that they are highly invasive and metastatic. (240). However what was surprising was the presence of high levels of vimentin in M19 cells but not in IF6 and FM82 cell lines. Since M19 shows a strong mesenchymal like morphology, vimentin expression may be

increased in these cells but this protein may not contribute to metastatic features such as motility or invasion in this particular cell type. It is still unclear as to why vimentin levels in FM82 cell lines are low even though they exhibit mesenchymal morphology. Additionally, these cells seem to be highly motile and invasive. It is possible that the central mechanism that contributes to these key features in FM82 revolves around BRAF-NHE1 interaction rather than vimentin. The lack of vimentin in IF6 cells was expected as these cells displayed a more epithelial like morphology rather than a mesechymal morphology. However it should be noted that among the intermediate filaments, vimentin is not the only protein involved in maintaining cell structure. Other cytoskeletal proteins such as Desmin and Nestin also interact with vimentin to support plasma membrane structure and maintain cell shape (230). It is possible that these proteins could compensate for lower levels of vimentin in FM82 cell lines.

2.6 Summary & Future Directions

Our current study has overall demonstrated the importance of NHE1-BRAF interaction and regulation in melanoma cell lines and the impact of the interaction in various metastatic cellular processes such as migration and invasion. Our results also demonstrate that proliferation rates vary among cell lines expressing mutant BRAF versus the one cell line that expresses WT BRAF. Although NHE1 has been implicated in facilitating cell proliferation, we were unable to establish a link between NHE1 and cell proliferation in human melanoma cells line (6). Mutant BRAF with the V600E mutation induced activation of NHE1. This causes a significant increase in cell migration in IF6, FM82 and Mel2A and this effect is attenuated in the presence of specific inhibitors for either BRAF or NHE1 or a combination of both. M19 cells on the other hand

showed low levels of migration. M19 cells also showed very low levels of invasion. Mel2A and FM82 are highly invasive and treatment with inhibitors had a significant effect on their invasive potential. This part of the study highlights the individual roles of BRAF and NHE1 on invasion but we were unable to establish a link between the two proteins and invasion. IF6 did not invade most likely owing to its non-metastatic nature. Additionally FM82 and Mel2A cells showed the presence of mature NHE1, which was absent in both M19 cells and IF6 cells. Vimentin expression was high in M19 and Mel2A cells but very low levels were present in IF6 and FM82 cell lines.

Tumors exhibit complex oncogenic phenotype and often acquire the ability to survive through anchorage independent growth. They down regulate cell adhesion molecules in order to be able to detach from the primary site, migrate to distant sites and finally implant and colonize a new environment (233). Future experiments should focus on assessing other aspects of tumor cell biology such as the anchorage dependent and anchorage independent growth in the presence of NHE1 or BRAF inhibitors or a combination of both inhibitors.

Another key feature accompanying malignant transformation is alterations in the actin cytoskeleton and adheren junctions. In normal cells, E-cadherin, a calcium-dependent membrane glycoprotein, functions to maintain cell-cell contacts (233). However in a malignant cell, E-cadherin is down regulated and N-cadherin is upregulated, which destabilizes cell adhesion and allows the cell to escape growth control and relocate to other sites (234). It will be interesting to assess the levels of E and N-Cadherin protein and mRNA among the 4 melanoma cell lines. We hypothesize that E-Cadherin will be highest in M19 while the other cell lines (FM82 and Mel2A)

will have a higher level of N-Cadherin. NHE1 or BRAF inhibition, most likely, will have a strong effect on the expression levels of the N-Cadherin proteins in FM82 and Mel2A but not in M19 cells. A combination of BRAF and NHE1 inhibition will probably lead to a significant decrease in the levels of N-Cadherin when compared to individual treatments in the more aggressive melanoma cell lines. IF6, due its more epithelial like morphology is more likely to have higher levels of E-Cadherin as opposed to N-Cadherin and inhibitor treatment may not have an effect on protein levels in this cell line.

Just like the EMT markers, an E-cadherin associated protein called Beta-Catenin (β-Catenin) is involved in carcinogenesis. Being the downstream signaling target of the Wnt pathway its primary role is to be a transcriptional activator of specific genes during embryogenesis (237, 238). However some studies have shown that the deregulation of this protein promotes tumor progression in various types of cancers including melanoma, colon cancer, ovarian cancer as well as prostate cancer (238). Previous studies conducted in the Fliegel lab have looked at the levels of β-Catenin in MDA-MB-231 cells with WTNHE1 and mutant S703A NHE1 (239). Although the study was unable to detect any changes in β-Catenin levels between untreated cells versus inhibitor treated cells, given the importance of β-Catenin in melanoma cells, it might be helpful to study the role of this protein in the 4 melanoma cell lines. We hypothesize that β-Catenin levels will be higher in the more aggressive cells lines (FM82 and Mel2A) when compared to M19 and IF6. Perhaps an inhibition of NHE1 in the aggressive cell lines might lead to a dramatic reduction in β-Catenin protein levels in the two cell lines. However an interesting observation from the breast cancer study was the effect of mutation S703A on vimentin levels. That study demonstrated that the S703A mutation not only caused a

dramatic change in cell morphology but also a significant reduction in the levels of vimentin (239). It would be interesting to see if inhibition of NHE1 leads to a significant reduction in vimentin levels in Mel2A cells. Additionally it would be interesting to evaluate the role of T653 residue in modulating vimentin and β-Catenin levels in Mel2A cells.

Matrix metalloproteinases (MMPs) also play a vital role in melanoma progression by aiding in the degradation of basement membrane and digestion of the ECM. Melanoma cells express a wide variety of MMPs including, MMP-1, MMP-2, MMP-9, MMP-13, and MT1-MMP. Studies conducted in MDA-MB-231 cell lines have shown that NHE1 mediates activation of MT1-MMP via the ERK1/2-p38 MAPK pathway and inhibition of NHE1 using cariporide caused a significant reduction in the levels and activation of MT1-MMP (235). Given the importance of MMPs in tumor cell invasion and regulation by NHE1 it will be interesting to investigate the expression profile including protein and mRNA levels of the various MMPs in the four melanoma cells. We hypothesize that the presence of NHE1 inhibitors will lead to a reduction in the expression levels of MMPs and a combination with BRAF inhibitors will enhance the effect.

Since the Fliegel laboratory discovered that BRAF phosphorylates NHE1 at T653, it would be interesting to study the cellular effects caused by the mutation of this residue (193). The invasive melanoma cells (FM82 and Mel2A) can be designed to lack endogenous NHE1 and stably express WTNHE1 or T653A mutant and various cellular effects such as proliferation, migration, invasion, anchorage independent growth can be assessed. Since cancer cells evade apoptosis, the mutant and WT cells can be tested to evaluate their susceptibility to apoptosis

when treated with staurosporine (161). We hypothesize that the mutation will cause more cell death than in cells expressing WTNHE1.

To fully understand the role of NHE1-BRAF interaction and regulation *in vivo* it would be ideal to use nude mice to gain further insights. Melanoma cells expressing WT and mutant NHE1 can be injected into the flanks of the mice and the tumor growth can be monitored over a period of 35 days to assess the importance of T653 residue in BRAF directed regulation of NHE1. Given that FM82 and Mel2A are highly invasive, we would expect them to form large tumors, which will metastasize to form multiple tumors in the animals at different sites. However T653A cells may not be as aggressive and may also lead to smaller tumors in the animal. A similar effect might be observed with M19 cells. Although IF6 cells did not invade *in vitro* it would be helpful to use these cell lines in an animal model to confirm the findings from the cellular context. This would also serve as a good control to confirm the results we obtained with the other cell lines. It would be interesting to conduct an expression profile of various tumor biomarkers from tumor samples obtained from the mice tumor tissue to identify novel proteins that are up regulated in the cancer phenotype in a physiological setting. The control animal samples can be compared against the T653A animal samples to identify these key targets that rely on NHE1 for up regulation during carcinogenesis.

Although this study has helped dissect the potential molecular mechanism that governs various cell effector functions in melanoma cell lines, the biggest challenge was detection of mycoplasma in all the stock samples of the cell lines. We attempted to treat the cells with plasmocin over a period of 30 days and were successful in eliminating the contamination. Some

experimental results presented in this thesis were obtained from mycoplasma free samples such as migration, invasion and western blotting. Cell proliferation was conducted when we were unaware of this contamination. Preliminary experiments with mycoplasma free cells were conducted (data not shown) to show a similar trend in cellular proliferation. More experiments will have to be conducted in the future with treated cells in order to strengthen our findings.

Metastatic melanoma has been an area of interest particularly to researchers focusing on developing small-molecule inhibitors to selectively target mutant BRAF. Although some success has been achieved in clinical response, melanoma cells acquire the capacity to bypass the MAPK cascade to promote survival (241). Therefore instead of targeted therapy alone, combinatorial therapy might provide better treatment outcomes. Taken together our study provides a deeper insight into the role of NHE1 and BRAF in these cell lines and may help improve drug design for the treatment of melanoma.

3. Stop codon Polymorphisms in NHE1

3.1 Discussion

NHE1 has been well studied in various diseases as described previously and there are very few studies exploring its role in development. Genetic defects in NHE1 have been shown to cause developmental delays, ataxia and convulsive seizures (172). Reports have also demonstrated that complete ablation of NHE1 leads to neuro-degeneration, ataxia, seizures and mortality in mice (173). The discovery of stop codon polymorphisms (SCP) in NHE1 and their role with respect to the exchanger's function and regulation is of great interest to researchers. Since the C-terminal tail of NHE1 is important for protein-protein interaction and regulation of the exchanger as a whole, the presence of SCPs within this region would be expected to cause defects in exchanger function at varying levels.

The current study examined the role played by three SCPs in the NHE1 gene wherein the mutations led to premature termination of the protein. NHE1 protein truncated at amino acid 735, 449 and 321 were studied. 543STOP was included as an additional control for comparison. We examined the localization pattern of these proteins in AP1 cells. It was observed that the 735STOP protein was able to localize to the plasma membrane similar to WTNHE1 although it lacked the last 80 amino acids of the C-terminal tail (191). This indicates that this region of the C-terminal tail is not vital for the targeting of NHE1 to the membrane. However the 543STOP, 449STOP and 321STOP all remained intracellular as evident from the immunofluorescence experiments. This effect maybe due to the fact that the truncated proteins are more rapidly

degraded when compared to WTNHE1 or 735STOP as observed in the same study. Protein degradation is a vital process in the normal functioning of a cell and several mechanisms exist within the cell to tightly regulate this phenomenon (260). Some studies have investigated the role of degradation motifs present within the protein that are crucial in determining the rate of degradation (243). Our hypothesis is that in WTNHE1 or 735STOP, these motifs are not accessible due to the conformation of the C-terminal tail. However truncation of the tail leads to a drastic effect on the structure, exposing these motifs and triggering rapid degradation of the truncated protein, which may explain why 543STOP does not get targeted to the plasma membrane. In the case of 449STOP and 321STOP, the complete loss of the C-terminal tail impedes the interaction of these proteins with other regulatory proteins in the cell thereby making them more susceptible to degradation. Therefore these proteins are not processed to be able to be targeted to the appropriate location in the cell. In addition to this, a study conducted by Kragelund and Pederson *et al*., looked at conserved regions of transient structures within the intrinsically disordered C-terminal tail of NHE1 (amino acids 686-815) (47). Point mutations within these conserved regions led to impaired trafficking of NHE1 in AP1 cells (47). The 543STOP, 449STOP and 321STOP mutants lack these conserved regions that might be crucial for targeting the exchanger to the plasma membrane and therefore they remain in the cytosol. The 735STOP on the other hand, retains most of these regions and therefore is trafficked to the membrane like full length WTNHE1.

Another reason for the mistargeting could be due to the absence of the Hsp70 binding sites on the truncated versions of NHE1 protein. Previous studies have demonstrated that Hsp70 binds to C-terminal tail of NHE1 and a recent study from the Fliegel laboratory has highlighted

the importance of the association of this protein with NHE1 in MDCK cells (242). Although the exact binding site of Hsp70 remains unclear, it is possible that the target site lies somewhere upstream of the amino acid 543, which is why 735STOP is targeted efficiently to the membrane while the other truncated proteins remain intracellular.

Since NHE1 has been shown to exist as a dimer, the next step was to see if co-expression of these truncated mutants along with full length NHE1 affected or rescued their co-localization pattern (244). In the case of the cystic fibrosis mutant (Δ508-CFTR), the protein remains in the endoplasmic reticulum rather than localize to the plasma membrane like the wild type cystic fibrosis transmembrane conductance receptor (CFTR). As a result of this the protein is rapidly degraded by the proteasome (245). However a report has demonstrated that the presence of wild type full length CFTR caused the defective protein (Δ508-CFTR) to fold correctly, mature and localize to the membrane (245). We tried to implement the same model in our study and hypothesized that trans-complementation may help in membrane targeting of the truncated NHE1 protein. AP1 cells were used to transiently transfect WTNHE1 along with 735STOP (which served as a control) and 321STOP. This experiment however did not yield the expected results. A possible explanation could be that loss of most of the C-terminal tail led to a loss of the dimerization domain and therefore WTNHE1 was unable to form a hetero-dimer with the mutant and therefore 321STOP was trapped in the cytosol. It is important to note that proteins with premature termination codons are often targets of non-sense mediated decay. This is an evolutionarily conserved mechanism, which aids in the degradation of such transcripts in order to protect the cells from any detrimental effects that might be caused due to the presence of such proteins (248). So even if the WTNHE1 and the truncated proteins do in fact form a dimer, the

quality control mechanism that exist in the cell may recognize this defective dimer and degrade it rapidly.

3.2 Summary & Future Directions

Overall the current study demonstrated that 735STOP behaves similar to WTNHE1 and retains most of the regulatory mechanisms although it lacks the last 80 amino acids. However the truncated mutants, 543STOP, 449STOP and 321STOP are unable to localize to the membrane. They also demonstrated low levels of expression, activity and rapid degradation as shown in other experiments conducted in this study (191). To our knowledge this is the first study to explore the cellular effects of SCPs in NHE1 especially with respect to cellular localization.

As future experiments the binding of these mutants to Hsp70 should be explored using immunoprecipitation assays, as this protein partner is vital for proper protein folding which then leads to correct targeting. Since the target-binding site of Hsp70 on NHE1 remains unknown, comparing 543STOP, 735STOP and WTNHE1 in immuneprecipitation experiments may provide vital clues to this question. This might also explain why co-expression of WTNHE1 with 321STOP did not rescue this mutant. Even if heterodimerization occurred lack of the Hsp70 binding site might contribute to misfolding of the dimer and subsequent degradation.

Since genetic mutations have led to growth retardation and other neurodegenerative defects it will be interesting to investigate the role of these SCPs in animal models. Previous reports have highlighted the importance of p38MAPK with respect to preimplantation

development in murine models. This is a vital process for viable pregnancy in mammals and inhibition of p38MAPK led to a reversible arrest in preimplantation development (246). It should be noted that the three stop codon mutants (543STOP, 449STOP and 321STOP) lack the p38MAPK phosphorylation sites (Thr718, Ser723, Ser726, and Ser729 residues) on the NHE1 C-terminal tail. Therefore we predict that mouse embryos expressing these truncated proteins may not be able to implant into the uterus and undergo development.

p38MAPK has also been implicated in tissue development and homeostasis especially bone development and maintenance. This kinase targets and activates several downstream signaling molecules that are vital for skeletogenesis as well as postnatal bone development (247). Genetically modified animals demonstrated disorders such as chondrodysplasia, cleidocranial dysplasia or faciogenital dysplasia (247). Since the p38MAPK target phosphorylation sites on NHE1 C-terminal tail lie within regions 718-729, we would expect severe developmental defects in animals that lack this region (543STOP, 449STOP and 321STOP). Even if the embryos survive the preimplantation developmental defects by using an alternative mechanism, the pups will most likely suffer from growth retardation, including a poorly developed spine and central nervous system.

Taken together future experiments will help understand the role of SCPs in the human context and perhaps be able to link these individuals to certain genetic disorders that are poorly defined. These studies will definitely pave the way to better diagnosis and management of the condition among individuals harboring these genetic mutations.

References

1. Loo, S. Y., Ker, M., Chang, X., Sui, C., Chua, H., Prem Kumar, A., Clement, M. V. (2012). NHE-1: A Promising Target for Novel Anti-cancer Therapeutics. *Current Pharmaceutical Design*, *18*, 1372–1382.

2. Karmazyn M., Avkiran M. and Fliegel L. (2003). The Sodium-Hydrogen Exchanger: From Molecule to its Role in Disease. *Kuwer Academic Publishers*, pp 1-318.

3. Karki, P., Li, X., Schrama, D., & Fliegel, L. (2011). B-Raf associates with and activates the NHE1 isoform of the Na +/H+ exchanger. *Journal of Biological Chemistry*, *286*(15), 13096 13105.

4. Karmazyn, M. (2013) NHE-1: still a viable therapeutic target. *J Mol Cell Cardiol*, *61*, 77-82.

5. Wakabayashi, S., Pang, T., Su, X., & Shigekawa, M. (2000). A novel topology model of the human Na+/H+ exchanger isoform 1. *Journal of Biological Chemistry*, *275*(11), 7942–7949.

6. Orlowski, J., & Grinstein, S. (2004). Diversity of the mammalian sodium/proton exchanger SLC9 gene family. *Pflugers Archiv European Journal of Physiology*, *447*(5), 549–565.

7. Hendus-Altenburger, R., Kragelund, B. B., & Pedersen, S. F. (2014). Structural dynamics and regulation of the mammalian SLC9A family of Na+/H+ exchangers. *Current Topics in Membranes*, 1(Vol. 73). Elsevier Inc.

8. Ohgaki, R., Van Ijzendoorn, S. C. D., Matsushita, M., Hoekstra, D., & Kanazawa, H. (2011). Organellar Na+/H+ exchangers: Novel players in organelle pH regulation and their emerging functions. *Biochemistry*, *50*(4), 443–450.

9. Fliegel, L., & Malo, M. E. (2006). Physiological role and regulation of the Na+/H+ exchanger. *Canadian Journal of Physiology and Pharmacology*, *84*(11), 1081–1095.

10. Fuster, D. G., & Alexander, R. T. (2014). Traditional and emerging roles for the SLC9 Na+/H+ exchangers. *Pflugers Archiv European Journal of Physiology*, *466*(1), 61–76.

11. Sardet C., Franchi A., Pouyssegur J. (1989) Molecular cloning, primary structure, and expression of the human growth factor- activatable Na+/H+ antiporter. *Cell*, *56*(2), 271-280.

12. Biemesderfer D., Reilly RF., Exner M., Igarashi P., Aronson PS. (1992). Immunocytochemical characterization of Na (+)-H+ exchanger isoform NHE-1 in rabbit kidney. *Am J Physiol*, *263*(5.2), F833–840.

13. Peti-Peterdi J., Chambrey R., Bebok Z., Biemesderfer D., St John PL., Abrahamson DR., Warnock DG., Bell PD. (2000) Macula densa Na+/H+ exchange activities mediated by apical NHE2 and basolateral NHE4 isoforms. *Am J Physiol Renal Physiol*, *278*(3), F452-463.

14. Petrecca K, Atanasiu R, Grinstein S, Orlowski J, Shrier A (1999) Subcellular localization of the Na+/H+ exchanger NHE1 in rat myocardium. *Am J Physiol*, *276*(2.2), H709–717.

15. Tse CM., Levine SA., Yun CH., Montrose MH., Little PJ., Pouyssegur J., Donowitz M. (1993) Cloning and expression of a rabbit cDNA encoding a serum-activated ethylisopropylamiloride-resistant epithelial Na+/H+ exchanger isoform (NHE-2). *J Biol Chem*, *268*(16), 11917–11924.

16. Wang Z., Orlowski J., Shull GE. (1993) Primary structure and functional expression of a novel gastrointestinal isoform of the rat Na/H exchanger. *J Biol Chem*, *268*(16), 11925–11928.

17. Ikuma M., Kashgarian M., Binder HJ., Rajendran VM. (1999) Differential regulation of NHE isoforms by sodium depletion in proximal and distal segments of rat colon. *AmJ Physiol*, *276*(2.1), G539–549.

18. Orlowski J. (1993) Heterologous expression and functional proper- ties of amiloride high affinity (NHE-1) and low affinity (NHE-3) isoforms of the rat Na/H exchanger. *J Biol Chem*, *268*(22), 16369– 16377

19. Chambrey R., Achard JM., Warnock DG. (1997) Heterologous expression of rat NHE4: a highly amiloride-resistant Na+/H+ exchanger isoform. *Am J Physiol*, *272*(1.1), C90–98.

20. Attaphitaya S., Park K., Melvin JE. (1999) Molecular cloning and functional expression of a rat Na+/H+ exchanger (NHE5) highly expressed in brain. *J Biol Chem*, *274*(7), 4383–4388.

21. Liu L., Schlesinger PH., Slack NM., Friedman PA., Blair HC. (2011) High capacity Na+/H+ exchange activity in mineralizing osteoblasts. *J Cell Physiol*, *226*(6), 1702–1712.

22. Nakamura N., Tanaka S., TekoY., Mitsui K., Kanazawa H. (2005) Four Na+/H+ exchanger isoforms are distributed to Golgi and post-Golgi compartments and are involved in organelle pH regulation. *J Biol Chem*, *280*(2), 1561–1572.

23. Hill JK., Brett CL., Chyou A., Kallay LM., Sakaguchi M., Rao R., Gillespie PG. (2006) Vestibular hair bundles control pH with (Na+, K+)/H+ exchangers NHE6 and NHE9. *J Neurosci*, *26*(39), 9944– 9955.

24. Wakabayashi, S., Pang, T., Su, X., & Shigekawa, M. (2000). A novel topology model of the human Na+/H+ exchanger isoform 1. *Journal of Biological Chemistry*, *275*(11), 7942–7949

25. Landau, M., Herz, K., Padan, E., & Ben-Tal, N. (2007). Model structure of the Na+/H+ exchanger 1 (NHE1): Functional and clinical implications. *Journal of Biological Chemistry*, *282*(52), 37854–37863.

26. Lee, B. L., Sykes, B. D., and Fliegel, L. (2013) Structural and functional insights into the cardiac Na+/H+ exchanger. *J Mol Cell Cardiol*, *61*, 60-67.

27. Coupaye-Gerard, B., Bookstein, C., Duncan, P., Chen, X. Y., Smith, P. R., Musch, M., Ernst, S. A., Chang, E. B., and Kleyman, T. R. (1996) Biosynthesis and cell surface delivery of the NHE1 isoform of Na+/H+ exchanger in A6 cells. *Am J Physiol 271*, C1639-1645

28. Liu, Y., Basu, A., Li, X., & Fliegel, L. (2015). Topological analysis of the Na+/H+ exchanger. *Biochimica et Biophysica Acta (BBA) - Biomembranes*, *1848*(10, Part A), 2385–2393.

29. Parker, M. D., Myers, E. J., and Schelling, J. R. (2015) Na+/H+ exchanger-1 (NHE1) regulation in kidney proximal tubule. *Cell Mol Life Sci 72*, 2061-2074.

30. Lee, S. H., Kim, T., Park, E. S., Yang, S., Jeong, D., Choi, Y., & Rho, J. (2008). NHE10, a novel osteoclast-specific member of the Na+/H+ exchanger family, regulates osteoclast differentiation and survival. *Biochemical and Biophysical Research Communications*, *369*(2), 320–326.

31. Coupaye-Gerard, B., Bookstein, C., Duncan, P., Chen, XY., Smith, PR., Musch, M., Ernst, SA., Chang, EB., Kleyman, TR. Biosynthesis and cell surface delivery of the NHE1 isoform of Na+/H+ exchanger in A6 cells. *Am J Physiol*, *271*(5.1), C1639-1645.

32. Counillon, L., Pouyssegur, J., Reithmeier, RA. (1994). The Na+/H+ exchanger NHE-1 possesses N- and O- linked glycosylation restricted to the first N-terminal extracellular domain. *Biochemistry*, *33*, 10463–10469.

33. Shrode, LD., Gan, BS., D'Souza, SJ., Orlowski, J., Grinstein, S. (1998). Topological analysis of NHE1, the ubiquitous Na+/H+ exchanger using chymotryptic cleavage. *Am J Physiol*, *275*, C431–C439.

34. Nygaard, EB., Lagerstedt, JO., Bjerre, GP., Shi, B., Budamagunta, M., Poulsen, KA., Meinild, S., Rigor, RR., Voss, JC., Cala, PM., Pedersen, SF. (2010). Structural modeling and electron paramagnetic resonance spectroscopy of the human Na+/H+ exchanger isoform 1, NHE1. *J Biol Chem*, *286*, 634– 648.

35. Tzeng, J., Lee, B. L., Sykes, B. D., and Fliegel, L. (2010) Structural and functional analysis of transmembrane segment VI of the NHE1 isoform of the Na+/H+ exchanger. *J Biol Chem*, *285*, 36656-36665.

36. Tzeng, J., Lee, B. L., Sykes, B. D., and Fliegel, L. (2011) Structural and functional analysis of critical amino acids in TMVI of the NHE1 isoform of the Na+/H+ exchanger. *Biochim Biophys Acta*, *1808*, 2327-2335.

37. Ding, J., Rainey, J. K., Xu, C., Sykes, B. D., and Fliegel, L. (2006) Structural and functional characterization of transmembrane segment VII of the Na+/H+ exchanger isoform 1. *J Biol Chem*, *281*, 29817-29829.

38. Ding, J., Ng, R. W., and Fliegel, L. (2007) Functional characterization of the transmembrane segment VII of the NHE1 isoform of the Na+/H+ exchanger. *Can J Physiol Pharmacol*, *85*, 319-325.

39. Reddy, T., Li, X., Fliegel, L., Sykes, B. D., and Rainey, J. K. (2010) Correlating structure, dynamics, and function in transmembrane segment VII of the Na+/H+ exchanger isoform 1. *Biochim Biophys Acta*, *1798*, 94-104.

40. Alves, C., Lee, B. L., Sykes, B. D., and Fliegel, L. (2014) Structural and functional analysis of the transmembrane segment pair VI and VII of the NHE1 isoform of the Na+/H+ exchanger. *Biochemistry*, *53*, 3658-3670.

41. Reddy, T., Ding, J., Li, X., Sykes, B. D., Rainey, J. K., & Fliegel, L. (2008). Structural and functional characterization of transmembrane segment IX of the NHE1 isoform of the Na+/H+ exchanger. *Journal of Biological Chemistry*, *283*(32), 22018–22030.

42. Khadilkar, A., Iannuzzi, P., & Orlowski, J. (2001). Identification of Sites in the Second Exomembrane Loop and Ninth Transmembrane Helix of the Mammalian Na+/H+ Exchanger Important for Drug Recognition and Cation Translocation. *Journal of Biological Chemistry*, *276*(47), 43792–43800.

43. Lee, B. L., Li, X., Liu, Y., Sykes, B. D., and Fliegel, L. (2009). Structural and functional analysis of transmembrane XI of the NHE1 isoform of the Na+/H+ exchanger. *J Biol Chem*, *284*, 11546-11556.

44. Slepkov, E. R., Chow, S., Lemieux, M. J., and Fliegel, L. (2004). Proline residues in transmembrane segment IV are critical for activity, expression and targeting of the Na+/H+ exchanger isoform 1. *Biochem J*, *379*, 31-38.

45. Slepkov, E., Ding, J., Han, J., and Fliegel, L. (2007) Mutational analysis of potential pore lining amino acids in TM IV of the Na+/H+ exchanger. *Biochim Biophys Acta*, *1768*, 2882-2889.

46. Lee, B. L., Li, X., Liu, Y., Sykes, B. D., & Fliegel, L. (2009). Structural and functional analysis of transmembrane XI of the NHE1 isoform of the Na+/H+ exchanger. *Journal of Biological Chemistry*, *284*(17), 11546–11556.

47. Nørholm, A. B., Hendus-Altenburger, R., Bjerre, G., Kjaergaard, M., Pedersen, S. F., & Kragelund, B. B. (2011). The intracellular distal tail of the Na+/H+ exchanger NHE1 is intrinsically disordered: Implications for NHE1 trafficking. *Biochemistry*, *50*(17), 3469-3480.

48. Gebreselassie, D., Rajarathnam, K., & Fliegel, L. (1998). Expression, purification, and characterization of the carboxyl-terminal region of the Na + / H+ exchanger. *Biochem. Cell. Biol 842*(76), 837–842.

49. Fliegel, L., & Fröhlich, O. (1993). The Na+/H+ exchanger: an update on structure, regulation and cardiac physiology. *The Biochemical Journal*, *296*(2.2), 273–285.

50. Aronson, P. S., Nee, J., & Suhm, M. A. (1982). Modifier role of internal H+ in activating the Na+–H+ exchanger in renal microvillus membrane vesicles. *Nature*, *299*(5879), 161-163.

51. Wakabayashi, S., Bertrand, B., Shigekawa, M., Fafournoux, P., and Pouyssegur, J. (1994) Growth factor activation and "H+-sensing" of the Na+/H+exchanger isoform 1 (NHE1). Evidence for an additional mechanism not requiring direct phosphorylation. *J Biol Chem*, *269*, 5583-5588.

52. Abu Jawdeh, B. G., Khan, S., Deschenes, I., Hoshi, M., Goel, M., Lock, J. T., Shinlapawittayatorn, K., Babcock, G., Lakhe-Reddy, S., DeCaro, G., Yadav, S. P., Mohan, M. L., Naga Prasad, S. V., Schilling, W. P., Ficker, E., and Schelling, J. R. (2011) Phosphoinositide binding differentially regulates NHE1 Na+/H+ exchanger-dependent proximal tubule cell survival. *J Biol Chem*, *286*, 42435-42445.

53. Aharonovitz, O., Zaun, H. C., Balla, T., York, J. D., Orlowski, J., & Grinstein, S. (2000). Intracellular pH regulation by Na(+)/H(+) exchange requires phosphatidylinositol 4,5-bisphosphate. *The Journal of Cell Biology*, *150*(1), 213–24.

54. Di Sole, F., Vadnagara, K., Moe, O. W., & Babich, V. (2012). Calcineurin homologous protein: a multifunctional Ca^{2+}-binding protein family. *American Journal of Physiology Renal Physiology*, *303*(2), F165–F179.

55. Lin, X., & Barber, D. L. (1996). A calcineurin homologous protein inhibits GTPase stimulated Na-H exchange. *Proceedings of the National Academy of Sciences of the United States of America*, *93*(22), 12631–6.

56. Pang, T., Su, X., Wakabayashi, S., & Shigekawa, M. (2001). Calcineurin Homologous Protein as an Essential Cofactor for Na +/H+ Exchangers. *Journal of Biological Chemistry*, *276*(20), 17367–17372.

57. Mishima, M., Wakabayashi, S., & Kojima, C. (2007). Solution structure of the cytoplasmic region of Na+/H + exchanger 1 complexed with essential cofactor calcineurin B homologous protein 1. *Journal of Biological Chemistry*, *282*(4), 2741–2751.

58. Pang, T., Wakabayashi, S., & Shigekawa, M. (2002). Expression of calcineurin B homologous protein 2 protects serum deprivation-induced cell death by serum-independent activation of Na+/H+ exchanger. *Journal of Biological Chemistry*, *277*(46), 43771–43777.

59. Li, X., Liu, Y., Kay, C. M., Muller-Esterl, W., and Fliegel, L. (2003) The Na+/H+ exchanger cytoplasmic tail: Structure, function, and interactions with tescalcin. *Biochemistry*, *42*, 7448-7456.

60. Denker, S. P., Huang, D. C., Orlowski, J., Furthmayr, H., and Barber, D. L. (2000) Direct binding of the Na-H exchanger NHE1 to ERM proteins regulates the cortical cytoskeleton and cell shape independently of H+ translocation. *Mol Cell*, *6*, 1425-1436.

61. Antelmi, E., Cardone, R. A., Greco, M. R., Rubino, R., Di Sole, F., Martino, N. A., Reshkin, S. J. (2013). β1 Integrin Binding Phosphorylates Ezrin at T567 to Activate a Lipid Raft Signalsome Driving Invadopodia Activity and Invasion. *PLoS ONE*, *8*(9), 1–19.

62. Darmellah, A., Rucker-Martin, C., and Feuvray, D. (2009) ERM proteins mediate the effects of Na+/H+ exchanger (NHE1) activation in cardiac myocytes. *Cardiovasc Res*, *81*, 294-300.

63. Bertrand, B., Wakabayashi, S., Ikeda, T., Pouyssegur, J., and Shigekawa, M. (1994) The Na+/H+ exchanger isoform 1 (NHE1) is a novel member of the calmodulin-binding proteins. Identification and characterization of calmodulin-binding sites. *J Biol Chem*, *269*, 13703-13709.

64. Eguti, D. M., Thieme, K., Leung, G. P., Mello-Aires, M., and Oliveira-Souza, M. (2010) Regulation of Na+/H+ exchanger isoform 1 (NHE1) by calmodulin-binding sites: role of angiotensin II. *Cell Physiol Biochem*, *26*, 541-552.

65. Li, X., Prins, D., Michalak, M., and Fliegel, L. (2013) Calmodulin-dependent binding to the NHE1 cytosolic tail mediates activation of the Na+/H+ exchanger by Ca2+ and endothelin. *Am J Physiol Cell Physiol*, *305*, C1161-1169.

66. Wakabayashi, S., Bertrand, B., Ikeda, T., Pouyssegur, J., and Shigekawa, M. (1994) Mutation of calmodulin-binding site renders the Na+/H+ exchanger (NHE1) highly H+ sensitive and Ca2+ regulation-defective. *J Biol Chem*, *269*, 13710-13715.

67. Li, X., Liu, Y., Alvarez, B. V., Casey, J. R., and Fliegel, L. (2006) A novel carbonic anhydrase II binding site regulates NHE1 activity. *Biochemistry*, *45*, 2414-2424.

68. Li, X., Alvarez, B., Casey, J. R., Reithmeier, R. A., and Fliegel, L. (2002) Carbonic anhydrase II binds to and enhances activity of the Na+/H+ exchanger. *J Biol Chem*, *277*, 36085-36091.

69. Vargas, L. A., Diaz, R. G., Swenson, E. R., Perez, N. G., and Alvarez, B. V. (2013) Inhibition of carbonic anhydrase prevents the Na+/H+ exchanger 1-dependent slow force response to rat myocardial stretch. *Am J Physiol Heart Circ Physiol*, *305*, H228-237.

70. Jung, Y. S., Kim, H. Y., Kim, J., Lee, M. G., Pouyssegur, J., and Kim, E. (2008) Physical interactions and functional coupling between Daxx and sodium hydrogen exchanger 1 in ischemic cell death. *J Biol Chem*, *283*, 1018-1025.

71. Lehoux, S., Abe, J., Florian, J. A., and Berk, B. C. (2001) 14-3-3 Binding to Na+/H+ exchanger isoform-1 is associated with serum-dependent activation of Na+/H+ exchange. *J Biol Chem*, *276*, 15794-15800.

72. Huang, C., Wang, J., Chen, Z., Wang, Y., and Zhang, W. (2013) 2 phenylethynesulfonamide Prevents Induction of Pro-inflammatory Factors and Attenuates LPS-induced Liver Injury by Targeting NHE1-Hsp70 Complex in Mice. *PLoS One*, *8*, e67582.

73. Silva, N. L., Haworth, R. S., Singh, D., and Fliegel, L. (1995) The carboxyl-terminal region of the Na+/H+ exchanger interacts with mammalian heat shock protein. *Biochemistry*, *34*, 10412-10420.

74. Zuiderweg, ER., Hightower, LE., Gestwicki, JE. (2017) The remarkable multivalency of the Hsp70 chaperones. *Cell Stress Chaperones*, *22*(2), 173-189.

75. Wakabayashi, S., Hisamitsu, T., Pang, T., & Shigekawa, M. (2003). Mutations of Arg440 and Gly455/Gly456 oppositely change pH sensing of Na+/H+ exchanger 1. *Journal of Biological Chemistry*, *278*(14), 11828–11835.

76. Sardet, C., Counillon, L., Franchi, A., and Pouyssegur, J. (1990) Growth factors induce phosphorylation of the Na+/H+ antiporter, glycoprotein of 110 kD. *Science*, *247*, 723-726.

77. Livne, A. A., Sardet, C., & Pouyssegur, J. (1991). The Na+/H+ exchanger is phosphorylated in human platelets in response to activating agents. *FEBS Letters*, *284*(2), 219–222.

78. Fliegel, L., Walsh, M. P., Singh, D., Wong, C., and Barr, A. (1992) Phosphorylation of the C-terminal domain of the Na+/H+ exchanger by Ca2+/calmodulin-dependent protein kinase II. *The Biochemical journal*, *282*(1), 139-145.

79. Bianchini, L., L'Allemain, G., and Pouyssegur, J. (1997) The p42/p44 mitogen-activated protein kinase cascade is determinant in mediating activation of the Na+/H+ exchanger (NHE1 isoform) in response to growth factors. *J Biol Chem*, *272*, 271-279.

80. Moor, A. N., and Fliegel, L. (1999) Protein kinase-mediated regulation of the Na+/H+ exchanger in the rat myocardium by mitogen-activated protein kinase-dependent pathways. *J Biol Chem*, *274*, 22985-22992.

81. Putney, L. K., Denker, S. P., and Barber, D. L. (2002) The changing face of the Na+/H+ exchanger, NHE1: structure, regulation, and cellular actions. *Annu Rev Pharmacol Toxicol*, *42*, 527-552.

82. Luo, J., Kintner, D. B., Shull, G. E., and Sun, D. (2007) ERK1/2-p90RSK-mediated phosphorylation of Na+/H+ exchanger isoform 1. A role in ischemic neuronal death. *J Biol Chem*, *282*, 28274-28284.

83. Malo, M. E., Li, L., and Fliegel, L. (2007) Mitogen-activated protein kinase-dependent activation of the Na+/H+ exchanger is mediated through phosphorylation of amino acids Ser770 and Ser771. *J Biol Chem*, *282*, 6292-6299.

84. Coccaro, E., Karki, P., Cojocaru, C., and Fliegel, L. (2009) Phenylephrine and sustained acidosis activate the neonatal rat cardiomyocyte Na+/H+ exchanger through phosphorylation of amino acids Ser770 and Ser771. *Am J Physiol Heart Circ Physiol*, *297*, H846-858.

85. Cuadrado, A., & Nebreda, A. R. (2010). Mechanisms and functions of p38 MAPK signalling. *The Biochemical Journal*, *429*, 403–417.

86. Kusuhara, M., Takahashi, E., Peterson, T. E., Abe, J., Ishida, M., Han, J., Ulevitch, R., and Berk, B. C. (1998) p38 Kinase is a negative regulator of angiotensin II signal transduction in vascular smooth muscle cells: effects on Na+/H+ exchange and ERK1/2. *Circ Res*, *83*, 824-831.

87. Bocanegra, V., Gil Lorenzo, A. F., Cacciamani, V., Benardon, M. E., Costantino, V. V., and Valles, P. G. (2014) RhoA and MAPK signal transduction pathways regulate NHE1 dependent proximal tubule cell apoptosis after mechanical stretch. *Am J Physiol Renal Physiol*, *307*, F881-889.

88. Grenier, A. L., Abu-ihweij, K., Zhang, G., Ruppert, S. M., Boohaker, R., Slepkov, E. R., Pridemore, K., Ren, J. J., Fliegel, L., and Khaled, A. R. (2008) Apoptosis-induced alkalinization by the Na+/H+ exchanger isoform 1 is mediated through phosphorylation of amino acids Ser726 and Ser729. *Am J Physiol Cell Physiol*, *295*, C883-896.

89. Khaled, A. R., Moor, A. N., Li, A., Kim, K., Ferris, D. K., Muegge, K., Fisher, R. J., Fliegel, L., and Durum, S. K. (2001) Trophic factor withdrawal: p38 mitogen-activated protein kinase activates NHE1, which induces intracellular alkalinization. *Mol Cell Biol*, *21*, 7545-7557.

90. Yan, W., Nehrke, K., Choi, J., & Barber, D. L. (2001). The Nck-interacting Kinase (NIK) Phosphorylates the Na+-H + Exchanger NHE1 and Regulates NHE1 Activation by Platelet derived Growth Factor. *Journal of Biological Chemistry*, *276*(33), 31349–31356.

91. Cardone, R. A., Bagorda, A., Bellizzi, A., Busco, G., Guerra, L., Paradiso, A., Casavola, V., Zaccolo, M., and Reshkin, S. J. (2005) Protein kinase A gating of a pseudopodial located RhoA/ROCK/p38/NHE1 signal module regulates invasion in breast cancer cell lines. *Molecular biology of the cell*, *16*, 3117-3127.

92. Tominaga, T., Ishizaki, T., Narumiya, S., and Barber, D. L. (1998) p160ROCK mediates RhoA activation of Na-H exchange. *Embo J*, *17*, 4712-4722.

93. Wallert, M. A., Hammes, D., Nguyen, T., Kiefer, L., Berthelsen, N., Kern, A., Anderson Tiege, K., Shabb, J. B., Muhonen, W. W., Grove, B. D., and Provost, J.J. (2015) RhoA Kinase (Rock) and p90 Ribosomal S6 Kinase (p90Rsk) phosphorylation of the sodium hydrogen exchanger (NHE1) is required for lysophosphatidic acid-induced transport, cytoskeletal organization and migration. *Cell Signal*, *27*, 498-509.

94. Meima, M. E., Webb, B. A., Witkowska, H. E., and Barber, D. L. (2009) The sodium hydrogen exchanger NHE1 is an Akt substrate necessary for actin filament reorganization by growth factors. *J Biol Chem*, *284*, 26666-26675.

95. Clement, D. L., Mally, S., Stock, C., Lethan, M., Satir, P., Schwab, A., Pedersen, S. F., and Christensen, S. T. (2013) PDGFRalpha signaling in the primary cilium regulates NHE1 dependent fibroblast migration via coordinated differential activity of MEK1/2-ERK1/2 p90RSK and AKT signaling pathways. *Journal of cell science*, *126*, 953-965.

96. Wu, K. L., Khan, S., Lakhe-Reddy, S., Jarad, G., Mukherjee, A., Obejero-Paz, C. A., Konieczkowski, M., Sedor, J. R., and Schelling, J. R. (2004) The NHE1 Na+/H+ exchanger recruits ezrin/radixin/moesin proteins to regulate Akt-dependent cell survival. *J Biol Chem*, *279*, 26280-26286.

97. Snabaitis, A. K., Cuello, F., and Avkiran, M. (2008) Protein kinase B/Akt phosphorylates and inhibits the cardiac Na+/H+ exchanger NHE1. *Circ Res, 103*, 881-890.

98. Misik, A. J., Perreault, K., Holmes, C. F., and Fliegel, L. (2005) Protein phosphatase regulation of Na+/H+ exchanger isoform I. *Biochemistry 44*, 5842-5852.

99. Snabaitis, A. K., D'Mello, R., Dashnyam, S., and Avkiran, M. (2006) A novel role for protein phosphatase 2A in receptor-mediated regulation of the cardiac sarcolemmal Na+/H+ exchanger NHE1. *J Biol Chem*, *281*, 20252-20262.

100. Wakabayashi, S., Bertrand, B., Shigekawa, M., Fafournoux, P., and Pouyssegur, J. (1994) Growth factor activation and "H+-sensing" of the Na+/H+exchanger isoform 1 (NHE1). Evidence for an additional mechanism not requiring direct phosphorylation. *J Biol Chem*, *269*, 5583-5588.

101. Bianchini, L., Woodside, M., Sardet, C., Pouyssegur, J., Takai, A., and Grinstein, S. 1991. Okadaic acid, a phosphatase inhibitor, induces activation and phosphorylation of the Na+/H+ antiport. *J Biol Chem*, *266,* 15406–15413.

102. Sardet, C., Fafournoux, P., & Pouysségur, J. (1991). α-thrombin, epidermal growth factor, and okadaic acid activate the Na+/H+ exchanger, NHE-1, by phosphorylating a set of common sites. *Journal of Biological Chemistry*, *266*(29), 19166–19171.

103. Takahashi, E., Abe, J., Gallis, B., Aebersold, R., Spring, D. J., Krebs, E. G., & Berk, B. C. (1999). p90 RSK Is a Serum-stimulated Na+/H+ Exchanger Isoform-1 Kinase. *The Journal of Biological Chemistry*, *274*(29), 20206–20214.

104. Maly, K., Strese, K., Kampfer, S., Ueberall, F., Baier, G., Ghaffari- Tabrizi, N., Grunicke, H.H., and Leitges, M. 2002. Critical role of protein kinase C alpha and calcium in growth factor induced activation of the Na(+)/H(+) exchanger NHE1. *FEBS Lett*, *521*, 205–210.

105. Sauvage, M., Maziere, P., Fathallah, H., and Giraud, F. 2000. Insulin stimulates NHE1 activity by sequential activation of phosphatidylinositol 3-kinase and protein kinase C zeta in human erythrocytes. *Eur J Biochem*, 267, 955–962.

106. Gunasegaram, S., Haworth, R. S., Hearse, D. J., and Avkiran, M. (1999) Regulation of sarcolemmal Na+/H+ exchanger activity by angiotensin II in adult rat ventricular myocytes: opposing actions via AT1 versus AT2 receptors. *Circ Res*, *85*, 919-930.

107. Costa-Pessoa, J. M., Figueiredo, C. F., Thieme, K., and Oliveira-Souza, M. (2013) The regulation of NHE1 and NHE3 activity by angiotensin II is mediated by the activation of the angiotensin II type I receptor/phospholipase C/calcium/calmodulin pathway in distal nephron cells. *Eur J Pharmacol*, *721*, 322-331.

108. Kramer, B. K., Smith, T. W., and Kelly, R. A. (1991) Endothelin and increased contractility in adult rat ventricular myocytes. Role of intracellular alkalosis induced by activation of the protein kinase C-dependent Na+-H+ exchanger. *Circ Res*, *68*, 269-279.

109. Touyz, R. M., Lariviere, R., and Schiffrin, E. L. (1995) Endothelin influences pHi of human platelets through protein kinase C mediated pathways. *Thromb Res*, *78*, 55-65.

110. Koliakos, G., Befani, C., Paletas, K., and Kaloyianni, M. (2007) Effect of endothelin on sodium/hydrogen exchanger activity of human monocytes and atherosclerosis-related functions. *Ann N Y Acad Sci*, *1095*, 274-291.

111. Khaled, A.R., Moor, A.N., Li, A., Kim, K., Ferris, D.K., Muegge, K., et al. 2001. Trophic factor withdrawal: p38 mitogen-activated protein kinase activates NHE1, which induces intracellular alkalinization. *Mol Cell Biol, 21*, 7545–7557.

112. Wallert, M. A., Hammes, D., Nguyen, T., Kiefer, L., Berthelsen, N., Kern, A., Anderson Tiege, K., Shabb, J. B., Muhonen, W. W., Grove, B. D., and Provost, J.J. (2015) RhoA Kinase (Rock) and p90 Ribosomal S6 Kinase (p90Rsk) phosphorylation of the sodium hydrogen exchanger (NHE1) is required for lysophosphatidic acid-induced transport, cytoskeletal organization and migration. *Cell Signal*, *27*, 498-509.

113. Biichini, L., & Pouyssegur, J. (1996). Regulation of the Na+/H+ exchanger isoform NHE1 : Role of phosphorylation. *Kidney Int*, *49*, 1038–1041.

114. Stock, C., & Schwab, A. (2006). Role of the Na+/H+ exchanger NHE1 in cell migration. *Acta Physiologica*, *187*(1–2), 149–157.

115. Nakamura, K., Kamouchi, M., Kitazono, T., Kuroda, J., Matsuo, R., Hagiwara, N., Iida, M. (2008). Role of NHE1 in calcium signaling and cell proliferation in human CNS pericytes. *American Journal of Physiology. Heart and Circulatory Physiology*, *294*(4), H1700-7.

116. Valles, P. G., Bocanegra, V., Gil Lorenzo, A., & Costantino, V. V. (2015). Physiological Functions and Regulation of the Na+ /H+ Exchanger [NHE1] in Renal Tubule Epithelial Cells. *Kidney and Blood Pressure Research*, *40*(5), 452–466.

117. Odunewu-Aderibigbe, A., & Fliegel, L. (2014). The Na(+) /H(+) exchanger and pH regulation in the heart. *IUBMB Life*, *66*(10), 679–85.

118. Stock, C., & Pedersen, S. F. (2016). Roles of pH and the Na+/H+ exchanger NHE1 in cancer: From cell biology and animal models to an emerging translational perspective? *Seminars in Cancer Biology*, 1–12.

119. Fliegel, L. (2005). The Na+/H+ exchanger isoform 1. *International Journal of Biochemistry and Cell Biology*. *37*(1), 33-37.

120. Wang, H., Singh, D., & Fliegel, L. (1997). The Na+/H+ antiporter potentiates growth and retinoic-acid induced differentiation of P19 embryonal carcinoma cells. *J Biol Chem*, *272*, 26545–26549.

121. Cox, G. A., Lutz, C. M., Yang, C.-L., Biemesderfer, D., Bronson, R. T., & Fu, A. et al., (1997). Sodium/hydrogen exchanger gene defect in slow-wave epilepsy mice. *Cell*, *91*, 139– 148.

122. Bell, S. M., Schreiner, C. M., Schultheis, P. J., Miller, M. L., Evans, R. L., & Vorhees, C. V. et al., (1999). Targeted disruption of the murine Nhe1 locus induces ataxia, growth retardation, and seizures. *Am J Physiol*, *276*, C788– C795.

123. Reshkin, S.J., Bellizzi, A., Cardone, R.A., Tommasino, M., Ca- savola, V., and Paradiso, A. 2003. Paclitaxel induces apoptosis via protein kinase A- and p38 mitogen-activated protein-dependent inhibition of the Na+/H+ exchanger (NHE) NHE isoform 1 in human breast cancer cells. *Clin Cancer Res*, 9, 2366–2373.

124. Rich, I.N., Worthington-White, D., Garden, O.A., and Musk, P. 2000. Apoptosis of leukemic cells accompanies reduction in intracellular pH after targeted inhibition of the Na+/H+ exchanger. *Blood*, *95*, 1427–1434.

125. Odunewu-Aderibigbe, A., & Fliegel, L. (2014). The Na+/H+ exchanger and pH regulation in the heart. *IUBMB Life*, *66*(10), 679–85.

126. Avkiran M. (2003). Basic Biology and pharmacology of the cardiac sarcolemmal sodium/hydrogen exchanger. *J Card Surg*, *18*, suppl 1, 3-12.

127. Dyck, J. R., Maddaford, T. G., Pierce, G.N., and Fliegel, L. (1995) Induction of expression of the Sodium-Hydrogen exchanger in rat myocardium. *Cardiovasc Res, 29*, 203-208.

128. Karmazyn, M., Sostaric, J. V., & Gan, X. T. (2001). The myocardial Na+/H+ exchanger: a potential therapeutic target for the prevention of myocardial ischaemic and reperfusion injury and attenuation of postinfarction heart failure. *Drugs*, *61*(3), 375–389.

129. Wang, Y., Meyer, J. W., Ashraf, M., and Shull, G. E. (2003) Mice with a null mutation in the NHE1 Na+–H+ exchanger are resistant to cardiac ischemia- reperfusion injury. *Circ Res, 93*, 776–782.

130. Karmazyn, M. (1999). The role of the myocardial sodium-hydrogen exchanger in mediating ischemic and reperfusion injury. *Annals of the New York Academy of Sciences*, *874*, 326–334.

131. Karmazyn, M. (1999). The role of the myocardial sodium-hydrogen exchanger in mediating ischemic and reperfusion injury. *Annals of the New York Academy of Sciences*, *874*(519), 326–334.

132. Chakrabarti, S., Hoque, A. N., & Karmazyn, M. (1997). A rapid ischemia-induced apoptosis in isolated rat hearts and its attenuation by the sodium-hydrogen exchange inhibitor HOE 642 (Cariporide). *Journal of Molecular and Cellular Cardiology*, *29*, 3169–3174.

133. Scholz, W., Albus U., Counillon L., Gogelein, H., Lang, H. J., Linz, W., Weichert, A. and Scholkens, B. A. (1995). Protective effects of HOE642, a selective sodium-hydrogen exchange subtype 1 inhibitor, on cardiac ischaemia and reperfusion. *CardioVasc Res*, *29*, 260-268.

134. Frey, N., Katus, H. A., Olson, E. N., & Hill, J. A. (2004). Hypertrophy of the Heart: A New Therapeutic Target? *Circulation*, *109*(13), 1580–1589.

135. Rockman HA, Koch WJ, Lefkowitz RJ. (2002). Seven-transmembrane-spanning receptors and heart function. *Nature, 415*, 206–212.

136. Esposito G., Rapacciuolo A., Naga Prasad SV., (2002). Cardiac hypertrophy: role of G protein-coupled receptors. *J Card Fail*, *8*, S409–S414.

137. Yamazaki, T., Komuro, I., Kudoh, S., Zou, Y., Shiojima, I., Mizuno, T., Tobe, K. (1995). Mechanical stress activates protein kinase cascade of phosphorylation in neonatal rat cardiac myocytes. *The Journal of Clinical Investigation*, *96*, 438–446.

138. Cingolani, H. E., and Ennis, I. L. (2007) Sodium-hydrogen exchanger, cardiac overload, and myocardial hypertrophy. *Circulation*, *115*, 1090–1100.

139. Mraiche, F., Oka, T., Gan, X. T., Karmazyn, M., & Fliegel, L. (2011). Activated NHE1 is required to induce early cardiac hypertrophy in mice. *Basic Research in Cardiology*, *106*(4), 603-616.

140. Karmazyn, M., Liu, Q., Gan, X. T., Brix, B. J., and Fliegel, L. (2003) Aldosterone increases NHE-1 expression and induces NHE-1-dependent hypertrophy in neonatal rat ventricular myocytes. *Hypertension*, *42*, 1171–1176.

141. Alvarez, B. V., Johnson, D. E., Sowah, D., Soliman, D., Light, P. E., et al. (2007) Carbonic anhydrase inhibition prevents and reverts cardiomyocyte hypertrophy. *J Physiol*, *579*, 127–145.

142. Kusumoto, K., Haist, J. V, & Karmazyn, M. (2001). Na+/H+ exchange inhibition reduces hypertrophy and heart failure after myocardial infarction in rats. *Am J Physiol Heart Circ Physiol*, *280*(2), H738-45.

143. Javadov, S., Rajapurohitam, V., Kilic, A., Hunter, J. C., Zeidan, A., et al. (2011). Expression of mitochondrial fusion–fission proteins during post- infarction remodeling: the effect of NHE-1 inhibition. *Basic Res Cardiol 106*, 99–109.

144. Villa-Abrille, M. C., Cingolani, E., Cingolani, H. E., and Alvarez, B. V. (2011) Silencing of cardiac mitochondrial NHE1 prevents mitochondrial permeability transition pore opening. *Am J Physiol Heart Circ Physiol, 300*, H1237– H1251.

145. Orlov, S. N., Adragna, N. C., Adarichev, V. A., Hamet, P., Sergei, N., Adragna, N. C., & Adarichev, V. A. (1999). Genetic and biochemical determinants of abnormal monovalent ion transport in primary hypertension. *Am J Physiol*, *276*, C511-536.

146. Siczkowski, M., Davies, J. E., Ng, L L. (1994). Sodium-hydrogen antiporter protein in normotensive Wistar-Kyoto rats and spontaneously hypertensive rats. *J Hypertension*, *12*(7), 775-781.

147. Bobulescu, I. A., Di Sole, F., & Moe, O. W. (2005). Na+/H+ exchangers: physiology and link to hypertension and organ ischemia. *Current Opinion in Nephrology and Hypertension*, *14*(5), 485–494.

148. Canessa, M., K. Morgan., R. Goldzer., T. J. Moore., and A. Spalvins. (1991). Kinetics abnormalities of the red blood cell sodium-proton exchange in hypertensive patients. *Hypertension*, *17*, 340–348.

149. Fortuno, A., J. Tisaire., R. Lopez., J. Bueno., and J. Diez. (1997). Angiotensin converting enzyme inhibition corrects Na+/H+ exchanger overactivity in essential hypertension. *Am J Hypertension*, *10*, 84–93.

150. Lifton R.P., Hunt S.C., Williams R. R, (1991). Exclusion of the Na+-H+ antiporter as a candidate gene in human essential hypertension. *Hypertension*, *17*, 8–14.

151. Phan, V.N., Kusuhara, M., Lucchesi, P.A. and Berk, B. C., (1997). A 90-kD Na+-H+ exchanger kinase has increased activity in spontaneously hypertensive rat vascular smooth muscle cells. *Hypertension*, *29*(6), 1265-72.

152. Iwamoto T, Kita S, Zhang J. (2004). Salt-sensitive hypertension is triggered by Ca2+ entry via Na+/ Ca2+ exchanger type-1 in vascular smooth muscle. *Nat Med*, *10*, 1193–1199.

153. Blair M. (2016). Diabetes Mellitus Review. *Urol Nurs*, *36*(1), 27-36.

154. Williams, B., & Howard, R. L. (1994). Glucose-induced changes in Na+/H+ antiport activity and gene expression in cultured vascular smooth muscle cells. Role of protein kinase C. *The Journal of Clinical Investigation*, *93*(6), 2623–31.

155. El-Seifi, S., Freiberg, JM., Kinsella, J., Cheng, L., Sacktor, B. (1987) Na+-H+ exchange and Na+-dependent transport systems in streptozotocin diabetic rat kidneys. *Am J Physiol*, *252*(1.2), R40-47.

156. Cukiernik, M., Hileeto, D., Downey, D., Evans, T., Khan, Z. A., Karmazyn, M., & Chakrabarti, S. (2004). The role of the sodium hydrogen exchanger-1 in mediating diabetes-induced changes in the retina. *Diabetes/Metabolism Research and Reviews*, *20*(1), 61–71.

157. Webb, B. A., Chimenti, M., Jacobson, M. P., & Barber, D. L. (2011). Dysregulated pH: A perfect storm for Cancer Progression. *Nature Reviews Cancer*, *11*, 1–7.

158. Reshkin, S. J., Cardone, R. A., & Harguindey, S. (2013). Na+-H+ Exchanger, pH Regulation and Cancer. *Recent Patents on Anti-Cancer Drug Discovery*, *8*(1), 85–99.

159. Huber, V., Milito, A. De, Harguindey, S., Reshkin, S. J., Wahl, M. L., Rauch, C., Fais, S. (2010). Proton dynamics in cancer. *J Transl Med,* 8, 57-60.

160. Cardone, R. A., Casavola, V., & Reshkin, S. J. (2005). The role of disturbed pH dynamics and the Na+/H+ exchanger in metastasis. *Nature Reviews. Cancer*, *5*(10), 786–795.

161. Hanahan, D., & Weinberg, R. A. (2011). Hallmarks of cancer: The next generation. *Cell*, *144*(5), 646–674.

162. Sharma M., Astekar M., Soi S., Manjunatha BS., Shetty DC., Radhakrishnan R. (2015). pH Gradient Reversal: An Emerging Hallmark of Cancers. *Recent Pat Anticancer Drug Discov*, *10*(3): 244-258.

163. Rotin, D., Steele-norwood, D., Grinstein, S., Steele-norwood, D., & Tannock, I. (1989). Requirement of the Na+/ H+ Exchanger for Tumor Growth. *Cancer Res, 49*(1), 205–211.

164. Reshkin SJ., Bellizzi A., Caldeira S., Albarani V., Malanchi I., Poignee M., Alunni Fabbroni M., Casavola V., Tommasino M. (2000). Na+/H+ exchanger-dependent intracellular alkalinization is an early event in malignant transformation and plays an essential role in the development of subsequent transformation-associated phenotypes. *FASEB J*, *14*(14), 2185-2197.

165. Reshkin, S. J., Bellizzi, A., Cardone, R. A., Tommasino, M., Casavola, V., & Paradiso, A. (2003). Paclitaxel Induces Apoptosis via Protein Kinase A- and p38 Mitogen-activated Protein-dependent Inhibition of the Na+/H+ Exchanger (NHE) NHE Isoform 1 in Human Breast Cancer Cells 1. *Clinical Cancer Research*, *9*, 2366–2373.

166. Amith, S. R., & Fliegel, L. (2013). Regulation of the Na/H Exchanger (NHE1) in breast cancer metastasis. *Cancer Research*, *73*(4), 1259–1264.

167. Lacroix, J., Poet, M., Maehrel, C., Counillon, L. (2004). A mechanism for the activation of the Na/H exchanger NHE-1 by cytoplasmic acidification and mitogens. *EMBO Rep*, *5*(1), 91- 96.

168. Fuster, D., Moe, OW., Hilgemann, DW. (2008). Steady-state function of the ubiquitous mammalian Na/H exchanger (NHE1) in relation to dimer coupling models with 2Na/2H stoichiometry. *J Gen Physiol*, 132(4), 465-480.

169. Cardone, RA., Bagorda, A., Bellizzi, A., Busco, G., Guerra, L., Paradiso, A. (2005). Protein kinase A gating of a pseudopodial-located RhoA/ROCK/p38/NHE1 signal module regulates invasion in breast cancer cell lines. *Mol Biol Cell*, 16, 3117–3127.

170. Bourguignon, LY., Singleton, PA., Diedrich, F., Stern, R., Gilad, E. (2004). CD44 interaction with Na+ -H+ exchanger (NHE1) creates acidic microenvironments leading to hyaluronidase-2 and cathepsin B activation and breast tumor cell invasion. *J Biol Chem*, *279*(26), 26991-7007.

171. Lin, Y., Chang, G., Wang, J., Jin, W., Wang, L., Li, H. (2011). NHE1 mediates MDA MB-231 cells invasion through the regulation of MT1-MMP. *Exp Cell Res, 317*, 2031 2040.

172. Bell, S. M., Schreiner, C. M., Schultheis, P. J., Miller, M. L., Evans, R. L., Vorhees, C. V, Scott, W. J. (1999). Targeted disruption of the murine Nhe1 locus induces ataxia, growth retardation, and seizures. *The American Journal of Physiology*, *276*(4.1), C788–C795.

173. Cox, G. A., Lutz, C. M., Yang, C. L., Biemesderfer, D., Bronson, R. T., Fu, A., Frankel, W. N. (1997). Sodium/hydrogen exchanger gene defect in slow-wave epilepsy mutant mice. *Cell*, *91*(1), 139–148.

174. Guissart, C., Li, X., Leheup, B., Drouot, N., Montaut-Verient, B., Raffo, E., Koenig, M. (2015). Mutation of SLC9A1, encoding the major Na^+/H^+ exchanger, causes ataxia-deafness Lichtenstein-Knorr syndrome. *Human Molecular Genetics*, *24*(2), 463–470.

175. Li, X., & Fliegel, L. (2015). A novel human mutation in the SLC9A1 gene results in abolition of Na+/H+ exchanger activity. *PLoS ONE*, *10*(3), 1–9.

176. Zhu, X., Petrovski, S., Xie, P., Ruzzo, E. K., Lu, Y.F., McSweeney, K. M., Goldstein, D.B. (2015). Whole-exome sequencing in undiagnosed genetic diseases: interpreting 119 trios. *Genetics in Medicine*, *17*(10), 774–781.

177. Roskoski, R. (2010). RAF protein-serine/threonine kinases: Structure and regulation. *Biochemical and Biophysical Research Communications*, *399*(3), 313–317.

178. Mccubrey, J. A., Steelman, L. S., Chappell, W. H., Abrams, S. L., Wong, W. T., Chang, F., Elena, R. (2007). Roles Of The RAS/MEK/ERK pathway in Cell Growth, Malignant Transformation and Drug Resistance. *Biochimica et Biophysica Acta - Molecular Cell Research*, *1773*(8), 1263–1284.

179. Carlino, M. S., Long, G. V., Kefford, R. F., & Rizos, H. (2015). Targeting oncogenic BRAF and aberrant MAPK activation in the treatment of cutaneous melanoma. *Critical Reviews in Oncology/Hematology*, *96*(3), 385–398.

180. Roberts, P., & Der, C. (2007). Targeting the Raf-MEK-ERK mitogen-activated protein kinase cascade for the treatment of cancer. *Oncogene*, *26*, 3291–3310.

181. Johnson, GL., Lapadat, R. (2002). Mitogen-activated protein kinase pathways mediated by ERK, JNK, and p38 protein kinases. *Science, 298*, 1911–1912.

182. Garnett, M.J., Rana, S., Paterson, H., Bardford, D., Marias, R. (2005). Wild-type and mutant B-RAF activate C-RAF through distinct mechanisms involving heterodimerization. *Mol. Cell, 20*, 963-969.

183. Chong, H., Vikis, H. G., & Guan, K. L. (2003). Mechanisms of regulating the Raf kinase family. *Cell Signal*, *15*(5), 463–469.

184. A. Zebisch., J. Troppmair. (2006). Back to the roots: the remarkable RAF oncogene story, *Cell. Mol. Life Sci*, *63*, 1314–1330.

185. Wessels, D., Lusche, DF., Scherer, A., Kuhl, S., Myre, MA., Soll, DR. (2014). Huntingtin regulates Ca chemotaxis and K-facilitated cAMP chemotaxis, in conjuction with the monovalent cation/H exchanger Nhe1, in a model developmental system: insights into its possible role in Huntingtons disease. *Dev Biol, 394*, 24–38.

186. Li, W., Han, M., Guan, KL. (2000) The leucine-rich repeat protein SUR-8 enhances MAP kinase activation and forms a complex with Ras and Raf. *Genes Dev, 14*(8), 895–900.

187. Therrien, M., Wong, AM., Rubin, GM. (1998) CNK, a RAF-binding multidomain protein required for RAS signaling. *Cell, 95*(3), 343–53.

188. Durbin, R. M., Altshuler, D. L., Durbin, R. M., Abecasis, G. R., Bentley, D. R., Chakravarti, A., Africa, W. (2010). A map of human genome variation from population scale sequencing. *Nature*, *467*(7319), 1061–73.

189. Lee, Y. C. G., & Reinhardt, J. A. (2012). Widespread polymorphism in the positions of stop codons in Drosophila melanogaster. *Genome Biology and Evolution*, *4*(4), 533–549.

190. Chang, YF., Imam, JS., Wilkinson, MF. (2007). The nonsense-mediated decay RNA surveillance pathway. *Annu Rev Biochem*, *76*, 51–74.

191. Li, X., Augustine, A., Chen, S., & Fliegel, L. (2016). Stop Codon Polymorphisms in the Human SLC9A1 Gene Disrupt or Compromise Na + /H + Exchanger Function. *PLoS One, 11*(9), 1-19.

192. Rose, B. A., Force, T., & Wang, Y. (2010). Mitogen-Activated Protein Kinase Signaling in the Heart: Angels Versus Demons in a Heart-Breaking Tale. *Physiol Rev*, *90*(4), 1507-1546.

193. Li, X., Augustine, A., Sun, D., Li, L., & Fliegel, L. (2016). Activation of the Na + /H + exchanger in isolated cardiomyocytes through β-Raf dependent pathways. Role of Thr 653 of the cytosolic tail. *Journal of Molecular and Cellular Cardiology*, *99*, 65–75.

194. Stüwe, L., Müller, M., Fabian, A., Waning, J., Mally, S., Noël, J., Stock, C. (2007). pH dependence of melanoma cell migration: protons extruded by NHE1 dominate protons of the bulk solution. *J Physiol*, *5852*, 351–360.

195. Schwab, A., & Stock, C. (2014). Ion channels and transporters in tumour cell migration and invasion. *Philos Trans R Soc Lond B Biol Sci, 369*(1638), 1-8.

196. Stock, C., & Schwab, A. (2015). Ion channels and transporters in metastasis. *Biochimica et Biophysica Acta – Biomembranes*, *10.B,* 2638-2646.

197. Kalal, B. S., Upadhya, D., & Pai, V. R. (2017). Chemotherapy resistance mechanisms in advanced skin cancer, *Oncol Rev*, *11*, 19–25.

198. Jakob, J.A., Bassett, R.L.J., r, Ng, C.S., Curry, J.L., Joseph, R.W., Alvarado, G.C., et al., 2012. NRAS mutation status is an independent prognostic factor in metastatic melanoma. *Cancer*, *118*, 4014–4023.

199. Davies, H., Bignell, G.R., Cox, C., Stephens, P., Edkins, S., Clegg, S., et al., 2002. Mutations of the BRAF gene in human cancer. *Nature*, *417*, 949–954.

200. Frontzek, F., Nitzlaff, S., Horstmann, M., Schwab, A., & Stock, C. (2014). Functional interdependence of NHE1 and merlin in human melanoma cells. *Biochem Cell Biol*, *92*(6), 530-540.

201. Stock, C., & Schwab, A. (2006). Role of the Na+/H+ exchanger NHE1 in cell migration. *Acta Physiologica*, *187*(1–2), 149–157.

202. Vahle, A. K., Domikowsky, B., Schwöppe, C., Krähling, H., Mally, S., Schäfers, M., Stock, C. (2014). Extracellular matrix composition and interstitial pH modulate NHE1 mediated melanoma cell motility. *Int J Oncol*, *44*(1), 78-90.

203. Bravo-Cordero, J. J., Hodgson, L., & Condeelis, J. (2012). Directed cell invasion and migration during metastasis. *Current Opinion in Cell Biology*, *24*(2), 277–283.

204. Yamaguchi, H. (2012). Pathological roles of invadopodia in cancer invasion and metastasis. *European Journal of Cell Biology*, *91*(11–12), 902–907.

205. Sibony-Benyamini, H., & Gil-Henn, H. (2012). Invadopodia: The leading force. *European Journal of Cell Biology*, *91*(11–12), 896–901.

206. Weeks, K. L., & Avkiran, M. (2014). Exchanging cardiac phenotype: Is AKT-mediated NHE1 inhibition a permissive switch in physiological hypertrophy? *Journal of Molecular and Cellular Cardiology*, *77*, 175–177.

207. Hausenloy, D., & Yellon, D. (2013). Myocardial ischemia-reperfusion injury: a neglected therapeutic target. *J Clin Invest*, *123*(1), 92–100.

208. Karmazyn, M. (2013). NHE-1: Still a viable therapeutic target. *Journal of Molecular and Cellular Cardiology*, *61*, 77–82.

209. Pike, M.M., Kitakaze, M., Marban, E. (1990). 23Na-NMRmeasurements of intracellular sodium in intact perfused ferret hearts during ischemia and reperfusion. *Am J Physiol*, *259*, H1767–73.

210. Murphy, E., Perlman, M., London, RE., Steenbergen, C. (1991). Amiloride delays the ischemia- induced rise in cytosolic calcium. *Circ Res*, *68*, 1250–8.

211. Pike, M.M., Luo, C.S., Clark, M.D., Kirk, K.A., Kitakaze, M., Madden, MC., et al. (1993). NMR measure- ments of Na+ and cellular energy in ischemic rat heart: role of Na+/H+ exchange. *Am J Physiol*, *265*, H2017–26.

212. Hartmann, M., Decking, U.K. (1999). Blocking Na+\H+ exchange by cariporide reduces Na+-overload in ischemia and is cardioprotective. *J Mol Cell Cardiol*, *31*, 1985–95.

213. Wallert, M. A., Hammes, D., Nguyen, T., Kiefer, L., Berthelsen, N., Kern, A., Provost, J. J. (2015). RhoA Kinase (Rock) and p90 Ribosomal S6 Kinase (p90Rsk) phosphorylation of the sodium hydrogen exchanger (NHE1) is required for lysophosphatidic acid-induced transport, cytoskeletal organization and migration. *Cellular Signalling*, *27*(3), 498–509.

214. Dechant, R., & Peter, M. (2014). Cytosolic pH : A conserved regulator of cell growth ? *Mol Cell Oncol*, *1*(4), 3–5.

215. Dechant, R., Saad, S., Ibáñez, A. J., & Peter, M. (2014). Cytosolic pH regulates cell growth through distinct gtpases, Arf1 and Gtr1, to promote ras/PKA and TORC1 activity. *Molecular Cell*, *55*(3), 409–421.

216. Jelinek, T., Catling, A. D., Reuter, C. W., Moodie, S. A., Wolfman, A., & Weber, M. J. (1994). RAS and RAF-1 form a signalling complex with MEK-1 but not MEK-2. *Molecular and Cellular Biology*, *14*(12), 8212–8.

217. Rabkin, S. W. (2002). Lovastatin induces cell death in cardiomyocytes that is not reversible by coenzyme Q 10. *Pharmacol Toxicol*, *90*(6), 343–345.

218. Zhao, L., & Zhang, B. (2017). Doxorubicin induces cardiotoxicity through upregulation of death receptors mediated apoptosis in cardiomyocytes. *Scientific Reports*, *7*, 44735.

219. Streng, A. S., Jacobs, L. H. J., Schwenk, R. W., Cardinaels, E. P. M., Meex, S. J. R., Wodzig, W. K. W. H., & Van Dieijen-Visser, M. P. (2014). Cardiac troponin in ischemic cardiomyocytes: Intracellular decrease before onset of cell death. *Experimental and Molecular Pathology*, *96*(3), 339–345.

220. Hofschröer, V., Koch, K. A., Ludwig, F. T., Friedl, P., Oberleithner, H., Stock, C., & Schwab, A. (2017). Extracellular protonation modulates cell-cell interaction mechanics and tissue invasion in human melanoma cells. *Scientific Reports*, *7*, 42369.

221. Miller, A. J., & Mihm, M. C. Jr. (2006) Melanoma. *The New England journal of medicine*, *355*, 51–65.

222. Ascierto, P. A., Kirkwood, J. M., Grob, J.-J., Simeone, E., Grimaldi, A. M., Maio, M., Mozzillo, N. (2012). The role of BRAF V600 mutation in melanoma. *Journal of Translational Medicine*, *10*(1), 85.

223. Reshkin, S. J., Greco, M. R., & Cardone, R. A. (2014). Role of pHi, and proton transporters in oncogene-driven neoplastic transformation. *Philosophical Transactions of the Royal Society of London. Series B, Biological Sciences*, *369*(1638), 20130100.

224. Luo, J., & Tannock, I. F. (1994). Inhibition of the regulation of intracellular pH: potential of 5-(N,N-hexamethylene) amiloride in tumour-selective therapy. *British Journal of Cancer*, *70*(4), 617–624.

225. Friedl, P., & Wolf, K. (2003). Tumour-cell invasion and migration: diversity and escape mechanisms. *Nature Reviews Cancer*, *3*(5), 362–374.

226. Van Muijen, G.N., Danen, E.H., Veerkamp, J.H., Ruiter, D.J., Lesley J., van den Heuvel L.P. (1995). Glycoconjugate profile and CD44 expression in human melanoma cell lines with different metastatic capacity. *Int J Cancer, 61*(2), 241-8.

227. Senbanjo, L. T., & Chellaiah, M. A. (2017). CD44: A Multifunctional Cell Surface Adhesion Receptor Is a Regulator of Progression and Metastasis of Cancer Cells. *Frontiers in Cell and Developmental Biology*, *5*.

228. Bourguignon, L. Y. W., Singleton, P. A., Diedrich, F., Stern, R., & Gilad, E. (2004). CD44 interaction with Na+-H+ exchanger (NHE1) creates acidic microenvironments leading to hyaluronidase-2 and cathepsin B activation and breast tumor cell invasion. *Journal of Biological Chemistry*, *279*(26), 26991–27007.

229. Chernoivanenko, I.S., Minin, A.A., Minin, A.A. (2013). Role of Vimentin in Cell Migration. *Ontogenez, 44*(3): 186-202.

230. Sun, B., Fang, Y., Li, Z., Chen, Z., & Xiang, J. (2015). Role of cellular cytoskeleton in epithelial-mesenchymal transition process during cancer progression (Review). *Biomedical Reports*, 603–610.

231. Xu, Z., Alloush, J., Beck, E., & Weisleder, N. (2014). A Murine Model of Myocardial Ischemia-reperfusion Injury through Ligation of the Left Anterior Descending Artery, *J Vis Exp*, *86*, 1–7.

232. Brooks, W. W., & Conrad, C. H. (2009). Isoproterenol-Induced Myocardial Injury and Diastolic Dysfunction in Mice : Structural and Functional Correlates, *Comp Med, 59*(4), 339–343.

233. Guadamillas, M. C., Cerezo, A., & Pozo, M. A. (2011). Overcoming anoikis pathways to anchorage- independent growth in cancer, *J Cell Sci*, *124*(19), 3189-3197.

234. Hao, L., Ha, J. R., Kuzel, P., Garcia, E., & Persad, S. (2012). Cadherin switch from E- to N-cadherin in melanoma progression is regulated by the PI3K/PTEN pathway through Twist and Snail. *British Journal of Dermatology*, *166*(6), 1184–1197.

235. Lin, Y., Chang, G., Wang, J., Jin, W., Wang, L., Li, H., Ma, L., Li, Q., Pang, T. (2011). NHE1 mediates MDA-MB-231 cells invasion through the regulation of MT1-MMP. *Exp Cell Res*, *317*(14), 2031-40.

236. Hofmann, U.B., Westphal, J.R., Van Muijen, G.N., Ruiter, D.J. (2000). Matrix metalloproteinases in human melanoma**.** *J Invest Dermatol, 115*(3), 337-44.

237. Sinnberg, T., Menzel, M., Ewerth, D., Sauer, B., Schwarz, M., Schaller, M., Schittek, B. (2011). β-Catenin Signaling Increases During Melanoma Progression and Promotes Tumor Cell Survival and Chemoresistance. *PLoS ONE*, *6*(8).

238. Morin, P. J. (1999). Beta-Catenin Signaling and Cancer. *Bioessays*, *21*(12), 1021–1030.

239. Amith, S. R., Wilkinson, J. M., & Fliegel, L. (2016). Na+/H+ exchanger NHE1 regulation modulates metastatic potential and epithelial-mesenchymal transition of triple-negative breast cancer cells. *Oncotarget*, *5*(16).

240. Qendro, V., Lundgren, D. H., Rezaul, K., Mahony, F., Ferrell, N., Bi, A., Han, D. K. (2014). Large-scale proteomic characterization of melanoma expressed proteins reveals nestin and vimentin as biomarkers that can potentially distinguish melanoma subtypes. *Journal of Proteome Research*, *13*(11), 5031–5040.

241. Winder, M., Virós, A. (2017). Mechanisms of Drug Resistance in Melanoma. *Handb Exp Pharmacol.* [Epub ahead of print].

242. Odunewu-Aderibigbe, A., Fliegel, L. (2017). Protein mediated regulation of the NHE1 isoform of the Na+/H+ exchanger in renal cells. A regulatory role of Hsp90 and AKT kinase. *Cell Signal*, *36*, 145-153.

243. Gardner, R. G., Cronin, S. R., Leader, B., Rine, J., Hampton, R. Y., & Leder, B. (1998). Sequence determinants for regulated degradation of yeast 3-hydroxy-3-methylglutaryl CoA reductase, an integral endoplasmic reticulum membrane protein. *Molecular Biology of the Cell*, *9*(9), 2611–26.

244. Moncoq, K., Kemp, G., Li, X., Fliegel, L., & Young, H. S. (2008). Dimeric structure of human Na+/H+ exchanger isoform 1 overproduced in Saccharomyces cerevisiae. *Journal of Biological Chemistry*, *283*(7), 4145–4154.

245. Cormet-Boyaka, E., Jablonsky, M., Naren, A. P., Jackson, P. L., Muccio, D. D., & Kirk, K. L. (2004). Rescuing cystic fibrosis transmembrane conductance regulator (CFTR) processing mutants by transcomplementation. *Proceedings of the National Academy of Sciences of the United States of America*, *101*(21), 8221–8226.

246. Natale, D. R., Paliga, A. J. M., Beier, F., D'Souza, S. J. A., & Watson, A. J. (2004). p38 MAPK signaling during murine preimplantation development. *Developmental Biology*, *268*(1), 76–88.

247. Thouverey, C., & Caverzasio, J. (2015). Focus on the p38 MAPK signaling pathway in bone development and maintenance. *BoneKEy Reports*, *4*, 1–8.

248. Olga Anczuko´W., Mark D. Ware., Monique, Buisson., Almoutassem, B., Zetoune,1 Dominique Stoppa-Lyonnet,2 Olga M. Sinilnikova,1,3 and Sylvie Mazoyer. (2008). Does the Nonsense-Mediated mRNA Decay Mechanism Prevent the Synthesis of Truncated BRCA1, CHK2, and p53 Proteins? *HUMAN MUTATION 29* (1), 65-73.

249. Hisamitsu, T., Yamada, K., Nakamura, T.Y., Wakabayashi, S. (2007). Functional importance of charged residues within the putative intracellular loops in pH regulation by Na^+/H^+ exchanger NHE1. *FEBS J*, *274*, 4326–4335.

250. Matsushita, M., Tanaka, H., Mitsui, K., & Kanazawa, H. (2011). Dual functional significance of calcineurin homologous protein 1 binding to Na+/H+ exchanger isoform 1. *American Journal of Physiology. Cell Physiology*, *301*(2), C280-8.

251. Wakabayashi, S., Bertrand, B., Ikeda, T., Pouysségur, J., & Shigekawa, M. (1994). Mutation of calmodulin-binding site renders the Na+/H+ exchanger (NHE1) highly H+ sensitive and Ca2+ regulation-defective. *Journal of Biological Chemistry*, *269*(18), 13710–13715.

252. Slepkov, E. R., Chow, S., Lemeuix, M. J., & Fliegel, L. (2004). Proline residues in transmembrane segment IV are critical for activity, expression and targeting of the Na+/H+ exchanger isoform 1. *Biochemical Journal*, *379*(1), 31–38.

253. Lorenz, K., Schmitt, J. P., Vidal, M., & Lohse, M. J. (2009). Cardiac hypertrophy: Targeting Raf/MEK/ERK1/2-signaling. *International Journal of Biochemistry and Cell Biology*, *41*(12), 2351–2355.

254. Verweij J., & Pinedo HM. ().Mitomycin C: mechanism of action, usefulness and limitations. *Anticancer Drugs*, *1*(1), 5-13.

255. Coccaro, E., Mraiche, F., Malo, M., Vandertol-Vanier, H., Bullis, B., Robertson, M., & Fliegel, L. (2007). Expression and characterization of the Na+/H+ exchanger in the mammalian myocardium. *Molecular and Cellular Biochemistry*, *302*, 145–155.

256. Onishi I., Lin PJ., Numata Y., Austin P., Cipollone J., Roberge M., Roskelley CD., Numata M. (2012) Organellar (Na+, K+)/H+ exchanger NHE7 regulates cell adhesion, invasion and anchorage- independent growth of breast cancer MDA-MB-231 cells. *Oncol Rep*, *27*(2), 311–317.

257. Catling, A. D., Schaeffer, H.-J., Reuter, C. W. M., Rukmini Reddy, G., & Weber, M. J. (1995). A Proline-Rich Sequence Unique to MEK1 and MEK2 Is Required for Raf Binding and Regulates MEK Function. *Molecular and Cellular biology*, *15*(10), 5214-5225.

258. Moor, A. N., Gan, X. T., Karmazyn, M., & Fliegel, L. (2001). Activation of Na+/H+ Exchanger-directed Protein Kinases in the Ischemic and Ischemic-reperfused Rat Myocardium. *Journal of Biological Chemistry*, *276*(19), 16113–16122.

259. Karki, P., & Fliegel, L. (2010). Overexpression of the NHE1 isoform of the Na+/H+ exchanger causes elevated apoptosis in isolated cardiomyocytes after hypoxia/reoxygenation challenge. *Molecular and Cellular Biochemistry*, *338*(1–2), 47-57.

260. Chen, B., Retzlaff, M., Roos, T., Frydman, J., Dobson, C. M., Bosco, D. A., Finkbeiner, S. (2012). Cellular Strategies of Protein Quality Control. *Cold Spring Harb Perspect Biol*, *3*(8), 1–14.